ASPECT RATIO EFFECT OF FUNCTIONALIZED/NON-FUNCTIONALIZED MULTIWALLED CARBON NANOTUBES ON THE MECHANICAL PROPERTIES OF CEMENTITIOUS MATERIALS

A Thesis

by

AHMAD IBRAHIM ASHOUR

Submitted to the Office of Graduate Studies of
Texas A&M University
in partial fulfillment of the requirements for the degree of

MASTER OF SCIENCE

August 2011

Major Subject: Civil Engineering

ASPECT RATIO EFFECT OF FUNCTIONALIZED/NON-FUNCTIONALIZED MULTIWALLED CARBON NANOTUBES ON THE MECHANICAL PROPERTIES OF CEMENTITIOUS MATERIALS

A Thesis

by

AHMAD IBRAHIM ASHOUR

Submitted to the Office of Graduate Studies of
Texas A&M University
in partial fulfillment of the requirements for the degree of

MASTER OF SCIENCE

Approved by:

Chair of Committee,	Rashid Abu Al-Rub
Committee Members,	Zachary Grasley
	Eyad Masad
	Anastasia Muliana
Head of Department,	John Niedzwecki

August 2011

Major Subject: Civil Engineering

ABSTRACT

Aspect Ratio Effect of Functionalized/Non-Functionalized Multiwalled Carbon Nanotubes on the Mechanical Properties of Cementitious Materials. (August 2011)

Ahmad Ibrahim Ashour, B.S., The Hashemite University

Chair of Advisory Committee: Dr. Rashid Abu Al-Rub

The focus of this research was to investigate the use of functionalized/non-functionalized multi walled carbon nanotubes (MWCNTs) as reinforcements for the Portland cement paste. The unique geometrical characteristics of the carbon nanotubes (CNTs), as well as its unique mechanical properties such as high strength, ductility and stiffness, were the vital motivation for this study. In this research, we combined this unique material (CNTs) with concrete which is the most used man-made material. When compared to other composite materials, a limited amount of research has been conducted on the CNTs/cement composites.

In order to investigate how the aspect ratio of functionalized/non-functionalized MWCNTs affects the mechanical properties of cementitious composites, ten different mixes of the MWCNTs/cement composites were prepared and tested. The different batches had a fixed water/cement ratio of 0.4, and variations of MWCNTs length, concentration and surface treatment. The cement nanocomposites were cast in small-scale specimens (beams) for the three-point flexural testing. Four major mechanical

properties were evaluated at ages of 7, 14, and 28 days from the casting day: the maximum flexural strength, ultimate strain capacity (ductility), modulus of elasticity, and modulus of toughness. The results for the different nanocomposite batches were compared with the plain cement (reference) batch.

The mechanical testing results showed that at 28 days almost all of the MWCNTs composites increased the flexural strength of the cement nanocomposites. At 28 days, the long MWCNTs increased the flexural strength more than the short MWCNTs. In general, the ultimate strain (ductility) of the short MWCNTs nanocomposites was higher than the ultimate strain of the long MWCNTs nanocomposites. The flexural strength of short 0.2% MWNT and long 0.04% MWNT (OH) increased by 269% and 83%, respectively, compared to the plain cement sample at 28 days. The highest ductility at 28 days for the short 0.1% MWNT and the short 0.2% MWNT was 86% and 81%, respectively.

Clear evidence was obtained from the SEM images for micro-crack bridging; many of the MWCNTs were stretching across the micro-cracks.

In conclusion, CNTs as nano reinforcements, can effectively improve certain mechanical properties of the cement paste composites.

DEDICATION

To my family and friends in Jordan and the USA who have always been supportive and encouraging.

My appreciation to all of them extends beyond words.

To the soul of my grandfather Mohammad Shehdeh Al-Muhtaseb.

ACKNOWLEDGEMENTS

I would like to acknowledge the great support and guidance of my advisor, Dr. Rashid Abu Al-Rub. Along with Dr. Abu Al-Rub, I would like to recognize my committee members, Dr. Grasley, Dr. Masad, and Dr. Muliana, and fellow researchers Bryan Tyson and Dr. Sun-Myung Kim for their gracious help. This study was mainly sponsored by the Southwest University Transportation Center (SWUTC) through the US Department of Transportation.

NOMENCLATURE

CMF	Carbon micro-fiber
CNF	Carbon nanofiber
CNT	Carbon nanotube
FRC	Fiber reinforced cement
MWCNT	Multi walled carbon nanotube
MWNT	Multi walled nanotube
RC	Reinforced cement
SEM	Scanning electron microscope
SWCNT	Single walled carbon nanotube
TEM	Transmission electron microscope
μ	Mean of the associated normal distribution
σ	Standard deviation of the associated normal distribution

TABLE OF CONTENTS

Page

ABSTRACT iii

DEDICATION v

ACKNOWLEDGEMENTS vi

NOMENCLATURE vii

TABLE OF CONTENTS viii

LIST OF FIGURES xi

LIST OF TABLES xvi

1. INTRODUCTION 1

1.1 Problem Statement 1
1.2 Carbon Nanotubes (CNTs) 8
1.2.1 Nature of CNTs 8
1.2.2 Manufacturing of CNTs 11
1.2.3 Properties of CNTs 12
1.3 Literature Review 13
1.3.1 CNTs in Polymers, Metals and Ceramics 13
1.3.2 CNTs in Cementitious Materials 15
1.4 Research Objectives 20

2. FUNCTIONALIZATION AND DISPERSION OF CARBON NANOTUBES 23

2.1 Introduction 23
2.2 Mechanical Dispersion of CNTs 24
2.3 Chemical Treatment of CNTs 25
2.3.1 Noncovalent Functionalization 26
2.3.2 Covalent Functionalization 28
2.4 Dispersion and Acid Treatment of the MWCNTs (Experimental work) 31
2.4.1 Dispersion 31
2.4.2 Acid Treatment and Defect Site Functionalization 33
2.4.3 Functionalized MWCNTs Characterization 34

Page

3. MIXING CARBON NANOTUBES IN AQUEOUS SOLUTION WITH CEMENT TO MAKE THE NANOCOMPOSITE 38

3.1 Materials 38
3.1.1 Long MWCNTs 38
3.1.2 Short MWCNTs 38
3.1.3 Portland Cement and Superplasticizer 39
3.1.4 Mixing Water 40
3.2 Methodology 40
3.2.1 Carbon Nanotubes Solution Preparation 40
3.2.2 Mixing Carbon Nanotubes Solution with Portland Cement ..43
3.2.3 Casting the Nanocomposite into the Molds 44
3.3 Cement Composite Batches 48

4. EXPERIMENTAL RESULTS AND MICROSTRUCTURAL CHARACTERIZATION 50

4.1 Testing Fixture 50
4.2 Data Analysis 53
4.3 Mechanical Properties 54
4.3.1 Long vs. Short Non-functionalized MWCNTs Nanocomposites 60
4.3.2 Long vs. Short Functionalized MWCNTs Nanocomposites .68
4.4 Results and Discussions 74
4.4.1 Long vs. Short MWCNTs 74
4.4.2 MWCNTs Pull-outs and Results Variability 80
4.4.3 Weakening due to Functionalization 81
4.4.4 Effect of the Cement Paste Curing Method and the Superplasticizer 82
4.5 SEM and TEM Microstructural Imaging 90
4.5.1 CNTs Pull-out and Crack Bridging 91
4.5.2 Dispersion and Agglomeration 93

5. CONCLUSIONS AND FUTURE WORK 97

5.1 Conclusion 97
5.2 Limitations 100
5.3 Future Work 101

REFERENCES 103

Page

APPENDIX A 113

VITA 133

LIST OF FIGURES

Page

Fig. 1. A chart showing the aspect ratio effect on the surface area/volume ratio for different lengths of SWCNTs, MWCNTs, CNFs and CMFs. 5

Fig. 2. A chart showing the aspect ratio effect on the surface area/volume ratio for different lengths of SWCNTs and MWCNTs, and the relations between surface area/volume ratio with mass fraction of CNTs by cement weight and their number per 1 g of cement. 7

Fig. 3. First images of the carbon nanotubes (CNTs) published in 1952 by Russian scientists [14]. 8

Fig. 4. Comparison between (a) graphite structure [16], (b) graphene sheet [17], and (c) fullerenes (Buckyball) structure [18]. 10

Fig. 5. (a) Schematic of a SWCNT [19] and (b) MWCNT which are comprised of many concentric layers of carbon tubes [20]. 10

Fig. 6. CNT structural orientations, (a) armchair structure (b) zig-zag structure, (c) chiral structure [21]. 11

Fig. 7. Ultrasonic wave mixer from Sonics & Materials, Inc. used for mechanically disperse CNTs within aqueous solutions [66]. 25

Fig. 8. Cryo-TEM image for the MWCNTs dispersed in a water/surfactant solution. No obvious agglomerations of the MWCNTs were noticed after ultrasonication (picture courtesy of Bryan M. Tyson) [100]. 32

Fig. 9. SEM images for comparison of (a) an untreated MWCNTs and (b) an acid treated short MWCNTs (COOH) and (c) a treated long MWCNTs (OH). All the MWCNTs surfaces look similar, indicating no sever damage (defects) for the functionalized MWCNTs (pictures a and b courtesy of Bryan M. Tyson) [100]. 36

Fig. 10. Accurate scale used to weigh the CNTs. 41

Page

Fig. 11. Water jacketed beaker (250 ml.) to sonicate the CNTs within the water using the ultrasonic mixer. Constant flow of the water jacket will reduce the temperature of the solution and help preventing excessive evaporation.....42

Fig. 12. Ultrasonic wave mixer from Sonics & Materials, Inc. used for CNTs dispersion [66].....42

Fig. 13. Variable speed planetary mixing blender (Oster Fusion™). 44

Fig. 14. Vacuuming Chamber and the air pump. 45

Fig. 15. Vibration table used for casting the composite cement paste. 46

Fig. 16. View of the square acrylic mold. 47

Fig. 17. Soldering iron of 200 watt power used for demolding the specimens from the acrylic molds. 48

Fig. 18. Three-point bending testing frame dimensions (picture courtesy of Bryan M. Tyson). 51

Fig. 19. Testing frame setup, showing the aluminum frame, the specimen, the LVDT, the load cell and the actuator. 51

Fig. 20. The 2.5 kg capacity load cell, with a small loading bar welded at top of adjustable screw (left). The Newport NSA12 actuator (right). 52

Fig. 21. Example of stress – strain curve for the plain cement and the non-functionalized short and long MWCNTs specimens at age of 7 days. 57

Fig. 22. Example of stress – strain curve for the plain cement and the non-functionalized short and long MWCNTs specimens at age of 14 days. 57

Fig. 23. Example of stress – strain curve for the plain cement and the non-functionalized short and long MWCNTs specimens at age of 28 days. 58

Fig. 24. Example of stress – strain curve for the plain cement and the functionalized short and long MWCNTs specimens at age of 7 days. 58

Page

Fig. 25. Example of stress – strain curve for the plain cement and the functionalized short and long MWCNTs specimens at age of 14 days. 59

Fig. 26. Example of stress – strain curve for the plain cement and the functionalized short and long MWCNTs specimens at age of 28 days. 59

Fig. 27. Average flexural strength results for the plain cement and the non-functionalized short and long MWCNTs composite specimens with the standard error of the mean.....64

Fig. 28. Average ultimate strain results for the plain cement and the non-functionalized short and long MWCNTs composite specimens with the standard error of the mean.....64

Fig. 29. Average modulus of elasticity results for the plain cement and the non-functionalized short and long MWCNTs composite specimens with the standard error of the mean.....65

Fig. 30. Average modulus of toughness results for the plain cement and the non-functionalized short and long MWCNTs composite specimens with the standard error of the mean.....65

Fig. 31. Average flexural strength results for the plain cement and the functionalized short and long MWCNTs composite specimens with the standard error of the mean.....69

Fig. 32. Average ultimate strain results for the plain cement and the functionalized short and long MWCNTs composite specimens with the standard error of the mean. 69

Fig. 33. Average modulus of elasticity results for the plain cement and the functionalized short and long MWCNTs composite specimens with the standard error of the mean.....70

Fig. 34. Average modulus of toughness results for the plain cement and the functionalized short and long MWCNTs composite specimens with the standard error of the mean.....70

Page

Fig. 35. Average flexural strength results for the plain cement and the long MWCNTs composite specimens with the standard error of the mean.....76

Fig. 36. Average flexural strength results for the plain cement and the short MWCNTs composite specimens with the standard error of the mean.....76

Fig. 37. Average ultimate strain results for the plain cement and the long MWCNTs composite specimens with the standard error of the mean.....77

Fig. 38. Average ultimate strain results for the plain cement and the short MWCNTs composite specimens with the standard error of the mean.....77

Fig. 39. Average modulus of elasticity results for the plain cement and the long MWCNTs composite specimens with the standard error of the mean.....78

Fig. 40. Average modulus of elasticity results for the plain cement and the short MWCNTs composite specimens with the standard error of the mean.....78

Fig. 41. Average modulus of toughness results for the plain cement and the long MWCNTs composite specimens with the standard error of the mean.....79

Fig. 42. Average modulus of toughness results for the plain cement and the short MWCNTs composite specimens with the standard error of the mean.....79

Fig. 43. SEM image showing the C-S-H and the crystalized CH of the cement paste. 84

Fig. 44. Average flexural strength results for different plain cement specimens with the standard error of the mean.....88

Fig. 45. Average ultimate strain results for different plain cement specimens with the standard error of the mean.....88

Fig. 46. Average modulus of elasticity results for different plain cement specimens with the standard error of the mean.....89

Fig. 47. Average modulus of toughness results for different plain cement specimens with the standard error of the mean.....89

Page

Fig. 48. SEM image showing the micro-crack bridging and breakage of the MWCNTs within cement paste. 91

Fig. 49. SEM image showing a micro-crack bridging by few number of MWCNTs within cement paste. 92

Fig. 50. SEM image of MWCNTs agglomerations within a small area of cement paste. 94

Fig. 51. A cryo-TEM image of MWCNTs within cement paste (picture courtesy of Bryan M. Tyson). 95

Fig. 52. SEM image showing a huge formation of ettringite needles within the C-S-H of the cement paste. Notice the air void (space) within and surrounding the ettringite formation. 96

LIST OF TABLES

Page

Table 1 The atomic mass percentages of carbon and oxygen for the MWCNTs.....35

Table 2 Physical properties for the long treated MWCNTs(OH) and long untreated MWCNTs.....39

Table 3 Physical properties for the short MWCNTs(COOH) and short untreated MWCNTs.....39

Table 4 Mix design of the functionalized and the non-functionalized MWCNTs test specimens.....49

Table 5 Newport NSA12 Actuator Specifications. 53

Table 6 Average ultimate flexural strength for the functionalized and the non-functionalized MWCNTs test specimens (MPa). 60

Table 7 Average ultimate strain capacity for the functionalized and the non-functionalized MWCNTs test specimens (%). 61

Table 8 Average modulus of elasticity for the functionalized and the non-functionalized MWCNTs test specimens (GPa).....61

Table 9 Average modulus of toughness for the functionalized and the non-functionalized MWCNTs test specimens (kPa).....62

1. INTRODUCTION

1.1 Problem Statement

It is well-known that concrete is the most used and produced material made by man on earth. The importance of this fundamental material motivates scientists and engineers to investigate and study the properties and behavior of cementitious materials, in order to have a better understanding and to improve their mechanical properties, such as strength, ductility and toughness. Concrete is a brittle material that has low tensile strength, low ductility and early developing and propagation of micro cracks due to shrinkage at early ages. Beginning as early as 1980's, fiber reinforced concrete (FRC), using macro fibers as reinforcements, started to become very important in order to improve the tensile strength, ductility and toughness of concrete. However, the gain in ductility was obtained for the fiber reinforced concrete as a composite, not to the concrete itself as a cementitious material. Recently, a wide range of reinforcements, at macro, meso and micro scales, have been used to control the early stages of cracks propagations within the cementitious materials [1-7]. Reinforcing the cementitious materials varied from using macro fibers, like steel reinforcements rebars that are continuously aligned along the tensile material fibers of the cementitious element, to discrete micro and nano fibers, like micro fibers, carbon nano fibers (CNFs) and carbon nanotubes (CNTs).

This thesis follows the style of Cement & Concrete Composites.

The motivation of using these nano-filaments is based on their unique characteristics. The nano scale of the CNTs and CNFs reduces the defects in their molecular structure as well as increases their surface-to-volume ratio. This unique structure allows carbon nanotubes to have extraordinary mechanical, electrical, thermal, and chemical properties that make them promising filaments to many engineering materials and applications [8, 9]. CNTs and CNFs have shown a great potential as reinforcements to polymer-based materials [10-12].

In the last few years, scientists and researchers start to investigate and implement the use of these nano-filaments, CNTs and CNFs, in reinforcing the most used material on earth; concrete. The idea behind using the CNTs and CNFs is their potential to control and prevent the nucleation of cracks at the nano scale by crack-bridging mechanism; hence, preventing the growth and propagation of the cracks to a larger scale. This would result in high-performance cementitious materials, with higher stiffness and durability.

However, to date, many challenges and requirements have not been met in order to effectively utilize CNTs and CNFs in cementitious materials. The extraordinary aspect ratio of the nano-filaments (especially for SWCNTs, [13]) and the graphitic nature of their surfaces created major challenges for implementation in the cementitious materials. These challenges include well dispersion with optimum concentration of the nano-filaments within the cementitious matrix, good and uniform alignment of the nano-filaments, and finally good bonding between the nano-filaments and the surrounding cement matrix. These challenges associated with the implementation of the nano-

filaments as reinforcements to the cementitious materials were discussed in this study. For example, it has been shown that dispersion is a very important element to effectively utilize the CNTs in cementitious composites. CNTs form agglomerations and bundles (clumps) to each other in their normal state due to the high van der Waals forces at the nano scale. Theses agglomerations are difficult to be separated (dispersed) within any media. Poor dispersion of these CNTs within any media will not only prevent the CNTs from effectively reinforce the material, but also it would cause inclusions and voids that would degrade the properties of the matrix and weaken it. Good dispersion of the CNTs within the matrix will guarantee a uniform distribution and bonding of the CNTs within the matrix with evenly distributed stresses, and hence uniformly transfer the tensile stresses from the matrix to the CNTs.

Uniform alignment of the nano-filaments within cementitious composites is very difficult and challenging in practice. However, theoretically, due to their needle-like shape (long tubes), CNTs and CNFs can transfer the stresses mainly in one direction, the axial direction parallel to their length. Hence, if they are aligned perpendicular to the direction of the stresses, they will not be able to transfer the stresses. The optimum scenario is when these nano-filaments are aligned, within the matrix, parallel to the direction of the stresses. However, in practice, three-dimensional random distribution of the nano-filaments within different materials showed that it is still effective to some aspect; this is because the material will harden under the intersection of the cracks propagated randomly in the three-dimensions.

Bonding between the nano-filaments and cement paste matrix is very important to effectively transfer the stresses at the interface between the nano-filaments and the matrix. The adhesive and friction forces at the interface play a major role in determining the mechanical behavior of the nanocomposite. Unfortunately, these bonds between cement paste and CNTs are naturally very weak because of the very smooth surface of the CNTs, and due to the non-covalent bonds. Enhancing these bonds through chemical treatment of the CNTs surfaces, will result in increasing the forces needed to pull-out the nano-filaments from the cement paste matrix. In this study, it has been shown that the pull-out action of the CNTs has significantly increased the flexural strength, ductility and toughness of the CNTs/cement paste composites.

In this study, the aspect ratio effects of short and long MWCNTs implemented into cement paste have been investigated in order to improve its mechanical properties. The hypothesis adopted is that due to the large contact area between the long MWCNTs surfaces and the surrounding cement matrix -compared to the short MWCNTs-, then larger adhesive surface energy and friction forces will develop at the interface; and this should increase the pull-out action energy and hence improve the nanocomposite mechanical properties, like strength, ductility and toughness. However, this hypothesis requires good dispersion of these long MWCNTs within the cement composite, which is very challenging due to the high aspect ratio.

In order to physically visualize the effects of the aspect ratio of the nano-filaments, a chart was developed to show the aspect ratio effect on the surface area/volume ratio for different lengths of single-walled carbon nanotubes (SWCNTs),

multi-walled carbon nanotubes (MWCNTs), carbon nano-fibers (CNFs) and carbon micro fibers (CMFs) (as shown in Fig. 1). It is clear from the chart that only CNTs can provide extremely high aspect ratio, as well as a very high surface area to volume ratio. The high surface area to volume ratio is a very crucial and desired factor in order to provide the best and the most efficient fiber reinforced composite system. Higher the surface area means higher contact area with the matrix, and hence higher bonding strength and better reinforcing.

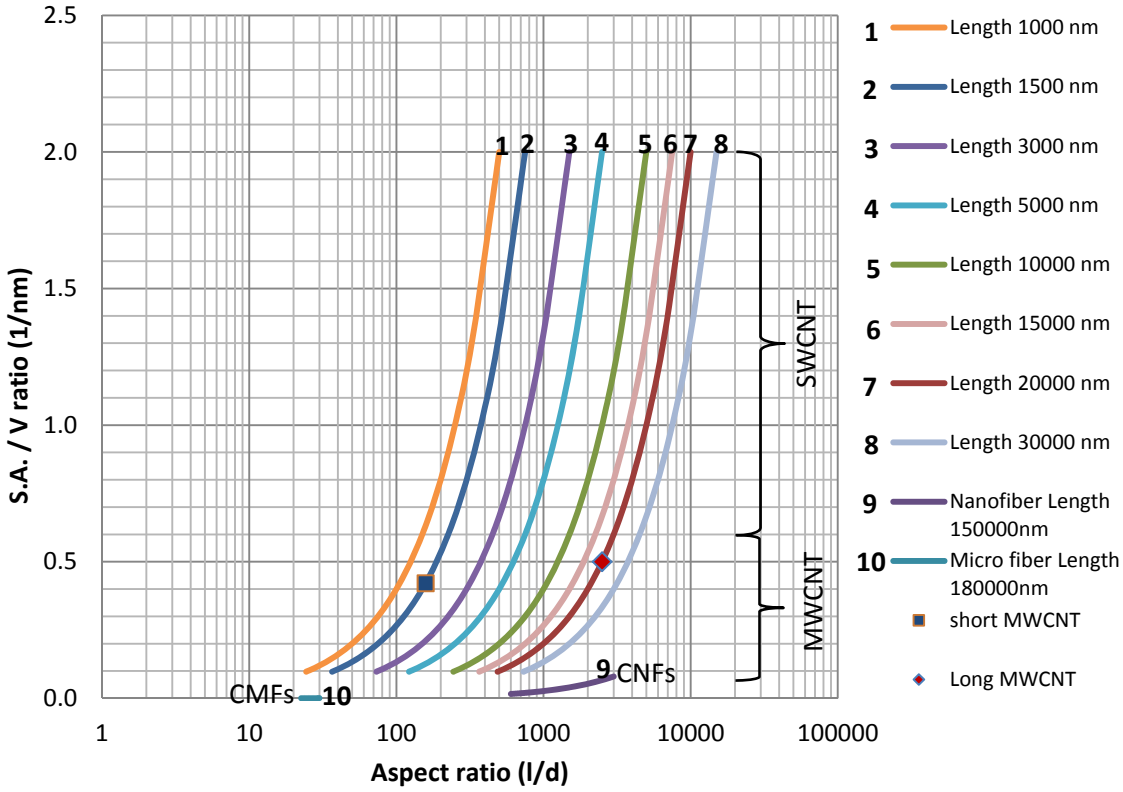

Fig. 1. A chart showing the aspect ratio effect on the surface area/volume ratio for different lengths of SWCNTs, MWCNTs, CNFs and CMFs.

It is also noticed from Fig. 1, that the SWCNTs can provide a surface area to volume ratio that exceed 1.0/nm. This is very unique and cannot be achieved in any material on earth except in the SWCNTs, especially when considering the ultra-long CNTs, which has aspect ratio of several millions. On the other hand, the CMFs and the CNFs show very limited ranges of aspect ratio and a relatively low surface area to volume ratio. These unique geometrical characteristics of the CNTs, as well as the unique mechanical properties, like high strength, ductility and stiffness, are the vital motivation for this study, trying to combine this unique material (CNTs) with concrete the most used material on earth after water.

After adopting the CNTs to be our case of study, additional physical/geometrical relationships between the different geometrical properties like length, aspect ratio, and surface area to volume ratio of the CNTs, along with cement paste/CNTs composite parameters such as mass fraction of CNTs by weight of dry cement, and the approximate number of the CNTs obtained for that specific mass fraction. Fig. 2 shows a chart showing these relationships for the CNTs and cement composites and the aspect ratio effect on the surface area/volume ratio for different lengths of SWCNTs and MWCNTs.

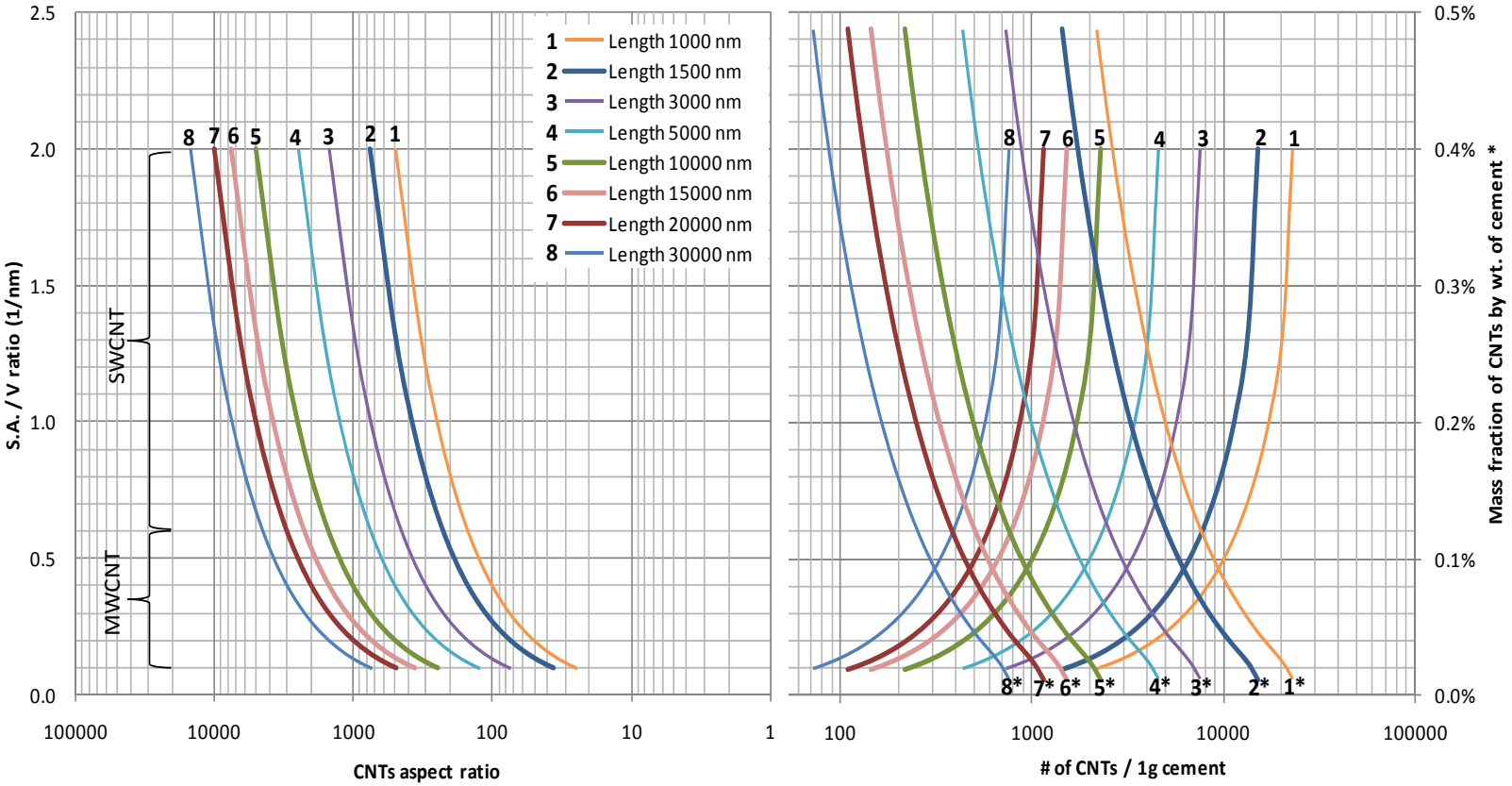

* Reading the mass fraction values shall be through the curves with "*" numbers.

Fig. 2. A chart showing the aspect ratio effect on the surface area/volume ratio for different lengths of SWCNTs and MWCNTs, and the relations between surface area/volume ratio with mass fraction of CNTs by cement weight and their number per 1 g of cement.

1.2 Carbon Nanotubes (CNTs)

1.2.1 Nature of CNTs

Carbon nanotubes (CNTs) have always existed in nature; however, they were first discovered by Russian scientists; L. V. Radushkevich and V. M. Lukyanovich, in 1952, where clear images of the CNTs were published in a journal paper (in Russian language) [14]. Fig. 3 shows the first images of the CNTs. However, CNTs have not been scientifically recognized and used until the last two decades. In 1991 Sumio Iijima [15], published the first article that systematically describes the formation of a helical microtubes made of pure carbon atoms linked together by carbon-carbon (C-C) bonds.

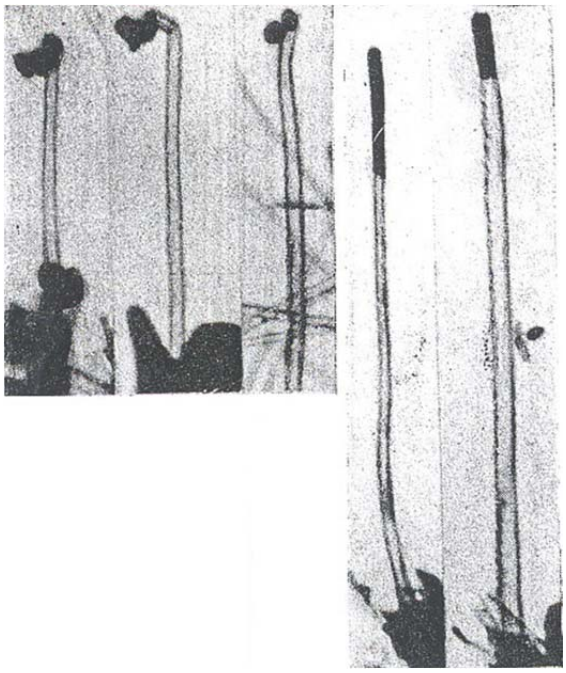

Fig. 3. First images of the carbon nanotubes (CNTs) published in 1952 by Russian scientists [14].

There are many known forms for carbon structures in nature, like diamond, graphite, graphene and fullerenes (Buckyballs) (Fig. 4). CNTs can be imagined as a rolled graphene sheet which its structure is made of a one layer of carbon atoms bonded by a carbon sp^2 bonds in hexagonal pattern. Graphene sheets were investigated by man for the first time in year 2004, by the Russian scientists Nobel Prize winners in physics (2010) Andre Geim and Konstantin Novoselov, from University of Manchester, UK. CNTs can be assumed to be a graphene sheet then rolled in a cylindrical (tube) shape and closed at the two ends by half fullerenes or another carbon structure.

These rolled tubes can be formed as a single tube with one cylinder and is called single walled carbon nanotube (SWCNT), or it may be made from multiple layers of the carbon nanotube, as if they are many cylinders inside each other (from 2 to 20 concentric layers), and called multi walled carbon nanotubes (MWCNTs). Fig. 5 shows schematic drawings for a SWCNT and a MWCNT. The size of the CNTs is in nano scale, the diameter could vary from 1 to 4 nanometers for SWCNTs, and 5 to 50 nanometers or more for the MWCNTs, where the length can extend into several micrometers. CNTs have different structural patterns for the carbon atoms; the orientation of the carbon hexagonal structure has different names; like armchair, zigzag, and chiral. Fig. 6 shows three different structural orientations for the CNTs.

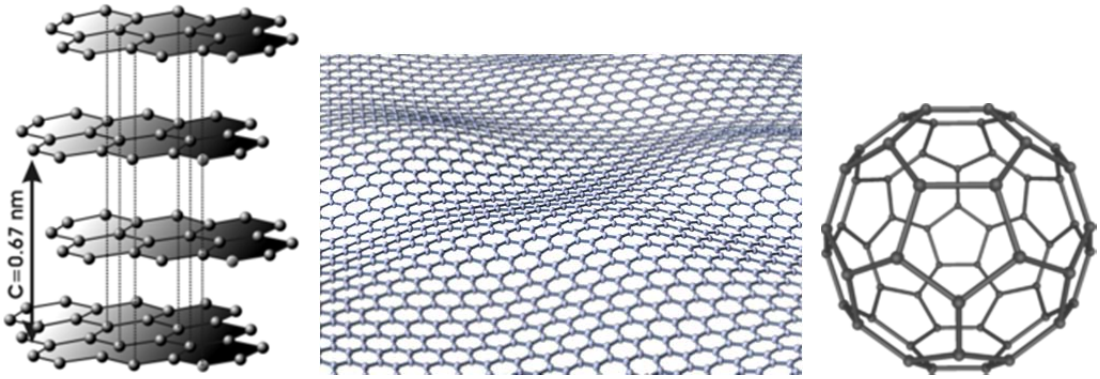

(a) (b) (c)

Fig. 4. Comparison between (a) graphite structure [16], (b) graphene sheet [17], and (c) fullerenes (Buckyball) structure [18].

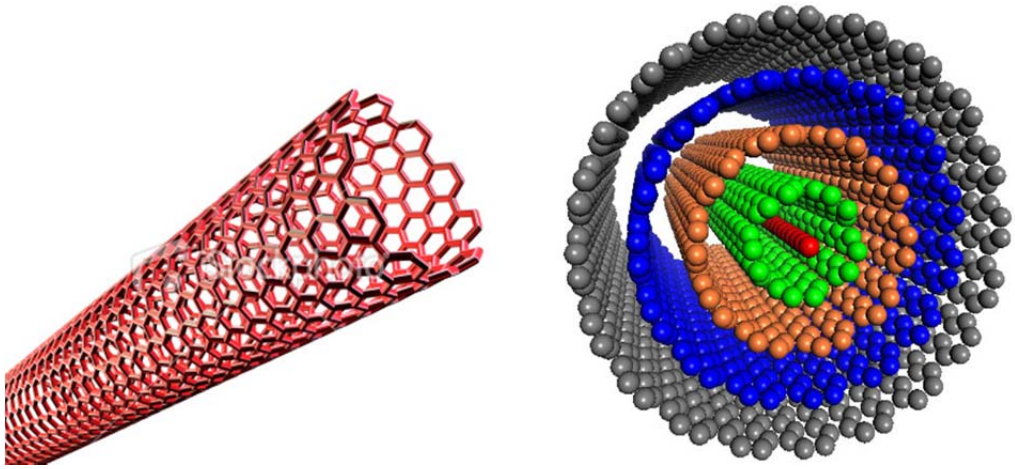

Fig. 5. (a) Schematic of a SWCNT [19] and (b) MWCNT which are comprised of many concentric layers of carbon tubes [20].

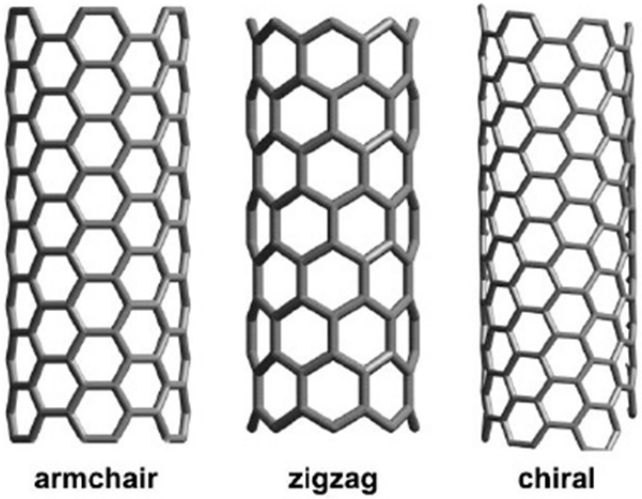

Fig. 6. CNT structural orientations, (a) armchair structure (b) zig-zag structure, (c) chiral structure [21].

1.2.2 Manufacturing of CNTs

There are three main approaches to manufacturing CNTs [22]; The chemical vapor deposition (CVD), the electric arc-discharge method, and laser ablation (LA) process.

The chemical vapor deposition (CVD) method is the most commonly used method; it is relatively less complicated and costly efficient for mass production of CNTs. In addition, it produces CNTs with relatively high purity. This method is based on using a metal catalyst to initiate the CNTs formation, by pumping high-carbon gases like acetylene, ethanol, or methane in a chamber at high pressure and temperature. The type and size of the metal catalyst, as long as the pressure and temperature in the reactor, will determine the produced CNTs properties like purity, length and size.

In the electric arc-discharge method, both SWCNTs and MWCNTs can be produced, by applying an electric arc through two carbon electrodes, which surrounded by an inert gas. The high temperature from the arc (up to 3000^{o}C) will sublimate the carbon atoms, and form the organized structure of the CNTs [23]. This method however, will not provide a high purity of CNTs (around 30% pure CNTs by weight).

The laser ablation (LA) process produces a high purity of CNTs (around 30% pure CNTs by weight). This method uses a laser beam to evaporate a piece of graphite at a very high temperature within an inert gas. The evaporated gas is then cooled and solidified to form the CNTs. The size of the CNTs will depend on the temperature of the reactor [24]. This method is the most expensive method; however, it provides high uniform and pure CNTs.

1.2.3 Properties of CNTs

The unique structure and the nano scale of carbon nanotubes (CNTs) reduce the defects in their molecular structure as well as increase their surface-to-volume ratio. CNTs properties would open a wide door for many mechanical, electrical, thermal, and chemical applications [9]. The applications for CNTs include structural and non-structural applications. Examples for non-structural functions may include self-sensing for measurements of strain, temperature, damage, self-heating (for deicing), electromagnetic interference shielding, and even drug delivery for medical applications. For structural applications, the unique structure allows carbon nanotubes to have unique

mechanical properties that make them promising reinforcements to many engineering materials [8].

The hexagonal structure of the carbon lattice in the CNTs provides a very strong structure that is stronger than diamond bonds. However, the van der Waals forces between the cylindrical tubes of the MWCNTs are much weaker, and hence will allow the inner tubes to slide with respect to each other.

The measured tensile strength for multi-walled CNTs was reported to reach 63 GPa (about 100 times stronger than steel), with ultimate strain capacity of more than 12% (about 60 times higher ductility than steel) and with elastic Young's modulus of about 950 GPa, [25]. Wong, et al. [26] have measured the flexural strength of MWCNTs -fixed as a cantilever beam- using atomic force microscope (AFM) tip, the results show the capability of the MWCNT to elastically store and absorb strain energy. The average flexural strength reported was 14.2 ± 8.0 GPa. Yet, CNTs has a very low mass density which varies based on the purity from 0.037 g/cm^3 like of the super-growth CNTs [27], to about 1.3-1.4 g/cm^3 in conventional CNTs [9] (about 1/6 of the density of the mild steel).

1.3 Literature Review

1.3.1 CNTs in Polymers, Metals and Ceramics

The structural applications for CNTs were mainly based on reinforcing material composites. The implementations of CNTs in polymeric materials have been widely used. Significant enhancements in the mechanical properties of polymers/CNTs composites were reported for by many researchers. The researches have implemented

both treated and untreated CNTs into the polymers/CNTs nanocomposites. Good bonding strength between the CNTs and the surrounding polymer matrix have been reported, this enhancement in bonding increases the elastic modulus, toughness and strength of the polymer/CNTs composites [28, 29]. The electrical conductivity of polymers/CNTs composites has increased significantly by the addition of the CNTs up to 10^8 times. CNTs have been also implemented in metals nanocomposites, for enhancing the electrical and the mechanical properties of the nanocomposites, such as CNTs-reinforced aluminum composites and Copper/CNTs composites [30-34]. In addition to metals, CNTs have been used as reinforcements in ceramics [35-38].

The dispersion of filaments and inclusions in composites is a major element in affecting the local characteristics of the matrix material, hence influencing the properties of the global composite. In polymers, effects of dispersion of inclusions on the mechanical and electrical properties of the composites are shown in the works of [39-43]. Also, some of the effects of dispersion in metals are shown in the works of Stoeffler et al. and Prasad, et al. [44, 45], where they showed that the increase of the filaments particle size comparing to the matrix particle size will result in poor dispersion, hence degrading the mechanical characteristic of the metal composites. This conclusion is important and very critical for the dispersion of CNTs in cementitious materials. The dispersion of filaments like fibers in cementitious materials is also studied in the works of [46-48].

1.3.2 CNTs in Cementitious Materials

When many researches have been done on the CNTs/polymers composites, only limited number of researches has been done on the CNTs/cement composites. As mentioned previously, two major challenges need to be solved in order to effectively obtain a successful CNTs/cement composite; the well-dispersion of the CNTs within the cement paste matrix, and the bonding or cohesive strength between the surface of the CNTs and the attached cement paste around them. Due to the high van der Waals forces due to their large surface area-to-volume ratio, CNTs tend to attract to each other and agglomerate, making it difficult to disperse and separate them. Using ultrasonic mixer with surfactants in aqueous solution, with a specific amount of energy and sonication time, could achieve a good dispersion of the CNTs within the cement paste. However, CNTs can dissolve in the solution or break down into smaller pieces if excessive amount of sonication energy is used. The compatibility of the surfactant used to disperse the CNTs with cement is another important issue. The hydration and the chemical reactions of cement could be badly affected; it could delay or even stop the hydration and the hardening process of the cement paste [49, 50].

Makar, et al. [51] have sonicated the CNTs in ethanol for two hours, and then sonicated the solution after adding the cement powder for another five hours. After that they evaporated the ethanol and grounded the resulted dried mixture. The SEM images for the grounded powder showed cement grains covered by the CNTs, however, some changes of the cement grains surface have been noticed, the author believes this is due to the ultrasonication process. On the other hand other researchers like Cwirzen, et al. [52]

tried to grow CNTs on the surface of the cement particles directly, in order to enhance the dispersion and reduce the time and efforts of mixing and dispersing the CNTs within the cement paste. Makar, et al. [53] have tested cement grains coated with SWCNT, before and after the hydration process, the SEM images showed differences in the distributed in the non-hydrated cement particles and hydrated matrix. The SEM images showed also micro-crack bridging by the CNTs and CNTs pull-out.

Li, et al. [54, 55] have tested both acid treated (H_2SO_4/HNO_3) functionalized MWCNTs and non-functionalized MWCNTs within cement composites of a 0.4 water/cement ratio by dispersing the MWCNTs into plain water using ultrasonic mixer, and then mix them with the cement powder with a surfactant. They reported that the compressive and flexural properties for the functionalized MWCNTs/cement composite were 4% more than non-functionalized MWCNTs/cement composite. SEM images showed that surface of the functionalized MWCNTs was covered by the C-S-H, which increased the strength.

Cwirzen, et al. [56] used solutions of poly (acrylic acid) and another solution of poly(acrylic acid) with gum Arabic to disperse treated and untreated MWCNTs with cement. It has been reported that the use of 0.8wt.% of gum Arabic delayed the cement hydration for three days, however, this delay in the hydration did not affect the material strength. Flexural and compressive tests have been conducted to evaluate the CNTs/cement composite mechanical properties. The nanocomposite was made of 0.045% MWCNTs by weight of the dry cement, and casted into (10 mm × 10 mm × 60

mm) molds for testing. The results show improvements in the compressive strength by 50%.

Nasibulin, et al. [57] provided a simple one-step process to grow carbon nanotubes (CNTs) and carbon nanofibers (CNFs) on cement particles surface using acetylene gas as the source of carbon in chemical vapor decomposition (CVD) technique. They used a continuous cement powder feeder rotating in a quartz tube. The CNTs-cement coated paste was casted into (10 mm × 10 mm × 60 mm) molds for testing. The experimental results show enhancements in compressive strength by more than 100% and increase in the electrical conductivity.

Shah et al. [58] have improved the mechanical properties of the MWCNTs/cement composites, by ultrsonicating the MWCNTs in water with surfactants. The results show increase in the flexural strength by 8% to 40 % and increase in the elastic modulus by 15% to 55 %. The reported optimum nanocomposite achieved was by using 0.1 wt% by dry cement with water/cement ratio of 0.3.

Konsta-Gdoutos et al. [59] reported a comparison between long and short MWCNTs. The experimental work implemented concentrations of 0.025 and 0.08 wt% for long MWCNTs as well as 0.025 and 0.1 wt% for short MWCNTs and were used. The experimental results implied that the concentrations of MWCNTs depend on their aspect ratios; optimum strength is obtained with the use of short MWCNTs at concentration of 0.08 wt%, while long MWCNTs at concentrations less than 0.048 wt%.

In another publication, Konsta-Gdoutos, et al. [60] suggested that the mechanical properties improved by proper dispersion by ultrasonicating the MWCNTs with dispersant solution; less concentration of long MWCNTs is needed in cement composites to improve their mechanical properties than short MWCNTs to reach the same level of the mechanical properties.

Abu Al-Rub et al. [61] and his student Tyson et al. [62], have investigated both CNFs and MWCNTs at different concentrations with cement paste (w/c ratio = 0.4) under three-point flexural testing. They also have investigated the functionalization effects on the CNFs and CNTs. The results were obtained at 7, 14 and 28 days from day of casting, and compared to plain cement specimens. Four mechanical properties have been investigated; strength, ductility, modulus of elasticity and toughness. The results showed that the CNFs/cement composites have better improvements in general when compared to the MWCNTs/cement composites. The non-functionalized CNFs and MWCNTs showed a delay in gaining strength before the 28 days. However, most of the nanocomposites showed improvements in the ductility when compared to the plain cement specimens. On the other hand, the functionalized CNFs and MWCNTs show degradation in the mechanical properties in general over the time. The authors suggest the reason to be related to formation of weak hydration products, or harmful components like excessive formation of ettringite. SEM imaging have been obtained to study the microstructure of the nanocomposites and to evaluate the nano-filaments dispersion.

Luo et al. [63] have tested MWCNTs with cement paste with fumed silica (FS, Grade I), at different concentrations of MWCNTs (0.1, 0.5 and 1 wt%). The dispersion

of the MWCNTs was by using a surfactant and ultrasonication. The nanocomposites where tested under three-point flexural testing with beams dimensions (160 mm × 18 mm × 36 mm). The water/cement ratio was 0.46. The results of testing at 28 days show improvements in the flexural strengths and the stress-intensity factor by 44.4% and 79.7%, respectively, with best enhancement for the 0.5 wt.% of MWCNTs.

In another publication, Luo et al. [64] have tested MWCNTs in cement paste using a surfactant and ultrasonication, at MWCNT/cement ratio of the same previous concentrations of 0.1, 0.5 and 1 wt%, and the results showed 44.5% increasing in the structural damping capacity of the MWNT/Cement composite compared to plain cement paste specimens.

Hunashyal et al. [65] have tested beams of dimensions (20 mm × 20 mm × 80 mm) under four-point bending test, for a composites of plain cement and carbon micro fibers (CFs) with MWCNTs. The WMCNTs and the CFs where separately sonicated with surfactant using ultrasonicator for long time (90 minutes for the MWCNTs and 20 minutes for the CFs). The sonicated solutions then were mixed with cement and sonicated again for another half an hour. After that the composite mixtures were casted and cured and tested at 28 days. Four different cement paste composites (w/c ratio of 0.4) with relatively high amount of MWCNTs were tested; 0.25, 0.5, 0.75, 1 wt% of dry cement. The results showed improvements in strength, ductility and toughness. The flexural strength increased by about 88% for the 0.75% MWCNTs specimens, compared to the plain cement specimens. It has been reported that the ductility has increased with the increase of the MWCNTs content in the composites.

Generally, only some results showed improvements in the mechanical properties of the CNTs/cement composites due to the obstacles of good dispersion and bonding.

1.4 Research Objectives

The main objective of this research is to investigate the effects of different lengths (aspect ratio) and types (functionalized of MWCNTs (functionalized and non-functionalized) as a nano reinforcements on the mechanical properties of the cement paste composite. The cementitious nanocomposite mechanical properties of interest in this study include flexural strength, ductility, modulus of elasticity, and modulus of toughness. Combining different types of MWCNTs at different concentrations to the cement paste is proposed to enhance the cement paste composite properties. Two aspect ratios will be used (long and short MWCNTs) to investigate the effects of large and small aspect ratios and their behavior in cementitious nanocomposites. It is expected that the MWCNTs would enhance the strength and toughness by bridging the nano-cracks, and limit the cracks propagation at the nano level. The modulus of toughness is expected to improve due to the CNTs pull-out mechanism from the cement paste.

As noticed in the literature, three challenging main points should be considered; firstly, the dispersion of the CNTs within the cement paste matrix. This is a very important element and very difficult to obtain, since CNTs tend to agglomerate and bundle together. Secondly, the bonding between the CNTs and the cement paste. This is another important issue to be considered in order to fully utilize the CNTs and fully transfer the stresses from the cement matrix to the CNTs and hence effectively bridging

the nano-cracks, otherwise, low pull-out strength would be resulted and poor enhancement for the mechanical properties will be obtained. Thirdly, the concentration of the CNTs used in the composite. Low concentrations may not be sufficient to fully reinforce the cement paste matrix, and high concentrations would have dispersivity problems and will be more costly.

This study will mainly cover four tasks:

- Dispersion and of CNTs within cement paste nanocomposite,
- Functionalization effects on bonding between the CNTs and the cement matrix,
- Testing of the mechanical properties of the CNTs/cement composite, and
- Microstructural characterization of the cement nanocomposite using SEM and TEM imaging.

The previous tasks will be achieved and discussed in the following sections:

- Section 2 will discuss the dispersion challenges of the CNTs within aqueous solution with the use of a chemical surfactant and within cement paste. It will also discuss the CNTs surface functionalization methods and evaluation.
- Section 3 will provide the details on mixing the CNTs with the cement paste and the preparation process for the CNTs/cement nanocomposites.
- Section 4 will provide the results of the mechanical testing, and a detailed discussion on the mechanical properties of the different batches of CNTs/cement nanocomposites. The microstructural characterization of the cement nanocomposites using SEM and TEM will be discussed too.

- Section 5 will summarize the work done and will provide conclusions based on the results obtained, and will provide plans for the future research.

2. FUNCTIONALIZATION AND DISPERSION OF CARBON NANOTUBES

2.1 Introduction

In order to effectively utilize carbon nanotubes (CNTs) and make use of their extraordinary properties, they should be well dispersed within the reinforced matrix. Dispersion of CNTs means spreading the tubes individually within the matrix by separating the agglomerations and bundle. In this study, dispersion of CNTs within the cement paste is a major element in controlling the mechanical properties of the cement nanocomposite (as discussed in the next sections). Poor dispersion of these nano-filaments within the matrix will not enhance the nanocomposite properties; in fact, it might significantly degrade and deteriorate the matrix properties. Carbon nanotubes in their dry state bundle together due to the van der Waals forces. These interfacial forces at the nano scale are strong enough to pull these nano tubes back to stick together, even after being dispersed in an aqueous solution. Chemical surfactants (provide non-covalent bonds) have been used to reduce the surface tension of the solution and keep the CNTs suspended and unbundled within the solution after they have been dispersed (separated) by mechanical dispersion. Regular hand soap is considered as a good chemical surfactant for the nano-filaments. Two main categories for dispersing techniques of the nano-filaments have been used; mechanical dispersion and chemical treatment. A third technique has been provided to guarantee a good dispersion of CNTs and CNFs within cement paste is by growing CNTs/CNFs directly on cement particles surface [57], the CNTs will be covering and attached on the surface of cement particles without the need to any further dispersion or sonication process.

2.2 Mechanical Dispersion of CNTs

The mechanical dispersion alone using ultrasonic wave mixer without any chemical surfactants is not effective for keeping the CNTs suspended and dispersed. However, the mechanical dispersion (using ultrasonic wave mixer) will be adequate to break the van der Waal forces between the CNTs and separate them in the aqueous solutions. The ultrasonic wave mixer (Fig. 7) induces high energy into the solution, with very high frequency waves (vibrations), causing micro and nano cavitations (vacuum-bubbles) to be formed among the solution molecules. These micro/nano vacuum bubbles will implode when they touch the CNTs surfaces. The imploded bubbles will cause a huge vacuuming force that will pull the nanotubes away into the solution; hence, the CNTs will be separated from each other and in the liquid. However, if no surfactant is used in the solution, the suspend CNTs will start to agglomerate and bundle again. In order to disperse the CNTs effectively, sufficient energy and sonication time should be applied. If excessive amount of energy or sonication time or both introduced to the CNTs solution, the huge forces from the imploded micro bubbles will break (shorten) the nanotubes. Optimizing the sonication process will require providing the optimum combination of sonication energy, duration, volume of solution, concentration of the nano-filaments, temperature, amount and type of the chemical surfactant (anionic, cationic, or nonionic) used in the solution.

Fig. 7. Ultrasonic wave mixer from Sonics & Materials, Inc. used for mechanically disperse CNTs within aqueous solutions [66].

2.3 Chemical Treatment of CNTs

The second technique is the chemical treatment of the surface of the CNTs. This technique is widely used. So many different approaches have been used for chemical treatment (functionalization) of the CNTs surface, and many of them show good results in effectively disperse the CNTs within the matrix and improve bonding between the CNTs and the surrounding matrix. Along with the mechanical dispersion of the CNTs, the chemical treatment of the surface of the CNTs will help in improving the efficiency of the dispersion and the bonding between the CNTs and the bonding with the material matrix. There are two main types for the chemical treatment; covalent bonding and non-covalent bonding (functionalization).

2.3.1 Noncovalent Functionalization

As mentioned before, the use of chemical surfactants in the sonication solution is the most common non-covalent functionalization approach. The existence of the surfactant will introduce non-covalent bonding or treatment for the CNTs surface and the surrounding liquid. The main purpose of these chemical surfactants is to reduce the surface tension of the water, so helping the separation of the CNTs and then to keep the CNTs suspended and separated within the solution. The non-covalent functionalization approach will provide the least amount of damage to the CNTs surface, since no defects are caused by the chemical surfactant to the surface of the CNTs, and the only damage (breakage) will be due to excessive sonication power induced.

Chemical surfactants are amphiphilic; they have two side groups in their chemical structure; hydrophilic (polar) as well as hydrophobic (nonpolar) end groups [67]. The hydrophobic side of the amphiphilic surfactants will be attracted to the CNTs surface (which is hydrophobic), where the hydrophilic end group will be attached to water molecules. Hence, the surfactant will be pulling the CNTs away from each other towards the water in the aqueous solution and the nano-filaments will stay suspended in the solution because of these non-covalent bonds.

While the focus of this study is on the CNTs/cement nanocomposites, it is important to mention that most of the CNTs composites and dispersion research have been done for polymers nanocomposites. Many researchers have combined CNTs within different types of polymers successfully [12, 67-72]. Many different surfactants have been used to disperse the CNTs within polymers, for example, Bandyopadhyaya, et al.

[73] have ultrasonicated the SWCNTs for 20 minutes with water solution with addition of Gum Arabic as a surfactant. They achieved homogeneous dispersions for the CNTs because of the absorption of the surfactant. Islam et al [74] disperse successfully high mass fractions of CNTs in different surfactants like sodium dodecylbenzene sulfonate (NaDDBS) which is a main component of laundry detergents, Triton X-100, and sodium dodecyl sulfate (SDS). While these surfactants and many others can be used in polymers, there is very limited number of surfactants options that can be used with cementitious materials. The nature and the chemistry of cement and its hydration process require certain surfactants that are compatible with cement, since many surfactants will delay or stop the hydration process of the cement paste [56]. It has been shown by Yazdanbakhsh, et al. [49], that using sodium dodecylbenzene sulfonate (NaDDBS) as a surfactant with cement will introduce much more air entrained in the cement paste (five times more than normal range), in addition, hindering the initial set of the cement paste for 24 hours.

One of the most successful surfactants that is compatible with cement without affecting the hydration process was proposed by Yazdanbakhsh, et al. [49]. It has been shown that using an ultrasonic mixer with a commercial superplasticizer, ADVA Cast 575 (polycarboxylate-based water reducing admixture) to disperse CNTs in the mixing water of cement paste provided a relatively good dispersion of the CNTs within the water. In this study this technique will be used, using ADVA Cast 575 superplasticizer as a surfactant to disperse the MWCNTs. The details of the experimental work done in this study for the CNTs/cement composites are discussed the next sections.

2.3.2 Covalent Functionalization

The covalent functionalization is widely used in the world of the nanocomposites, it is not only a powerful tool for CNTs and CNFs dispersion, but also it opened the door wide to many applications of different nanocomposites, by increasing the reactivity and bonding between the functionalized CNTs and the hosting matrix. Covalent functionalization has effectively utilized these nanofilaments into usable composite materials.

Many different approaches have been used to functionalize the CNTs for cement nanocomposites, like air Oxygen treatment [75-77], acid treatment [78], Ozone treatment [79, 80], and plasma oxidation [76, 81-84]. The main purpose of these processes is to provide a side group (functional group) at the surface of the CNTs to improve the dispersion and to increase the reactivity and the bonding strength between the functionalized CNTs and the matrix by covalent bonds. The most common functional groups used in CNTs/cement nanocomposites are the oxygen groups, which include hydroxyl, carboxyl, carbonyl, and ester side groups. Other side groups include halogen groups, like fluoro and chloro side groups, in addition to hydrocarbyl groups, which include alkenyl and alkyl side groups. Ago, et al. [81] used the X-ray photoelectron spectroscopy (XPS) to analyze the surface of MWCNTs and proposed the formation of hydroxyl and carbonyl groups using gas-phase treatment, and carboxylic acid groups by liquid-phase functionalization.

The functionalization of the CNTs will be targeting one of the following locations on the surface of the CNTs; the end caps of the CNTs [85, 86], or the defect sites on the

surface of the CNTs [87] or functionalization of the whole surface of the CNTs without introducing defects sites on the surface (sidewall functionalization) [88].

The defect sites functionalization includes using a strong oxidizing agent (like sulfuric acid) to attack and defect small locations on the surface of the CNTs. Usually a mixture of sulfuric and nitric acid is used for this type of functionalization. The level of functionalization depends on many factors, like the sulfuric/nitric acid ratio. The higher the concentration of the sulfuric acid the more defects on the CNTs surface it would cause, after that the nitric acid will interact with these defected sites and provide the functional group attached to the defected sites by covalent bonds [81, 88-91].

Wang et al. [92] have functionalized SWCNTs using sulfuric/nitric acids treatment. The CNTs were mixed at concentration of 10-20 mg/ 20 ml of 1:1 solution of the sulfuric and nitric acid. After that, the CNTs/acid solution was functionalized by microwave radiation at 450 watts for 1 to 20 minutes at a pressure of 20 psi. The Raman and Fourier transformation infrared (RTIR) spectroscopy showed that the optimum microwave time is three minutes, to prevent excessive damage of the CNTs. After drying the solution, SEM images have been taken for the CNTs. The images showed an average length of 1 μm, which is smaller than the original length of the CNTs. This indicates that the acid treatment along with the high energy of microwave radiations have damaged the CNTs and break them into smaller pieces.

End caps functionalization is similar to defect sites functionalization, but without using sulfuric acid to attack and defect the surface of the CNTs. This means that the

oxidizing agent will interact only with pre-defected locations on the surface of the CNTs (if they exist) and functionalize the end caps at the ends of the CNTs.

The last approach that is widely used for different types of nanocompossites is the sidewall functionalization. In this method, many different chemical s can be used to functionalize the surface of the CNTs [93], but the is no need to use strong acid for the functionalization. These chemicals include the use of some salts, like benzenediazonium salts [93], or oleum (pyrosulfuric acid) [94], or gases such as fluorine gas [95].

Other techniques that have been used for covalent functionalization includes ozone and plasma treatments. These techniques have showed good results of dispersion with minor defects for the CNTs and CNFs surfaces. For example, Fu, et al. [96] have showed an increase in the CNFs surface oxygen content, using ozone treatment by changing the surface oxygen configuration from C–O to C=O. The ozone treatment process included immersing in acetic acid, H_2O_2, and NaOH solution, then fibers washing and trying, and finally exposing the fibers to O_3 gas for 5 minutes at temperature of 160°C. Chen, et al. [97], used Microwave excited Ar/H_2O surface-wave plasma to functionalize the surface of the MWCNTs. The results showed enhancement in the surface oxygen content without damaging the MWCNTs surfaces.

Although it is very challenging to obtain a very good dispersion within cementitious composites, it is also more challenging to evaluate quantitatively the level of dispersion of the nano-filaments within many matrices, especially within cement paste. Only few works have been done to try defining quantitatively the level of dispersion [49, 50, 98]. However, experimentally, SEM and TEM imaging could give some idea on how

qualitatively CNTs are dispersed within the matrix. Some researchers assessed the dispersion of the nano-filaments in cement paste be measuring the electrical resistivity of the composite and comparing it with the electrical resistivity of the plain cement paste [99].

2.4 Dispersion and Acid Treatment of the MWCNTs (Experimental work)

2.4.1 Dispersion

In order to study the dispersion of the MWCNTs used in this study, two identical solutions were made of deionized water, with MWCNTs at 0.25 wt% by weight of water, and ADVA Cast 575 surfactant (superplasticizer) at 1.25 wt% by weight of water. The first CNTs solution was dispersed by mechanical shaking by hand for 7 minutes. The other CNTs solution was dispersed by ultrasonication at a power of 78.64 Watt (70% of maximum amplitude) for 20 minutes.

The dispersing results indicate clearly that the mechanical shaking by hand resulted in very poor dispersion. Large areas of big agglomerations and bundles of CNTs were seen in the mechanical shacked solution. In few minutes, the CNTs have bundled again and settled down in the suspension. On the other hand, the sonicated solution showed a uniform stable distribution of the CNTs within the solution. In order to visually evaluate the dispersion of the CNTs within the solution, a cryo TEM images for the dispersion were obtained at frozen liquid nitrogen temperatures (-196^{o}C) by an FEI Tecnai F20 transmission electron microscope. Fig. 8 shows a relatively good dispersion

of the CNTs within the aqueous solution. No significant clumps and agglomerations were noticed.

In general, CNTs are very difficult to be well dispersed in any media. ultrasonication is a good means to guarantee a relatively good dispersion of the CNTs. However, breakage of CNTs could occur due to excessive sonication power induced.

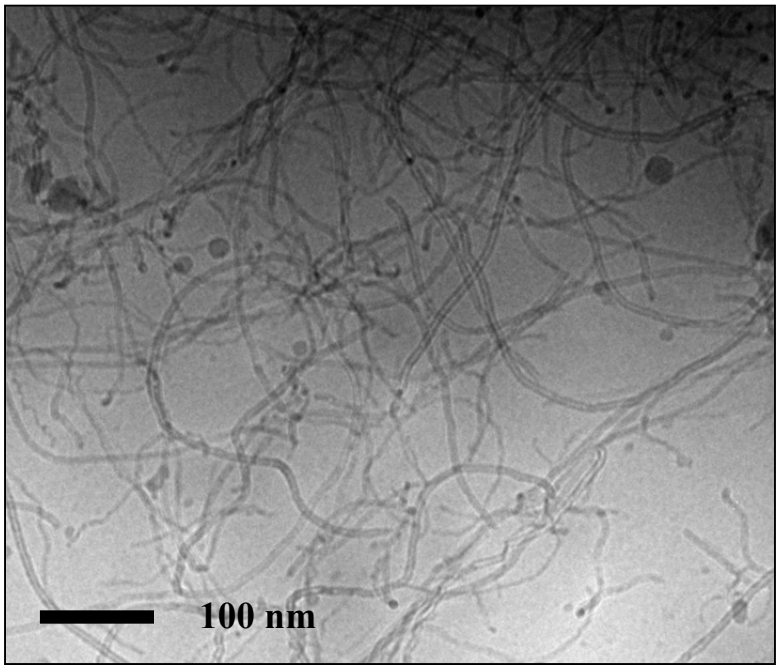

Fig. 8. Cryo-TEM image for the MWCNTs dispersed in a water/surfactant solution. No obvious agglomerations of the MWCNTs were noticed after ultrasonication (picture courtesy of Bryan M. Tyson) [100].

2.4.2 Acid Treatment and Defect Site Functionalization

Acid treatment using sulfuric/nitric acids is the technique adopted for functionalizing the MWCNTs that will be used for the CNTs/cement composites fabrication (as shown the following sections).

Four main variables control the acid functionalization process. First, the concentration of each of the acids used, i.e. the ratio between the sulfuric and nitric acids. The sulfuric acid (H_2SO_4) creates small defect sites on the surface of the CNTs, and the nitric acid (HNO_3) will oxidize these defect sites by providing a functional group (like carboxylic acid groups in our case). Increasing the concentration of the sulfuric will introduce more defects (roughness) on the CNTs surfaces. Hence, by changing the sulfuric/nitric acids concentrations, the level of the functionalization can be controlled. However, excessive surface treatment by sulfuric acid could break (shorten), damage, dissolve, or deteriorate the mechanical properties of the CNTs.

Another important element in the acid functionalization process is the temperature of the solution (reaction temperature). Appropriate temperature should be maintained constant over the functionalization process. High temperature would increase the reaction speed and a low temperature could slow it down. The duration of the acid treatment of the CNTs is another variable. The more the CNTs stay in contact with the acids, the more the functionalization will be introduced to the CNTs surfaces. Finally, the CNTs/acids ratio will affect the severity of the functionalization process. If the CNTs concentration is relatively high, then more acids will be needed to complete the chemical reactions.

The complete acid functionalization process for the MWCNTs was carried through three main stages as discussed in details in [100]. The first step was to place the untreated MWCNTs in a solution of sulfuric and nitric acids. Then the CNTs/acids solution was placed in oil bath at constant temperature of 85^{o}C. The sulfuric acid to nitric acid ratio was 2:1, where the CNTs/acids concentration was 100 mg of MWCNTs for every 100 ml of the acid solution. The acids treatment of the CNTs lasted for 60 minutes.

The next step after the acids treatment of the MWCNTs is to dilute the acidic solution and washing the CNTs. The dilution and washing have been done using deionized water. The CNTs have been placed a filter with a 0.45 μm pore size and washed by the deionized water multiple times until the pH value of the washing water reaches almost the neutral value between 6.0 and 7.0, which is the pH for the deionized water used.

The last step is to dry the functionalized MWCNTs. Oven drying at a temperature of 60^{o}C was used with a relative humidity set to approximately 0%. The drying process took 1 to 3 days, until the CNTs are completely dried with no change in the weight. The functional group introduced to these MWCNTs is carboxylic acid group (COOH). These CNTs will be denoted as MWCNTs (COOH) from now on.

2.4.3 Functionalized MWCNTs Characterization

After the functionalization process complete, the functionalized MWCNTs (COOH) were analyzed by an X-ray photoelectron spectroscopic (XPS) in order to

measure the oxidization level at the surface of the functionalized MWCNTs (COOH). The ratio of C1s to O1s was calculated in order to properly calculate the oxidation level. The XPS results (Table 1) showed that the functionalized MWCNTs (COOH) increased the amount of oxygen atoms by 10 times compared to the untreated ones.

In order to widen the area of this research, two new batches of MWCNTs were included. The new batches have higher aspect ratio, and the functional group for the long MWCNTs is (OH) provided by Cheap Tubes, Inc.[101]. Four different batches were used in this study. Untreated Short MWCNTs, Untreated long MWCNTs, Treated short MWCNTs (COOH), and Treated long MWCNTs (OH). Table 1 shows summary of the atomic mass percentages of carbon and oxygen for the four different types of MWCNTs used in this study.

Table 1
The atomic mass percentages of carbon and oxygen for the MWCNTs.

Sample	Carbon %	Oxygen %
Untreated short MWCNTs	98.78◊	1.22◊
Untreated long MWCNTs	97.44*	-
Treated short MWCNTs (COOH)	87.80◊	12.20◊
Treated long MWCNTs (OH)	94.42*	5.58*

* Using Energy Dispersive X-ray Spectroscopy [101]. ◊: data from [100].

In order to evaluate the functionalization effects on the surface of the functionalized short MWCNTs (COOH) and long MWCNTs (OH), SEM images have been taken at a high magnification to the individuals of these MWCNTs. Fig. 9 shows a

comparison between untreated MWCNTs and the treated short MWCNTs (COOH) and long MWCNTs (OH). The images show that there are no noticeable damage (defects or cuts) introduced on the surfaces structure for both of the functionalized MWCNTs. On the other hand, similar surface characteristics were noted and no significant differences between the untreated and the treated MWCNTs.

However, the mechanical properties of the functionalized and the non-functionalized MWCNTs in cement composites are different. The mechanical properties of the CNTs/cement composites will be discussed in Section 4.

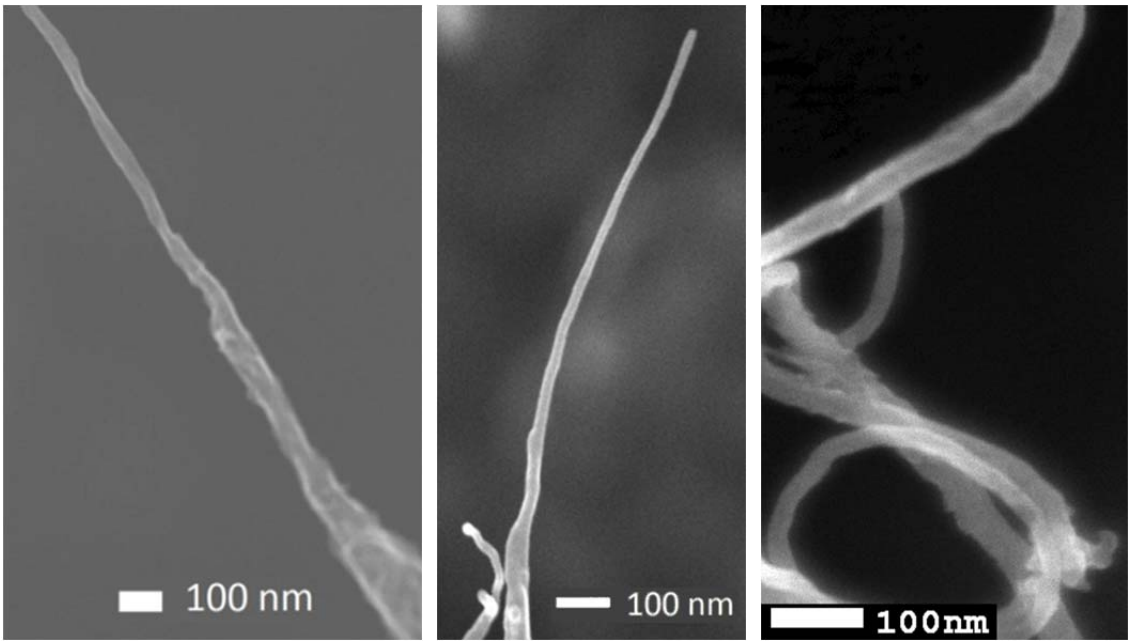

(a) (b) (c)

Fig. 9. SEM images for comparison of (a) an untreated MWCNTs and (b) an acid treated short MWCNTs (COOH) and (c) a treated long MWCNTs (OH). All the MWCNTs surfaces look similar, indicating no sever damage (defects) for the functionalized MWCNTs (pictures a and b courtesy of Bryan M. Tyson) [100].

In summary, using the proper chemical surfactant is very useful for maintaining the dispersion of the CNTs; however, that surfactant has to be compatible with cement. Excessive amount of surfactant will enhance the dispersivity of the CNTs, and reduce the amount of ultrasonication power and time, but will have negative effects on the cement paste hydration process. Less surfactant means more energy (sonication) needed for well dispersion, but that will cause breakage and dissolving of the CNTs. Optimum level of both surfactant and ultrasonication needed to be achieved, and more investigations are needed. On the other hand, the CNTs functionalization process is very important in order to improve the dispersion and to enhance the bonding between the CNTs and the surrounding matrix. Providing the specific type of the functional group that will bond with the matrix, and optimizing the level of functionalization is crucial, such that providing sufficient side functional groups without excessive damaging to the CNTs. A combination of all these parameters, will result in effectively utilize the unique properties of the CNTs.

3. MIXING CARBON NANOTUBES IN AQUEOUS SOLUTION WITH CEMENT TO MAKE THE NANOCOMPOSITE

3.1 Materials

3.1.1 Long MWCNTs

The long functionalized (OH functional group) and the long non-functionalized multi-walled CNTs were provided by Cheap Tubes, Inc. [101], batches names: (SKU 030201 and SKU 030101, respectively). The long MWNTs were produced by Catalytic Chemical Vapor Deposition (CCVD) process. The (OH) represents the hydroxyl functional group. The physical properties provided by the manufacturer are shown in Table 2. The average aspect ratio (length/diameter ratio) for the long MWCNTs was 1250 to 3750.

3.1.2 Short MWCNTs

The functionalized (COOH functional group) and non-functionalized short MWCNTs were NC7000 multi-walled carbon nanotubes provided by Nanocyl, Inc.[102], and were produced by (CCVD) process too. The (COOH) represents the carboxyl functional group. The physical properties are shown in Table 3. The average aspect ratio (length/diameter ratio) for the short MWCNTs was about 157. The functionalized MWCNTs were acid treated by Sulfuric and Nitric acids in order to get carboxylic functional groups, as discussed in the previous section.

Table 2
Physical properties for the long treated MWCNTs(OH) and long untreated MWCNTs.

	Long CNTs(OH)	Long CNTs
Outer Diameter	<8 nm	<8 nm
Length	10-30 μm	10-30 μm
Specific Surface Area	>500 m^2/g	>500 m^2/g
Purity	>95%	>95%
OH content	5.58wt%	--

Table 3
Physical properties for the short MWCNTs(COOH) and short untreated MWCNTs.

	Short CNTs(COOH)	Short CNTs
Outer Diameter	9.5 nm	9.5 nm
Length	1.5 μm	1.5 μm
Specific Surface Area	250–300 m^2/g	250–300 m^2/g
Purity	≥90%	≥90%
COOH content	12.20wt%	--

3.1.3 Portland Cement and Superplasticizer

The cement used in all mixtures was the commercial Type I/II Portland cement. A commercial water reducing admixture (polycarboxylate), provided by (Grace Corporation) named ADVA Cast 575 was used as a superplasticizer. This superplasticizer is used in this study as a surfactant to disperse the CNTs within the aqueous solution.

3.1.4 Mixing Water

The mixing water used for all batches was deionized water by a reverse osmosis water filtering technique. The measured pH value for the water was about 5.5 to 6.0.

3.2 Methodology

3.2.1 Carbon Nanotubes Solution Preparation

The preparation process of the nanocomposite cement mixture starts by weighing the required amount of the CNTs using an accurate scale (Fig. 10). The required quantities of the mixing water and the surfactant (ADVA Cast 575 superplasticizer) were measured and added together with the CNTs into a water jacketed beaker of a capacity of 250 ml. (Fig. 11). The dispersion process was performed using an ultrasonic mixer from Sonics & Materials, Inc. (Fig. 12). The high frequency of the ultrasonic waves that transferred through the 13 mm titanium alloy probe to the liquid medium, with a maximum power that could reach 500 watts and frequency of 20 kHz, will provide a good level of dispersion of the CNTs filaments in the water. Under adequate ultrasonic waves power and for a certain period of sonication time, the high energy put into the mixture will break the agglomerations and clumps of the CNTs by breaking the chemical bonding of the van der Waals forces between the nano-filaments.

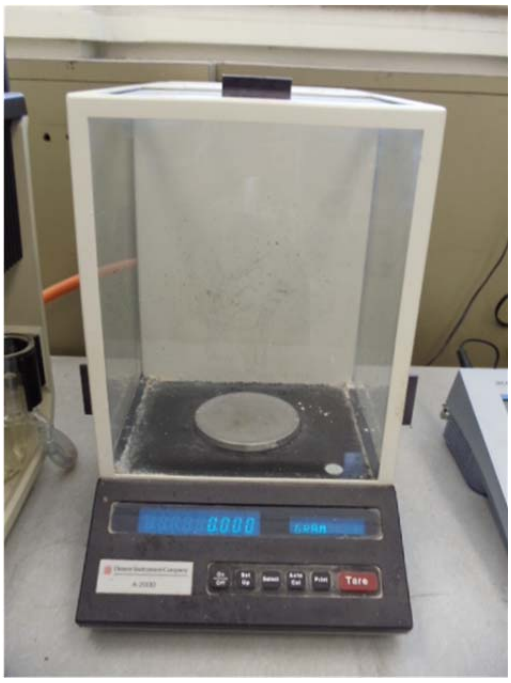

Fig. 10. Accurate scale used to weigh the CNTs.

The high energy introduced into the solution will heat it up, and causes part of the mixture water to evaporate. In order to reduce the solution temperature, a water jacket of flowing tap water at room temperature surrounding the beaker is used to help reducing the temperature below 45^{o}C throughout the dispersing period. The amount of power and period of dispersion is a critical element for achieving a good dispersion of CNTs; less energy and time could not guarantee a good dispersion, while more energy and time would dissolve and break the nano-filaments. The sonication power for all different types of the MWCNTs solutions was 78.64 Watt (70% of max. amplitude), and the power per solution volume was 0.4626 Watt/ml. of the solution. The sonication period for different MWCNTs lengths varied from 20 to 30 minutes.

Fig. 11. Water jacketed beaker (250 ml.) to sonicate the CNTs within the water using the ultrasonic mixer. Constant flow of the water jacket will reduce the temperature of the solution and help preventing excessive evaporation.

Fig. 12. Ultrasonic wave mixer from Sonics & Materials, Inc. used for CNTs dispersion [66].

3.2.2 Mixing Carbon Nanotubes Solution with Portland Cement

The required amount of the sonicated CNTs solution was then poured into blender jar of a variable speed planetary kitchen blender (Oster Fusion™) as shown in Fig. 13. Due to the small mix quantities made, the use of the standard Hobart mixer will not be effective, due to the relatively large mixing bowl. That is the reason why a smaller mixer bowl was needed. In previous step the cement powder was weighed and kept in another beaker. The blender is started with the dispersed solution only, and then cement powder was added gradually to the CNTs solution. After adding the cement powder, the mixing time was a total of 7 minutes; 3 minutes at low speed, 1 minute at medium speed, then 3 minutes at low speed. Another mixing protocol has been tried, where the CNTs solution was added to the cement powder in the blender. The last protocol will cause agglomerations of some parts of unhydrated cement that sticks on the blender jar walls. This required pausing of mixing and scraping down the sticking cement agglomerations to guarantee homogeneous mixing. However, the products of both mixing protocols did not show any significant effects on the mechanical properties from flexural testing.

Fig. 13. Variable speed planetary mixing blender (Oster Fusion™).

3.2.3 Casting the Nanocomposite into the Molds

Immediately after mixing is done, the composite cement paste is poured into a plastic bottle and placed into a small air vacuuming chamber for 3 minutes (Fig. 14). The air vacuuming will help in getting rid of the entrapped air bubbles that formed during mixing process.

Fig. 14. Vacuuming Chamber and the air pump.

After that the composite cement paste was poured into small vertical acrylic molds of square cross-section that have been placed on top of a vibrating table as shown in Fig. 15. The vibration during casting the cement paste will help to smoothly fill the molds and reduce the air voids and entrapped air bubbles. This is important to get solid uniform cross-sections of the material throughout the length of the small beams, without having defects due to air voids that would significantly affect the mechanical strength of the composite.

Fig. 15. Vibration table used for casting the composite cement paste.

The used extruded acrylic molds were chosen for their very smooth surfaces and small dimensional tolerances. Acrylic as a polymer will not absorb the mix water from the cement paste like some other polymeric materials. The molds inner cross-section dimensions are square (6.5 mm × 6.5 mm) as shown in Fig. 16. The molds were bought as long extruded tubes, and then were cut into the desired length of about 200 mm. Small square flat pieces (~ 2.5 cm × 2.5 cm) of acrylic were glued to the bottom of the acrylic tubes to seal the bottom and to be as a standing base.

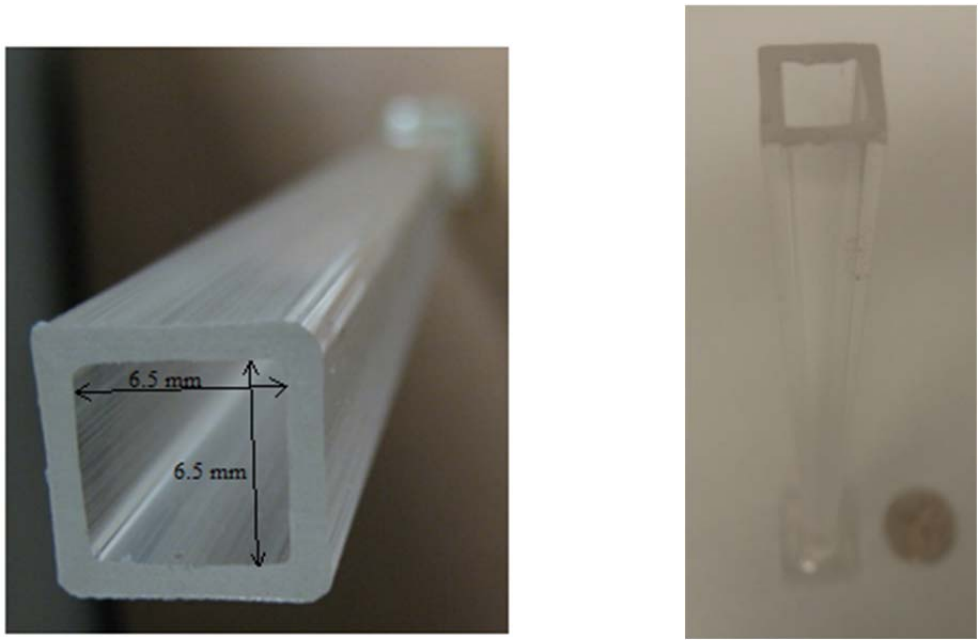

Fig. 16. View of the square acrylic mold.

The casted specimens were then allowed to air cured in the molds at room temperature for 7 days before demolding. Since only the upper side of the molds, which have a very small cross-sectional area, is exposed to air, the mix water content loss will be minimal.

After 7 days from casting, the specimens were demolded using a special soldering iron. The soldering iron used was provided by a custom made cutting edge made of copper, with a power of 200 Watt and temperature of 537^{o}C (1000^{o}F) as shown in Fig. 17. The sides of the acrylic molds were cut using the soldering iron by melting the acrylic at the cutting lines on the four sides.

Fig. 17. Soldering iron of 200 watt power used for demolding the specimens from the acrylic molds.

3.3 Cement Composite Batches

Ten different CNT-reinforced Portland cement paste batches were produced during the course of this study. The first batch was the plain cement batch (reference) sample; the other nine batches cover all different MWCNTs/cement composites. These include five batches using non-functionalized MWCNTs and four batches using functionalized MWCNTs. The different batches includes different CNTs aspect ratio (long and short), and three different concentrations of the CNTs by weight of dry cement (0.04%, 0.1% and 0.2%). All specimens including the plain cement reference sample have a water/cement ratio of 0.4. A summary of the mix design for all batches is shown in Table 4. For each testing day (7, 14 and 28 days), four or five replicates (samples) of each specimen were made to get a representative average value from the flexural testing. A total of about 12 to 15 replicates (samples) for each batch were casted. Note that a batch of 0.2% long MWCNTs could not be produced due to the difficulty in achieving satisfactory dispersion of the long MWCNTs within the aqueous solution.

The plain cement paste (reference) specimen was made with a water/cement ratio of 0.4, with addition of 0.1% of superplasticizer by the weight of cement. This amount of superplasticizer is equal to 25% of what has been added to the other MWCNTs/cement composite specimens. The reason why more amount of superplasticizer has been used in all other MWCNTs/cement composites is that larger amount of superplasticizer, which is used as a surfactant, is needed in the nano composites in order to improve the dispersion of the nano-filaments (see [49] and [98] for more details).

Table 4
Mix design of the functionalized and the non-functionalized MWCNTs test specimens.

Test Specimens	Superplasticizer: % weight of cement	CNTs: % weight of cement	Ultra-sonication time (minutes)
Plain cement (Reference)	0.1	0.0	-
Short CNTs 0.04	0.4	0.04	20
Short CNTs 0.1	0.4	0.1	30
Short CNTs 0.2	0.4	0.2	30
Long CNTs 0.04	0.4	0.04	30
Long CNTs 0.1	0.4	0.1	20
Short CNTs(COOH) 0.1	0.4	0.1	30
Short CNTs(COOH) 0.2	0.4	0.2	30
Long CNTs(OH) 0.04	0.4	0.04	30
Long CNTs(OH) 0.1	0.4	0.1	20

4. EXPERIMENTAL RESULTS AND MICROSTRUCTURAL CHARACTERIZATION

4.1 Testing Fixture

A custom made flexural testing apparatus [100] was needed due to the small scale of the specimens (beams) and to capture accurately the stress-strain behavior of the nanocomposites. The testing apparatus used was a three-point bending testing frame made of 6061 aluminum, of dimensions (170 mm × 25 mm × 114 mm), providing a flexural span of 160 mm. Fig. 18 shows the frame dimensions. The frame was fixed with an actuator (NSA12 from Newport Corp.), a load cell (from Strain Measurement Devices of 2.5 kg capacity) to measure the applied force, and a linear variable differential transformer (LVDT) (from Macro Sensors) to measure the displacement (deflection) at mid-span of the beam, connected to a data acquisition board DAQ (from National Instruments), and a micro-stepping controller (from Newport NSC200) to control and smooth the actuator motion.

A LabView program [103] was written to control the actuator and to record the measured load vs. displacement data. The testing frame setup showing the testing frame components is shown in Fig. 19.

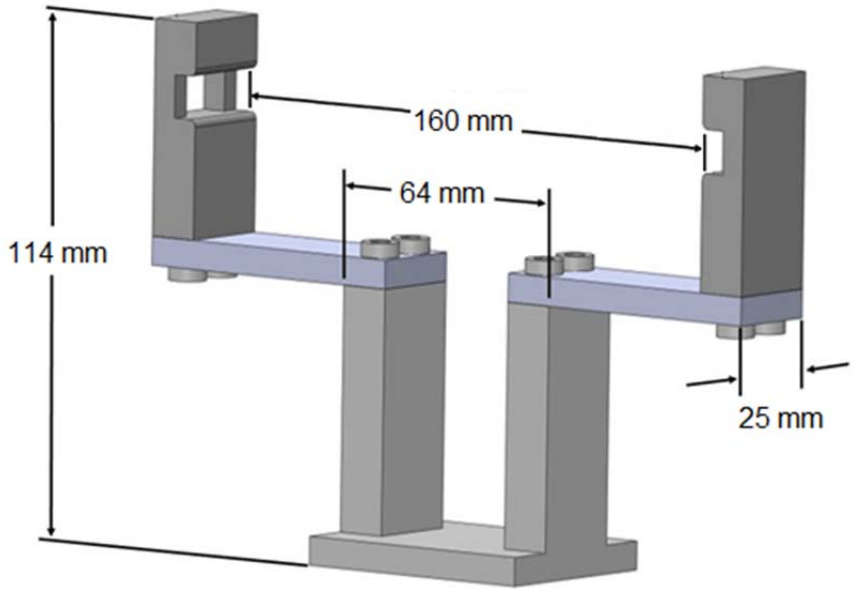

Fig. 18. Three-point bending testing frame dimensions (picture courtesy of Bryan M. Tyson).

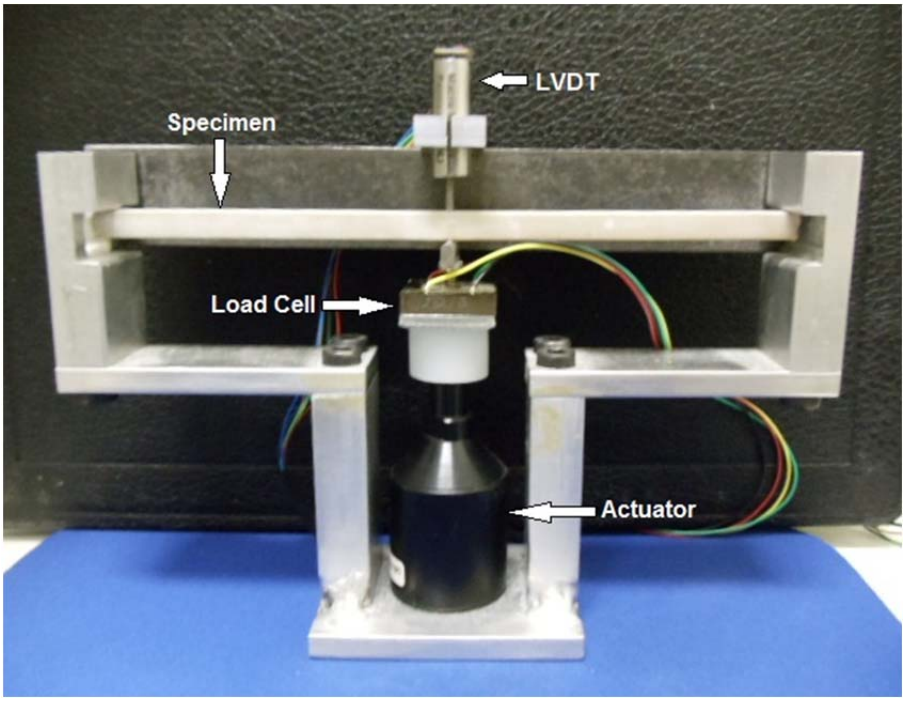

Fig. 19. Testing frame setup, showing the aluminum frame, the specimen, the LVDT, the load cell and the actuator.

The LVDT has a very high resolution that allows it to capture micro displacements with an error tolerance of ±0.002 mm and maximum displacement range of 5.0 mm. The load cell has a relatively small load capacity of 24.5 N in order to have high resolution for the load data recorded. The Newport NSA12 actuator has a motion speed range of 0.001 mm/s to 0.9 mm/s. This will allow higher accuracy for static loading (very low loading speed) which will allow measuring the mechanical properties like elastic modulus, strength and toughness. Fig. 20 shows the actuator and the load cell with a loading bar on the top to uniformly distribute the applied force across the beam width at mid-span.

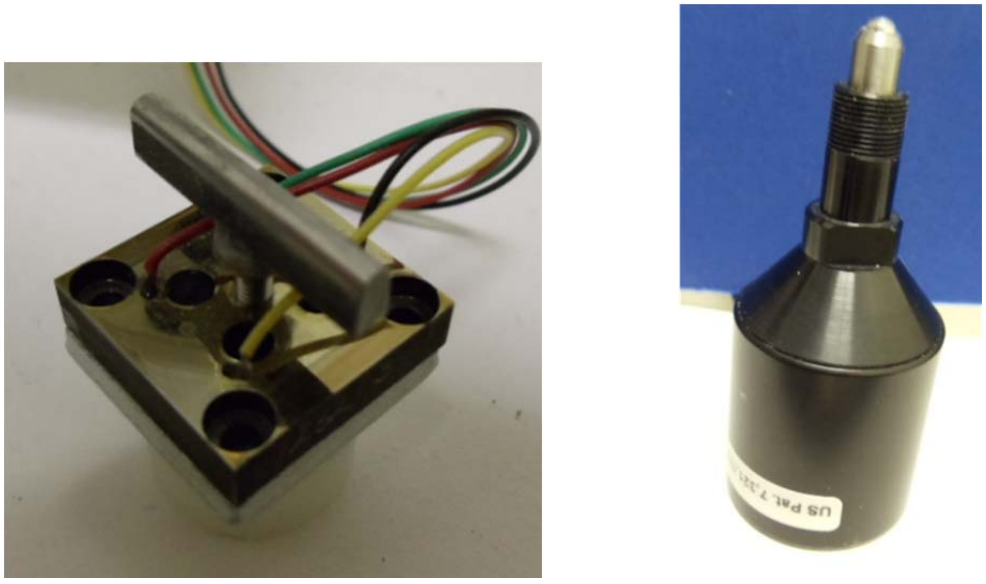

Fig. 20. The 2.5 kg capacity load cell, with a small loading bar welded at top of adjustable screw (left). The Newport NSA12 actuator (right).

All tests were performed at a loading speed of 0.003 mm/s. More information about the actuator specifications are shown in Table 5. The simply supported beams

under three-point bending was loaded from bottom by the actuator, and the load cell will be mounted on the actuator pushing the specimen up (cambering up), while the LVDT was measuring the deflection of the beam at mid-span from top. For more information about the testing fixture refer to the descriptions and discussions in [100].

Table 5
Newport NSA12 Actuator Specifications.

Feedback	Open loop, no encoder
Axial Load Capacity (N)	25
Maximum Speed (mm/s)	0.9
Travel Range (mm)	11
Minimum Incremental Motion (μm)	0.2
Drive Screw Pitch (mm)	0.3048

4.2 Data Analysis

The loads in (kg) and displacements in (mm) were measured and recorded by the software and then converted to stresses and strains using Euler-Bernoulli elastic beam theory, in order to calculate some mechanical properties.

$$\sigma_i = \frac{LC}{4I} \cdot F_i \qquad \text{and} \qquad \varepsilon_i = \frac{12C}{L^2} \cdot y_i \tag{1}$$

where σ_i is the flexural tensile stress at the extreme tension fibers of the beam at each load step. ε_i is the elastic strain at the extreme tension fibers of the beam at each load step. L is the span length of the beam (160 mm). C is the half-depth of the beam

cross-section ($6.5/2\ mm$). I is the second moment of area of the square cross-section beam ($6.5^4/12\ mm^4$). F_i is the applied force measured by the load cell at mid-span length at each load step (N), and y_i is the displacement measured by the LVDT at mid-span length at each load step (mm).

Data were analyzed and stress-strain diagrams were generated using Matlab software and Microsoft Excel spread sheets. The Excel software was used to generate the stress-strain diagrams and all the statistical analysis; the mean value, standard deviation and standard error of the mean. Matlab was used for curve fitting and smoothing. The modulus of toughness - "toughness"- of the beams was calculated by integrating the stress-strain curve function (total area under the stress-strain diagram).

4.3 Mechanical Properties

For each different batch, three to five replicates have been tested at each testing day of 7, 14 and 28 days from casting day. Stress-strain diagrams have been obtained for each single sample. The average value for the replicates for each batch has been computed for four major mechanical characteristics: The maximum flexural strength, ultimate strain capacity (ductility), modulus of elasticity (Young's modulus), and modulus of toughness. The results for the different nine nanocomposite batches have been compared along with the plain cement (reference) batch.

Examples of long vs. short non-functionalized MWCNTs composites stress-strain curves at age of 7 days are shown in Fig. 21 along with the plain cement reference

sample. The material behaves linearly till fracture, and both the long and short nanocomposites at different concentrations showed an increase in both the strength and ductility.

Most of the nanocomposites showed a change in the material characteristics at age of 14 days as seen in Fig. 22. The plain cement stress-strain curve is almost linear, similar to the 7 days behavior. However, most of the nanocomposites show softening and multi-peak behavior. After the first crack, the material softens or yields in some cases, and sometimes shows gradual increase in the strength to become higher than the first-crack strength. This behavior clearly indicates the CNTs pull-out action, which increases the composite ductility and toughness.

Fig. 23 shows examples of the behaviors after 28 days. The plain cement sample showed softening and nonlinearity post-peak. The non-functionalized nanocomposites showed a significant increase in strength and ductility compared to the plain cement reference sample. The progressive CNTs pull-out can be seen in most of the samples and the increase in strength after the first-crack shows how the CNTs are effectively bridging the cracks and enhancing the mechanical properties of the material.

Examples of long vs. short functionalized MWCNTs composites stress-strain curves are shown in Fig. 24, Fig. 25 and Fig. 26 for the results at 7, 14 and 28 days, respectively. Similar to the non-functionalized nanocomposites, most of the nanocomposites show a linear trend with a higher strength and ductility with respect to the plain cement reference sample. However, the 0.04% Long MWNT (OH) at 7 days showed softening and nonlinearity in the material with multi-peak behavior, it has low

strength and high ductility compared with the plain cement reference sample. Similar general trend between the functionalized and non-functionalized nanocomposites at ages of 14 days and 28 days was seen. Multi-peak behavior and increase in the strength after the first-crack drop is clearly noticed. This indicates how CNTs can improve the mechanical properties of the cement paste by effectively bridging the cracks and increasing the toughness by the progressive tubes pull-out. Some of the nanocomposites showed a linear behavior with a brittle failure at a higher strength and ductility comparing to the plain cement sample.

More details on the comparison between long and short MWCNTs nanocomposites mechanical properties are discussed in the following subsections.

The stress-strain diagrams for all the samples of all different batches are shown in the attached appendix.

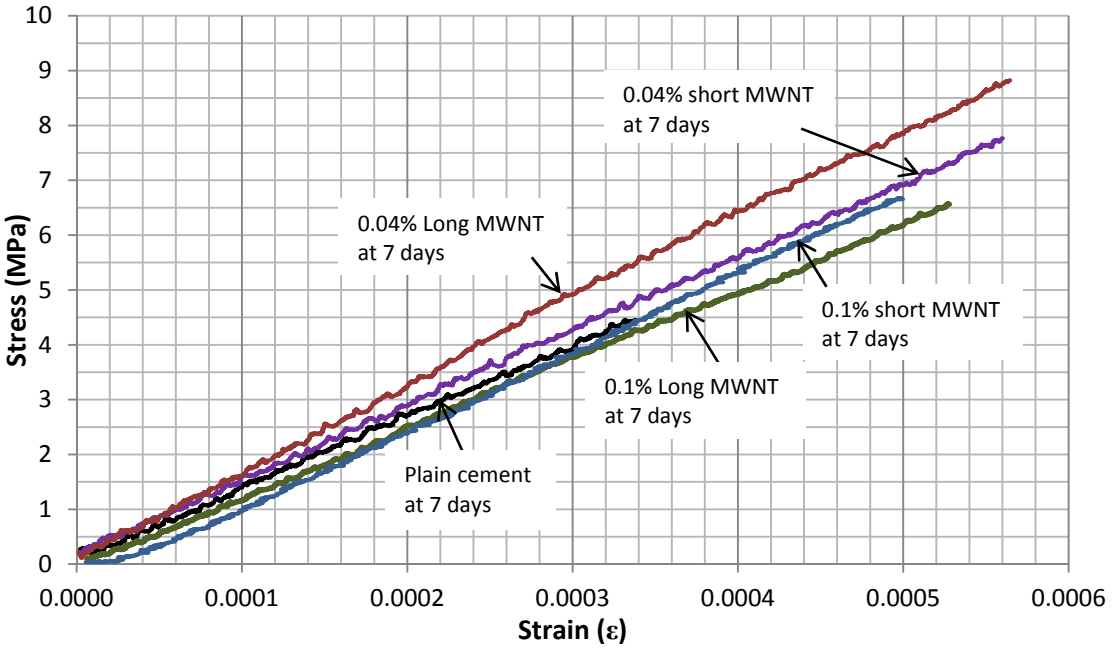

Fig. 21. Example of stress – strain curve for the plain cement and the non-functionalized short and long MWCNTs specimens at age of 7 days.

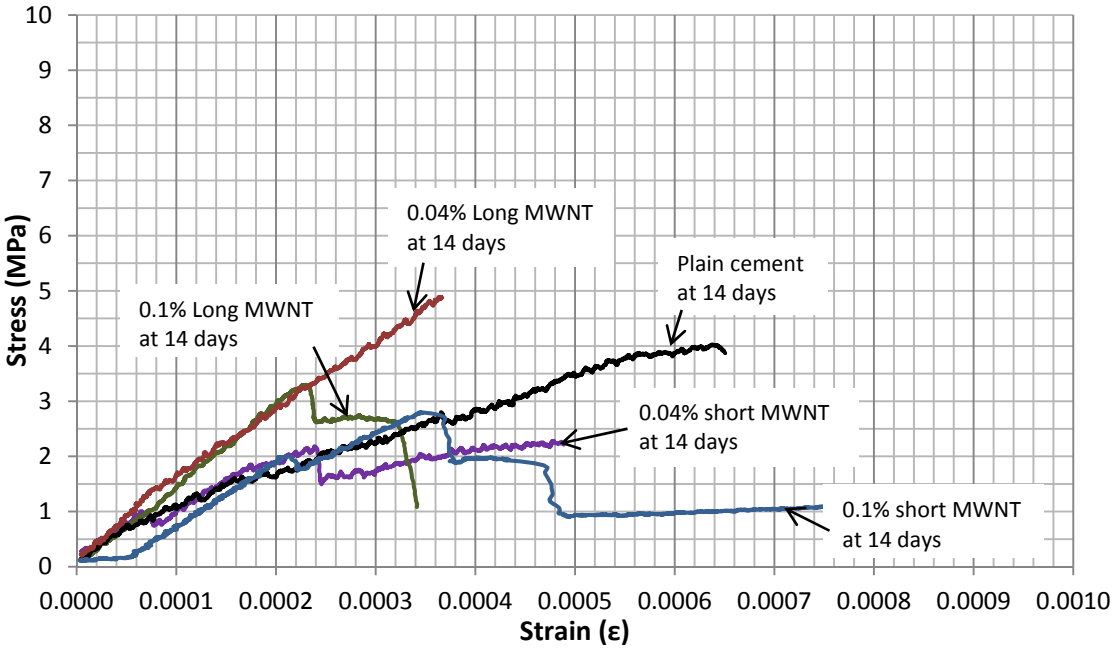

Fig. 22. Example of stress – strain curve for the plain cement and the non-functionalized short and long MWCNTs specimens at age of 14 days.

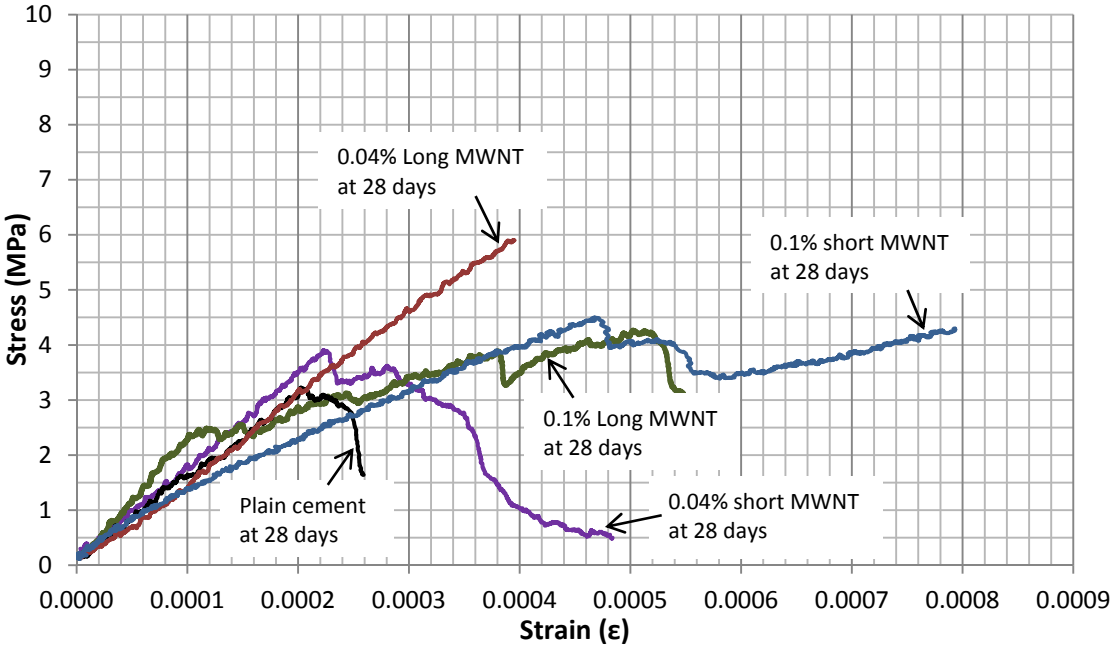

Fig. 23. Example of stress – strain curve for the plain cement and the non-functionalized short and long MWCNTs specimens at age of 28 days.

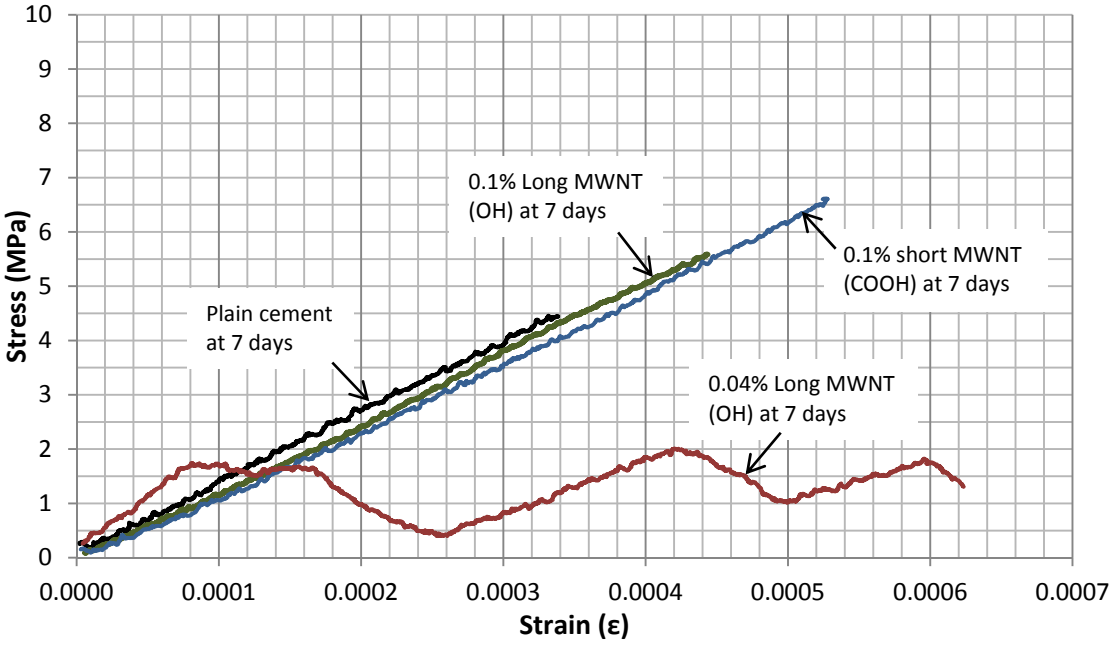

Fig. 24. Example of stress – strain curve for the plain cement and the functionalized short and long MWCNTs specimens at age of 7 days.

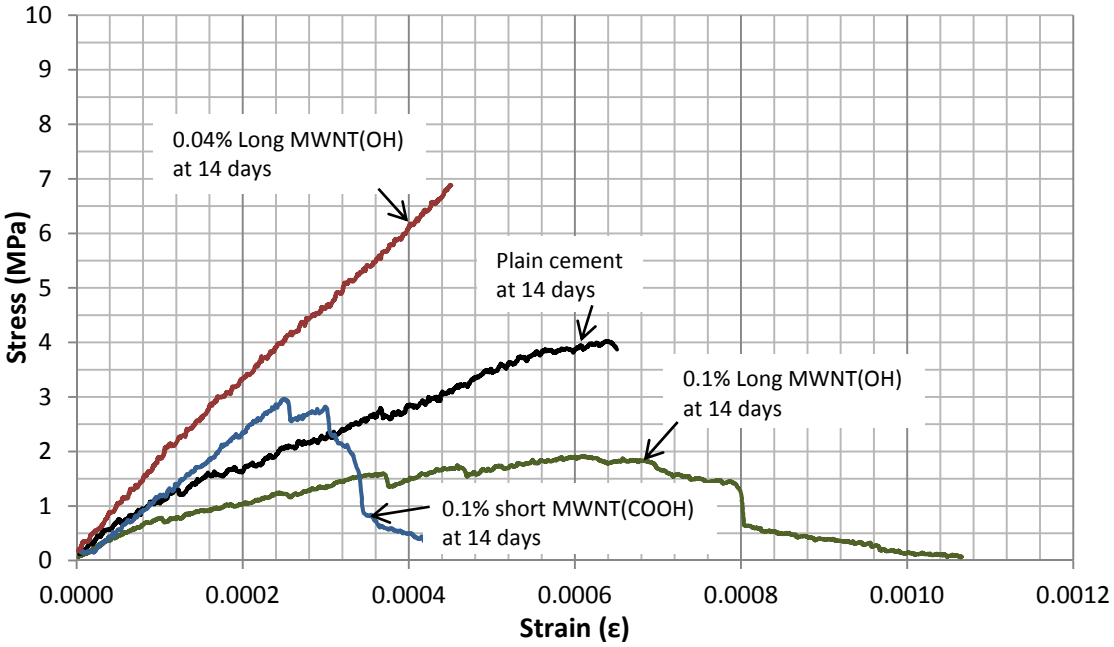

Fig. 25. Example of stress – strain curve for the plain cement and the functionalized short and long MWCNTs specimens at age of 14 days.

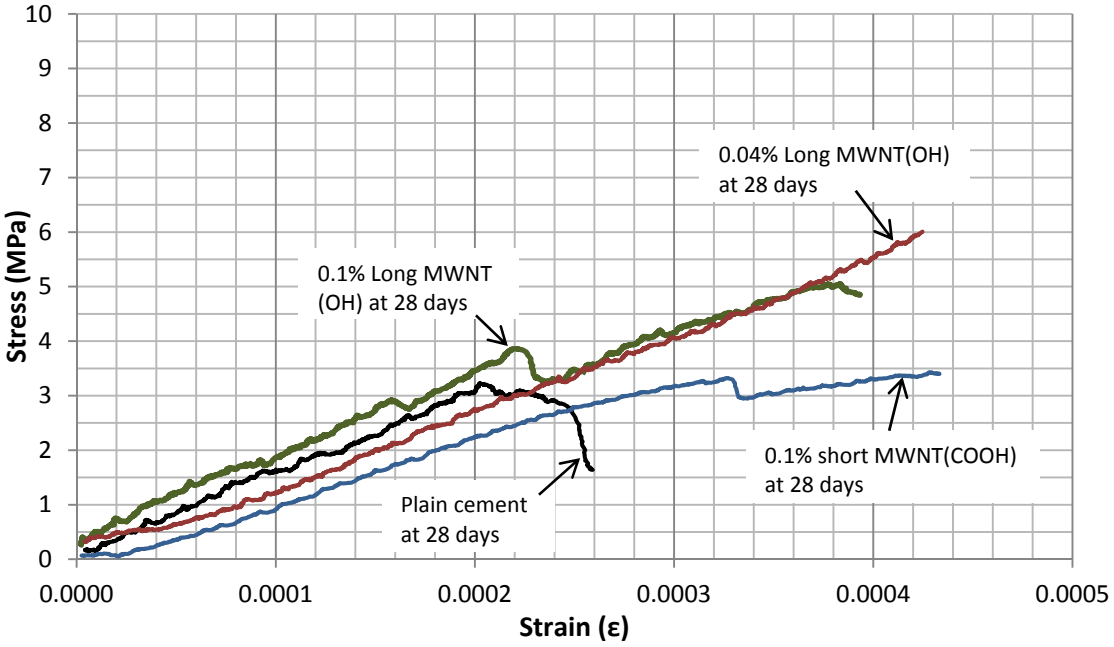

Fig. 26. Example of stress – strain curve for the plain cement and the functionalized short and long MWCNTs specimens at age of 28 days.

4.3.1 Long vs. Short Non-functionalized MWCNTs Nanocomposites

In this section, a detailed analysis for the data obtained from the mechanical testing will be discussed, comparing the four mechanical properties of the long and short non-functionalized MWCNTs nanocomposites with respect to the plain cement (reference) specimen. Summary tables for the average values of all different batches results are shown in Table 6 to Table 9 for average ultimate flexural strength, average ultimate strain, average modulus of elasticity and average modulus of toughness, respectively.

Table 6
Average ultimate flexural strength for the functionalized and the non-functionalized MWCNTs test specimens (MPa).

	Day		
Specimen	7	14	28
Plain cement (Reference)	4.50	4.51	3.22
Short CNTs 0.04	7.49	3.49	3.77
Short CNTs 0.1	5.19	2.39	4.36
Short CNTs 0.2	2.76	3.26	11.87
Long CNTs 0.04	5.47	5.64	4.94
Long CNTs 0.1	6.10	2.96	5.30
Short CNTs(COOH) 0.1	6.36	2.89	4.02
Short CNTs(COOH) 0.2	9.54	2.79	1.96
Long CNTs(OH) 0.04	1.37	6.82	5.88
Long CNTs(OH) 0.1	5.35	1.59	3.70

Table 7
Average ultimate strain capacity for the functionalized and the non-functionalized MWCNTs test specimens (%).

	Day		
Specimen	7	14	28
Plain cement (Reference)	0.0339	0.0603	0.0414
Short CNTs 0.04	0.0511	0.0498	0.0520
Short CNTs 0.1	0.0471	0.0894	0.0651
Short CNTs 0.2	0.0780	0.1040	0.0635
Long CNTs 0.04	0.0460	0.0539	0.0318
Long CNTs 0.1	0.0520	0.0401	0.0430
Short CNTs(COOH) 0.1	0.0471	0.0634	0.0409
Short CNTs(COOH) 0.2	0.0736	0.0453	0.0476
Long CNTs(OH) 0.04	0.0652	0.0471	0.0440
Long CNTs(OH) 0.1	0.0448	0.0840	0.0459

Table 8
Average modulus of elasticity for the functionalized and the non-functionalized MWCNTs test specimens (GPa).

	Day		
Specimen	7	14	28
Plain cement (Reference)	13.69	10.47	14.38
Short CNTs 0.04	12.49	12.17	12.40
Short CNTs 0.1	15.45	10.77	15.20
Short CNTs 0.2	14.36	8.72	16.98
Long CNTs 0.04	11.83	11.43	15.25
Long CNTs 0.1	7.51	8.50	12.99
Short CNTs(COOH) 0.1	12.71	11.93	11.90
Short CNTs(COOH) 0.2	11.99	11.02	8.58
Long CNTs(OH) 0.04	13.87	15.78	17.30
Long CNTs(OH) 0.1	6.79	3.48	14.39

Table 9
Average modulus of toughness for the functionalized and the non-functionalized MWCNTs test specimens (kPa).

	Day		
Specimen	7	14	28
Plain cement (Reference)	0.758	1.524	0.589
Short CNTs 0.04	1.926	1.003	1.013
Short CNTs 0.1	1.142	1.158	1.790
Short CNTs 0.2	1.083	1.704	3.712
Long CNTs 0.04	1.401	1.623	0.875
Long CNTs 0.1	0.946	0.347	0.797
Short CNTs(COOH) 0.1	1.537	0.709	0.860
Short CNTs(COOH) 0.2	3.380	0.769	0.596
Long CNTs(OH) 0.04	0.520	1.700	1.362
Long CNTs(OH) 0.1	0.711	0.474	0.533

For comparison purposes, results for plain cement as well as the long and short non-functionalized MWCNTs nanocomposites are shown in Fig. 27 to Fig. 30 for average ultimate flexural strength, average ultimate strain, average modulus of elasticity and average modulus of toughness, respectively. The column charts include the standard error of the mean, which is a statistical measure for the deviation (error) from the true mean value ($\bar{x}$), taking into account the number of samples (n) for each data point. The standard error of the mean is the value of the sample standard deviation (σ) divided by the square root of the number of the samples (n), such that:

$$Std.\,Error_{\bar{x}} = \frac{\sigma}{\sqrt{n}} \tag{2}$$

At age of 7 days, most of the non-functionalized MWCNTs/cement composites showed an increase in the flexural strength, ductility and modulus of toughness when compared to the plain cement (reference) specimen. The highest improvement in the flexural strength was seen in the short 0.04% MWNT specimens with an increase of 66% compared to the plain cement specimen. The long 0.1% MWNT, short 0.1% MWNT and long 0.04% MWNT flexural strength have increased also by 35%, 15%, and 22%, respectively. The short 0.2% MWNT specimens showed a decrease in their flexural strength by 38% while it showed the highest improvement in the ductility (ultimate strain) with an increase of 130% with respect to the plain cement specimen. All specimens of different batches have shown an increase in the ductility.

The modulus of elasticity values for most of the specimens at age of 7 days were close to the plain cement sample. However, the short 0.1% MWNT and short 0.2% MWNT showed a slight increase 13% and 5%, respectively, compared to the plain cement sample. All nanocomposite specimens have shown an improvement in modulus of toughness. The highest improvement in modulus of toughness was provided by the short 0.04% MWNT with a significant increase of 154% compared to the plain cement sample.

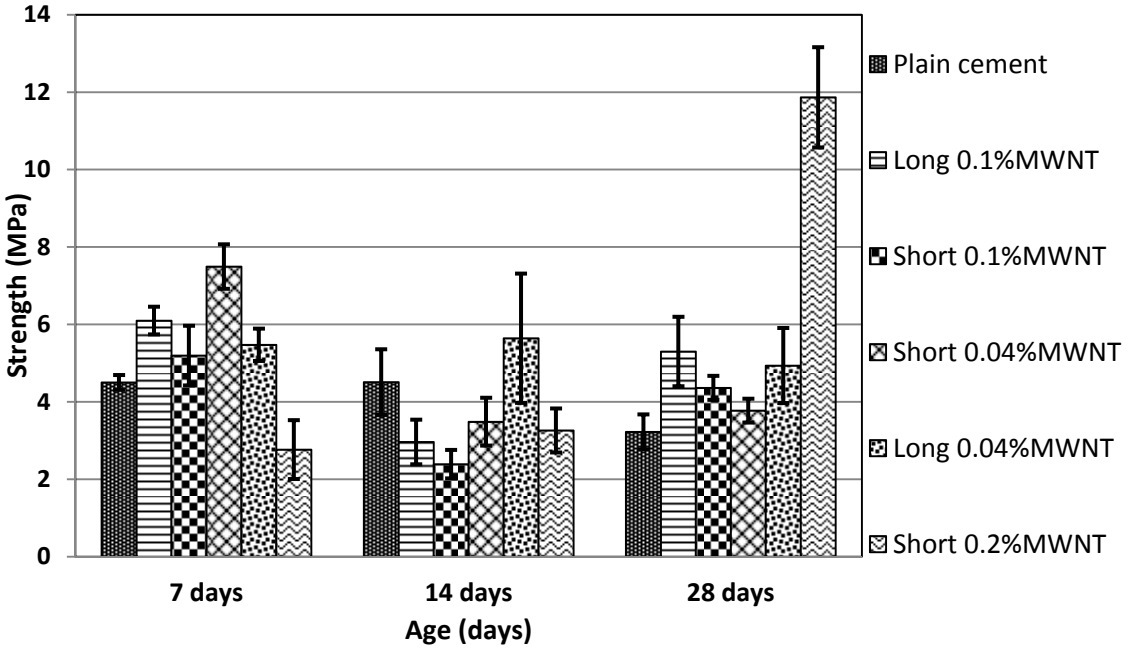

Fig. 27. Average flexural strength results for the plain cement and the non-functionalized short and long MWCNTs composite specimens with the standard error of the mean.

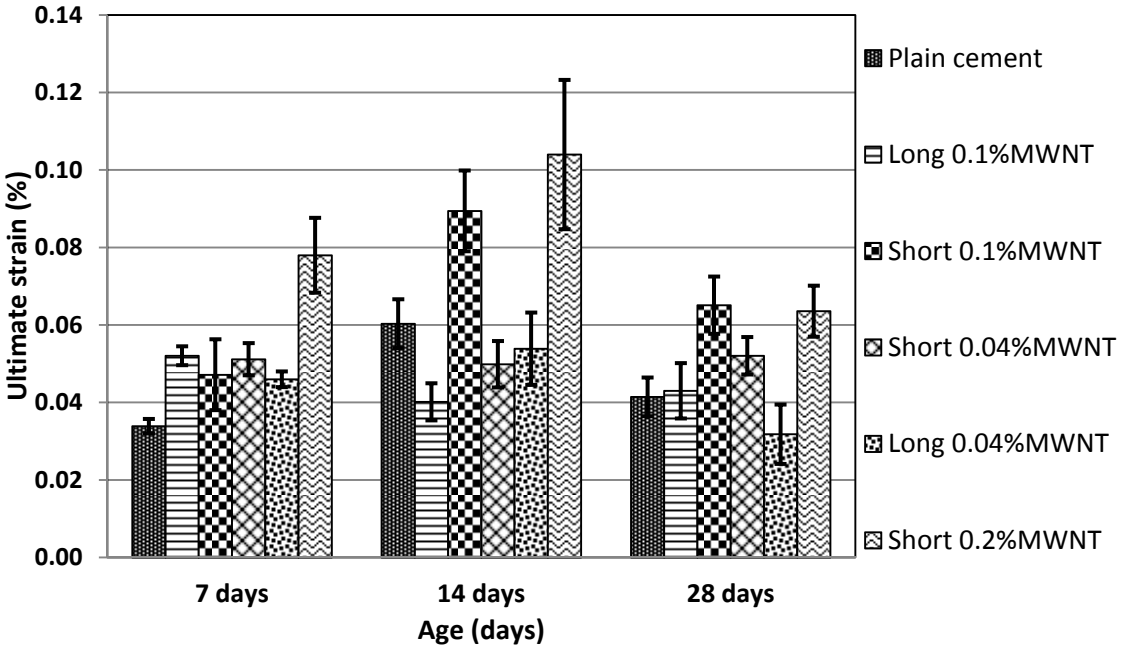

Fig. 28. Average ultimate strain results for the plain cement and the non-functionalized short and long MWCNTs composite specimens with the standard error of the mean.

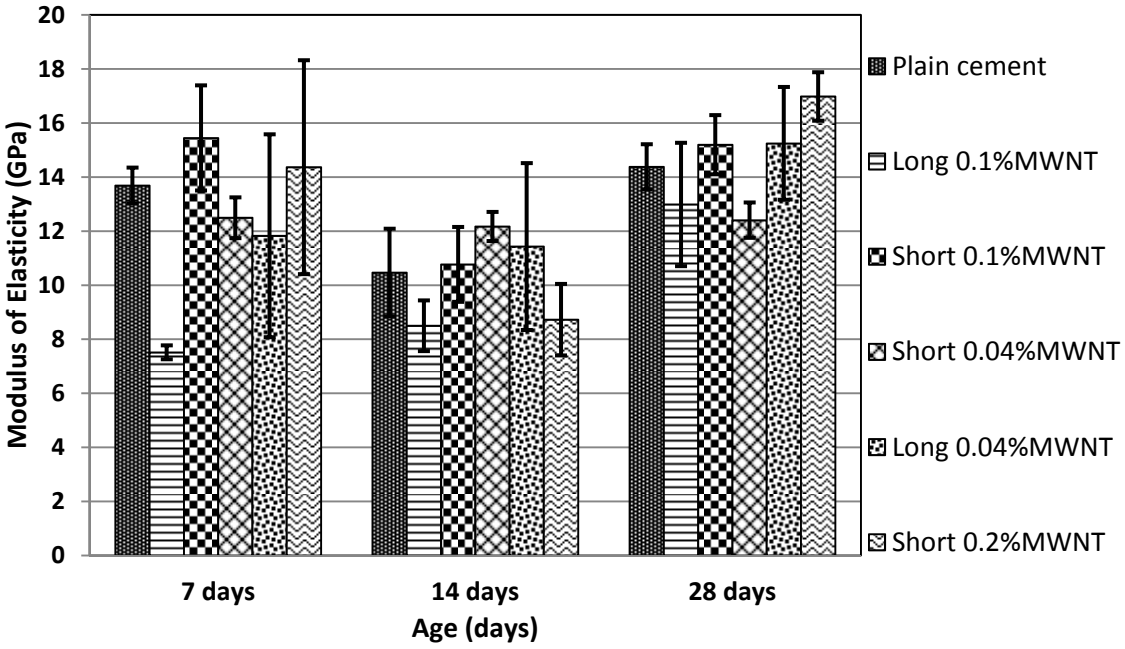

Fig. 29. Average modulus of elasticity results for the plain cement and the non-functionalized short and long MWCNTs composite specimens with the standard error of the mean.

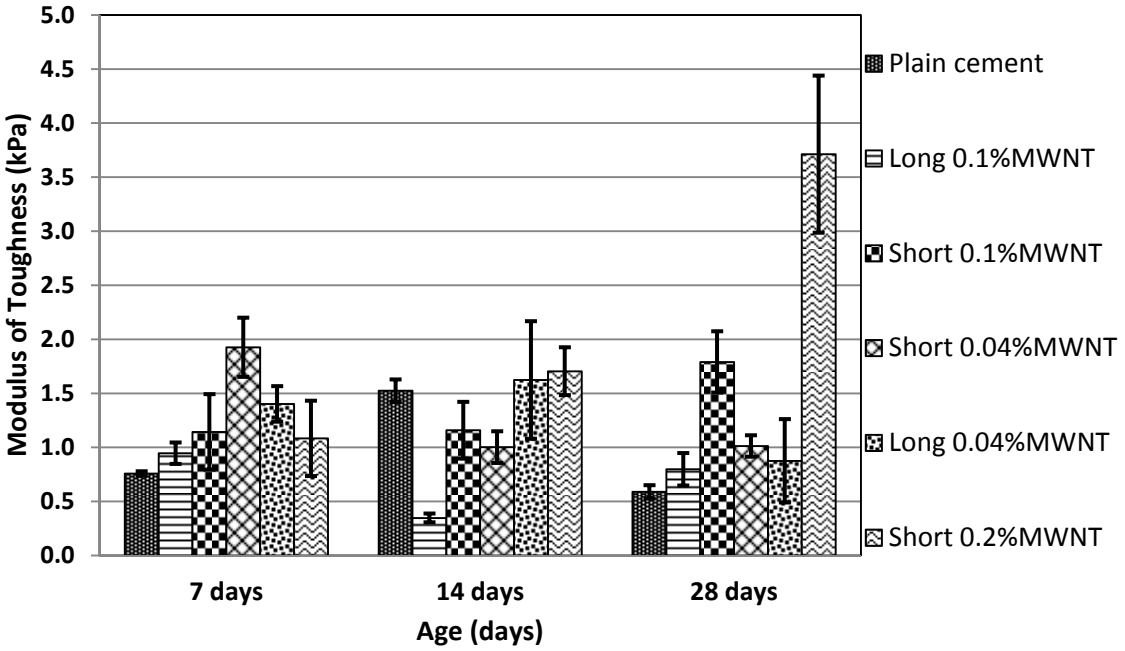

Fig. 30. Average modulus of toughness results for the plain cement and the non-functionalized short and long MWCNTs composite specimens with the standard error of the mean.

On the other hand, considerable changes in the behavior of the nanocomposites were observed at age of 14 days. Large drop in the flexural strength of most of the composites occurred, to be less than the plain cement sample strength, except for the long 0.04% MWNT that showed an increase in the average strength by 25% compared to the plain cement sample. The lowest flexural strength was recorded for the short 0.1% MWNT, with degradation of 89% with respect to the plain cement sample. Some of the nanocomposites showed a decrease in ductility, while some showed an increase. The highest ductility obtained after 14 days was for the short 0.2% MWNT with an increase of 72% from the corresponding value of the plain cement sample.

However, at age of 14 days, no significant changes in the general behavior of the composites regarding the modulus of elasticity values with respect to the plain cement samples, but in general most of the specimens showed a decrease in the modulus of elasticity compared to the values at 7 days. Degradation in modulus of toughness values was observed in many of the nanocomposites comparing to the plain cement sample, where large decrease is noticed in the long 0.1% MWNT with 339% degradation from the corresponding value of the plain cement sample.

After 28 days, all composites retrieved their strength values to become higher than the values at 14 days, and all of them showed higher strength than the plain cement sample. However, the short 0.2% MWNT showed a significant increase in the flexural strength, specifically increased by 269% compared to the plain cement sample value. The long 0.1%MWNT has also increased by 65%. Most of the nanocomposites showed a reduction in ductility in general, when compared to the ductility at 14 days. The highest

ductility at 28 days were for the short 0.1% MWNT and short 0.2% MWNT, with 86% and 81%, respectively, more than the plain cement sample. However, the short 0.04% MWNT showed almost a constant value for ductility from age of 7 days through age of 28 days.

All specimens showed an increase in their modulus of elasticity values at 28 days compared to 14 days values, and the short 0.2% MWNT has the highest increase of 18% compared to the plain cement sample. All the non-functionalized MWCNTs nanocomposites showed a significant improve in modulus of toughness compared to the plain cement sample. Due to the large increase in the flexural strength of the short 0.2% MWNT, it has recorded the highest modulus of toughness value, with an increase of 530%, and the short 0.1%.MWNT improved by 204% compared to the plain cement (reference) sample at age of 28 days.

Generally, one can notice the same trend for the variation of flexural strength and modulus of elasticity with variation in age and MWCNTs concentration; increase at age of 7 days, decrease at age of 14 days, and then increase at age of 28 days. On the other hand, the same trend of variation in the ductility and toughness is seen with variation in age and MWCNTs concentration; low values at age of 7 days, increase at age of 14 days, and then decrease at age of 28 days. Generally, an increase in strength corresponds to an increase in ductility and toughness. Moreover, generally, the short MWCNTs lead to better enhancements in the stress-strain response. This might be attributed to the better dispersivity of the short CNTs within the cement paste as compared to the long CNTs.

4.3.2 Long vs. Short Functionalized MWCNTs Nanocomposites

In this section, a detailed discussion on the results from the data obtained from the mechanical testing will be discussed, comparing the four mechanical properties of the long and short functionalized MWCNTs nanocomposites with respect to the plain cement (reference) specimen. Summary tables for the average values of all different batches results are shown in Table 6 to Table 9 for average ultimate flexural strength, average ultimate strain, average modulus of elasticity and average modulus of toughness, respectively.

For comparison purposes, results for plain cement as well as the long and short functionalized MWCNTs nanocomposites are shown in Fig. 31 to Fig. 34 for average ultimate flexural strength, average ultimate strain, average modulus of elasticity and average modulus of toughness, respectively. The four mechanical properties are shown at ages of 7, 14 and 28 days with the standard error of the mean.

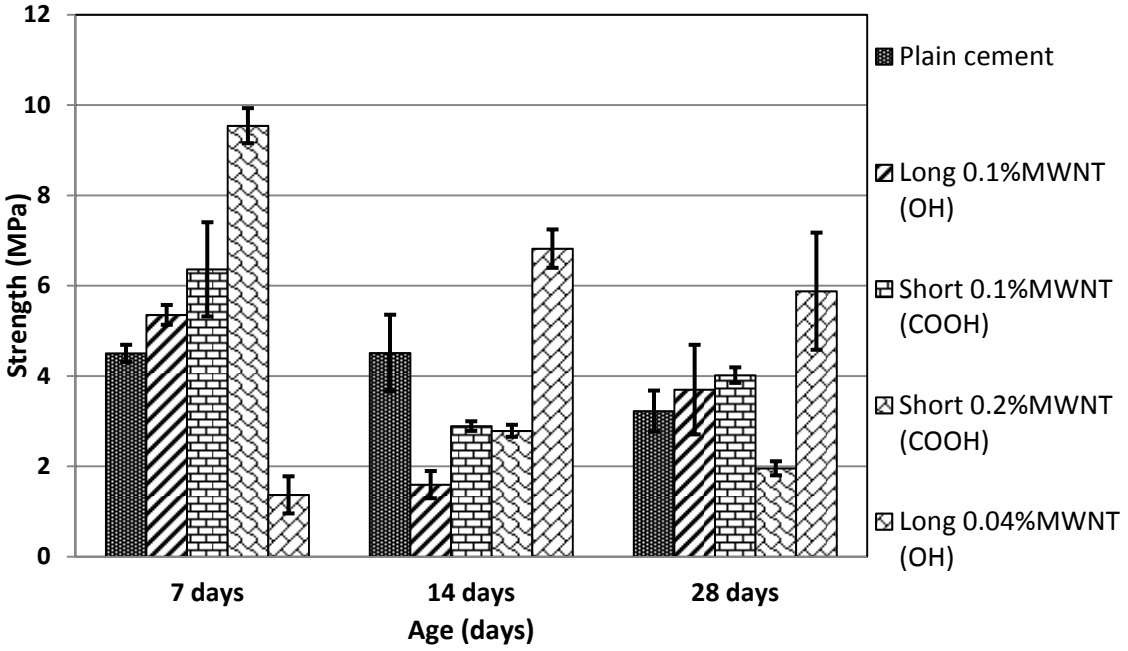

Fig. 31. Average flexural strength results for the plain cement and the functionalized short and long MWCNTs composite specimens with the standard error of the mean.

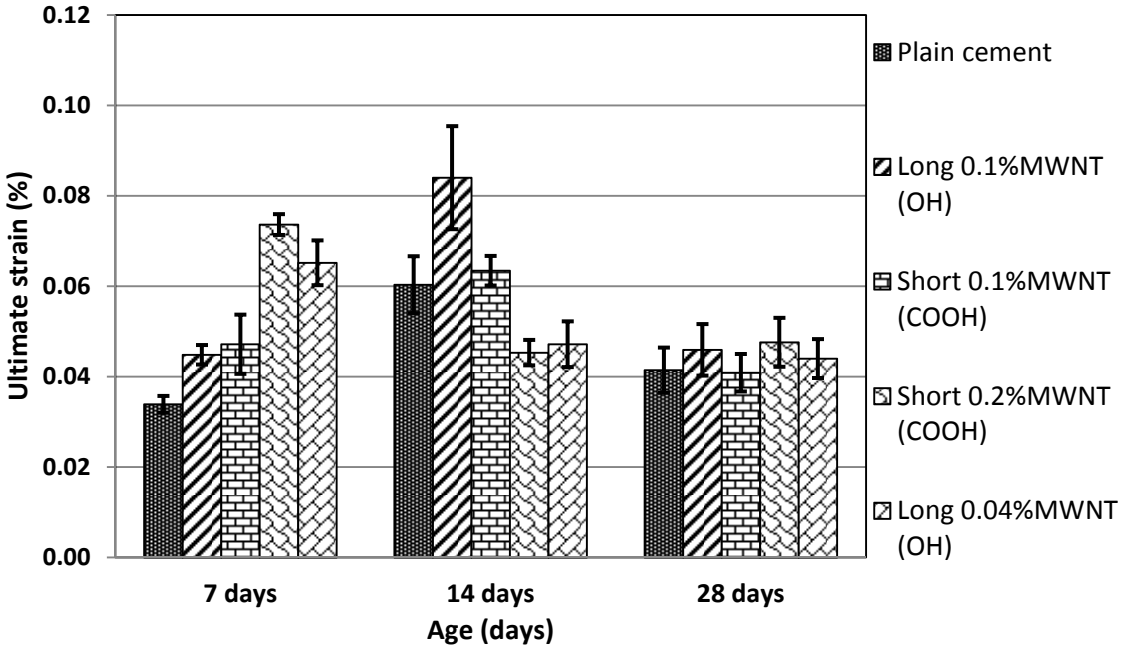

Fig. 32. Average ultimate strain results for the plain cement and the functionalized short and long MWCNTs composite specimens with the standard error of the mean.

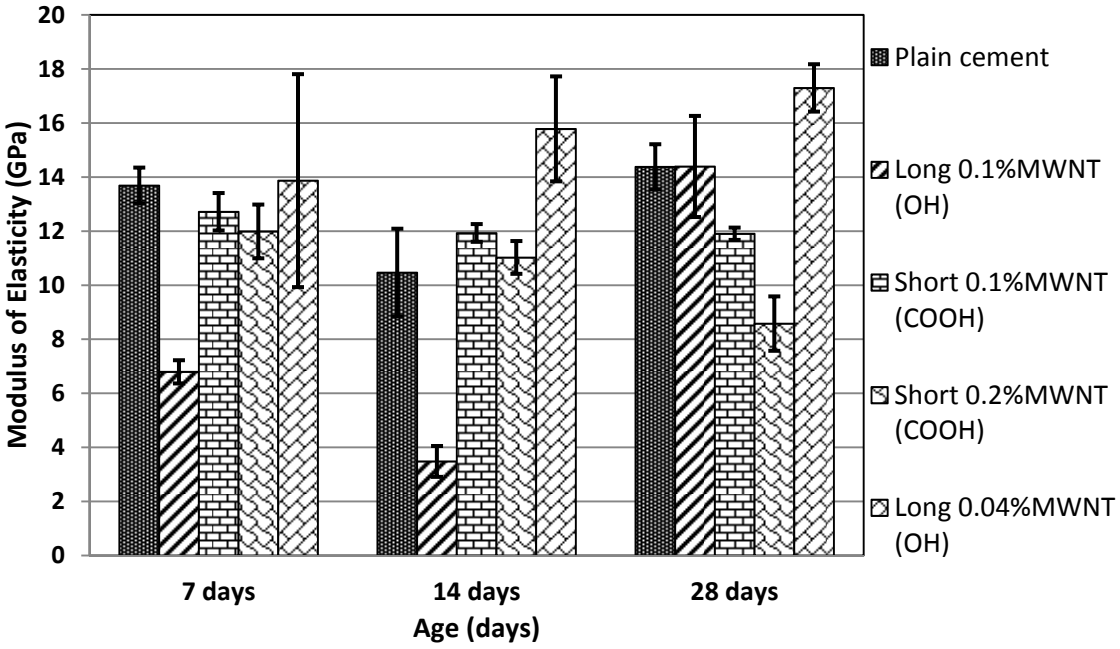

Fig. 33. Average modulus of elasticity results for the plain cement and the functionalized short and long MWCNTs composite specimens with the standard error of the mean.

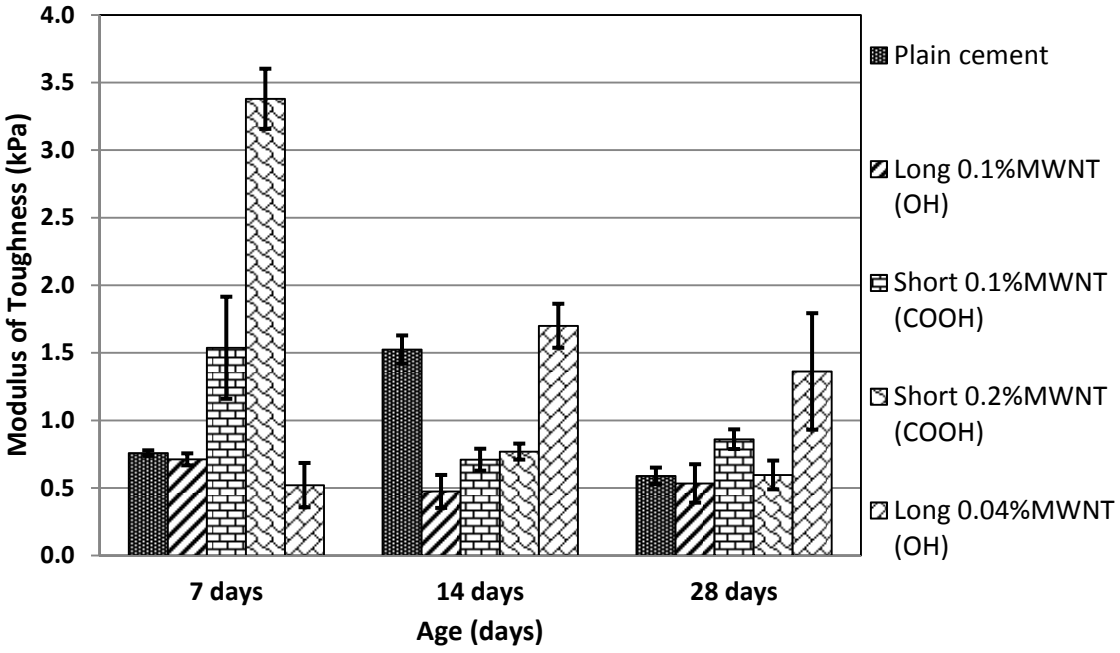

Fig. 34. Average modulus of toughness results for the plain cement and the functionalized short and long MWCNTs composite specimens with the standard error of the mean.

At age of 7 days, most of the functionalized MWCNTs/cement composites showed improvements in the flexural strength, ductility and some in modulus of toughness when compared to the plain cement (reference) sample. The highest improvement in the flexural strength was seen for the short 0.2% MWNT (COOH) specimens with increase of 112% compared to the plain cement specimen. The long 0.1% MWNT (OH) and the short 0.1% MWNT (COOH) flexural strength have also increased by 19% and 41%, respectively. The long 0.04% MWNT (OH) specimens showed a huge decrease in their flexural strength by 228% compared to the plain cement specimens.

All specimens of different batches have shown increase in the ductility. The highest ductility has been seen for the short 0.2% MWNT (COOH) and the long 0.04% MWNT (OH) specimens with an increase of 118% and 89%, respectively, with respect to the plain cement sample. The modulus of elasticity values for most of the specimens were close to the plain cement sample. However, the long 0.1% MWNT (OH) showed a decrease in the elastic modulus by 102%, compared to the plain cement (reference) sample. Only the short 0.1%MWNT (COOH) and short 0.2%MWNT (COOH) have shown improvement in modulus of toughness with increase of 103% and 346%, respectively, compared to the plain cement sample.

Considerable changes in the behavior of the composites were observed at age of 14 days. Large drop in the flexural strength of most of the nanocomposites occurred, to be less than the plain cement sample strength, except for the long 0.04% MWNT (OH) that showed an increase in the average strength by 51% compared to the plain cement

sample. The lowest flexural strength was recorded for the long 0.1% MWNT (OH), with degradation of 184% with respect to the plain cement sample. Some of the nanocomposites showed decrease in ductility, while some showed increase at 14 days. The highest ductility obtained after 14 days was for the long 0.1% MWNT (OH) with an increase of 42% from the corresponding value of the plain cement sample. The short 0.1% MWNT (COOH) showed a ductility close to the plain cement sample, while the short 0.2% MWNT (COOH) and the long 0.04% MWNT (OH) showed decrease in the ductility.

It is also noticed form Fig. 33 that, in general, no significant changes in the general behavior of the composites regarding the modulus of elasticity values with respect to the plain cement (reference) sample. However, the long 0.1% MWNT (OH) showed more degradation in modulus of elasticity, and the long 0.04% MWNT (OH) showed an increase, compared to the plain cement sample and to the 7 days values.

A significant degradation in modulus of toughness values was observed in most of the nanocomposites comparing to the plain cement sample. The lowest modulus of toughness is noticed in the long 0.1% MWNT (OH) with 222% degradation from the corresponding value of the plain cement sample. However, a significant increase in modulus of toughness is seen for the long 0.04% MWNT (OH) with respect to its value at 7 days.

When investigating the results at 28 days, some of the nanocomposites showed an increase in the flexural strength and some showed a decrease, when compared to the values at 14 days, but most of the nanocomposites results ended with a higher strength

than of the plain cement sample. The long 0.04% MWNT (OH) showed the highest flexural strength at 28 days, specifically with an improvement of 83% compared to the plain cement sample. All of the nanocomposites showed a higher ductility than the plain cement sample at 28 days. The highest ductility at 28 days was for the short 0.2% MWNT (COOH) and the long 0.1% MWNT (OH) with increase of 36% and 31%, respectively, compared to the plain cement sample. However, all of the nanocomposites ductility values were close to each other at 28 days. Only the long 0.04% MWNT (OH) has shown a significant increase in the elastic modulus compared to the plain cement sample by 20%. Unlike the non-functionalized MWCNTs nanocomposites, only the long 0.04% MWNT (OH) has shown a significant improvement in modulus of toughness by 131% compared to the plain cement (reference) sample. The rest of the nanocomposites showed a similar modulus of toughness to the plain cement sample, but the short 0.1% MWNT (COOH) showed an increase by 46% compared to the plain cement sample.

4.4 Results and Discussions

The experimental results obtained for different batches have shown clearly the variation in the mechanical properties between the functionalized non-functionalized short and long MWCNTs nanocomposites over time. It has been noticed that these nano-filaments at very small concentrations could extremely change and vary the cement paste behavior; hardening, softening, stiffening or weakening. In order to gain insight into the mechanical behavior of these MWCNTs nanocomposites in general, and to observe the real effects of the aspect ratio of the MWCNTs on the mechanical behavior of the cement nanocomposites, a different arrangement of the data presentation is provided in the following pages. This is done by comparing the same mechanical characteristic for long and short MWCNTs on two figures in the same page. The data point of the short 0.2% MWNT has been removed from this comparison -for strength and modulus of toughness- because it has much higher strength and modulus of toughness than all other batches.

4.4.1 Long vs. Short MWCNTs

For flexural strength, Fig. 35 and Fig. 36 show that at 28 days almost all of the MWCNTs composites have increased the flexural strength of the cement nanocomposites. At 28 days, the long MWCNTs have increased the flexural strength more than the short MWCNTs, although the short MWCNTs improved the flexural strength more at early ages of 7 days. This behavior is matching the expectations of that the longer fibers will need more energy (force) to be pulled out from the matrix. It is noticed also that at age of 28 days, the functionalized MWCNTs (OH) and MWCNTs

(COOH) at higher concentrations (mass fraction) would not effectively increase the flexural strength of the cement nanocomposites.

For the ultimate strain (ductility) of the nanocomposite beams, Fig. 37 and Fig. 38 show that over all ages, 7, 14 and 28 days, the ultimate strain (ductility) of the short MWCNTs nanocomposites is more than the ultimate strain of the long MWCNTs nanocomposites. This is not an expected behavior, since it was thought that the longer fibers have longer friction surfaces and would provide more ductility to the matrix. However, the author believes that this might be because of the dispersion variations between the long and short MWCNTs. Since a better level of dispersion can be achieved in the short MWCNTs, then a better distribution of the nanotubes in the composite material would be more critical to ductility than length (aspect ratio). Also, at 28 days, the short functionalized MWCNTs (COOH) did not help that much in improving the ductility, comparing to the short non-functionalized MWCNTs.

For the modulus of elasticity, Fig. 39 and Fig. 40 show a slightly better improvement for the long MWCNTs nanocomposites over the short ones, at age of 28 days. More consistent results were seen for the short MWCNTs nanocomposites over the long ones, at ages of 7 and 14 days.

For the modulus of toughness, Fig. 41 and Fig. 42 show a higher toughness for the short MWCNTs nanocomposites over the long MWCNTs nanocomposites, at age of 7 days. However, no significant differences in toughness general trend were noticed between the long and short MWCNTs nanocomposites at age of 28 days.

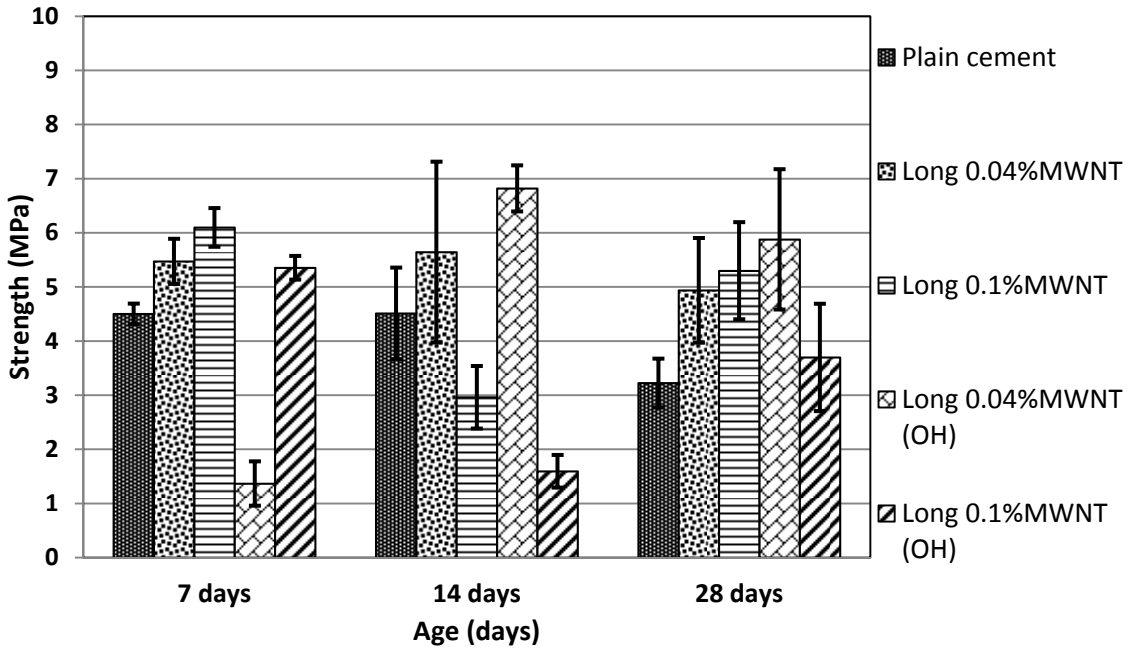

Fig. 35. Average flexural strength results for the plain cement and the long MWCNTs composite specimens with the standard error of the mean.

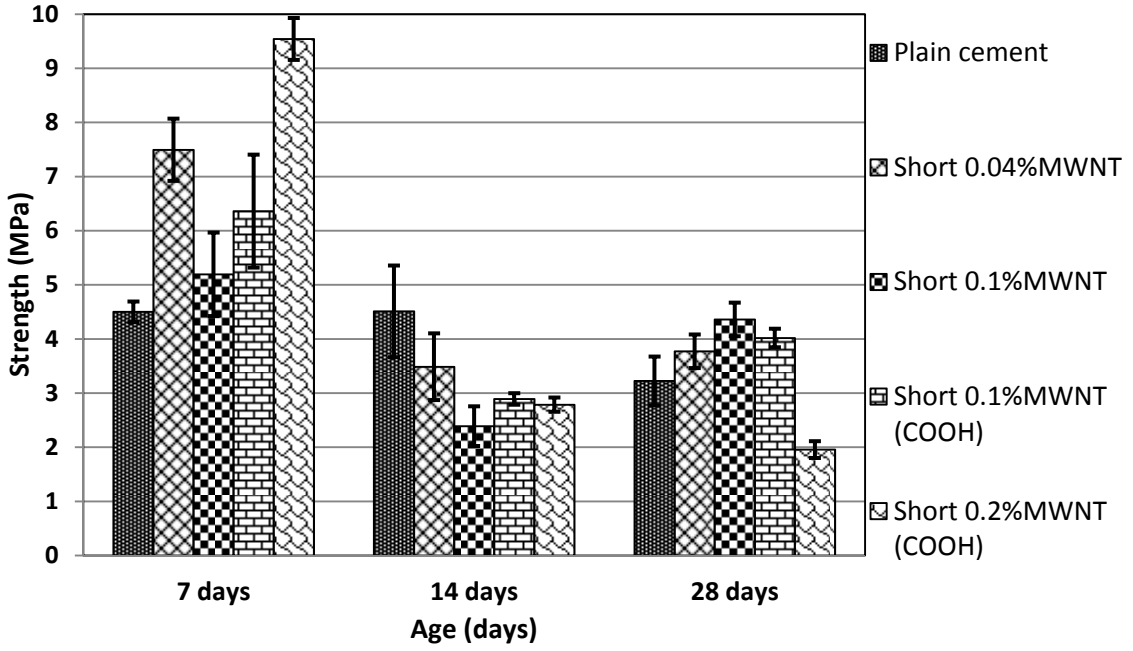

Fig. 36. Average flexural strength results for the plain cement and the short MWCNTs composite specimens with the standard error of the mean.

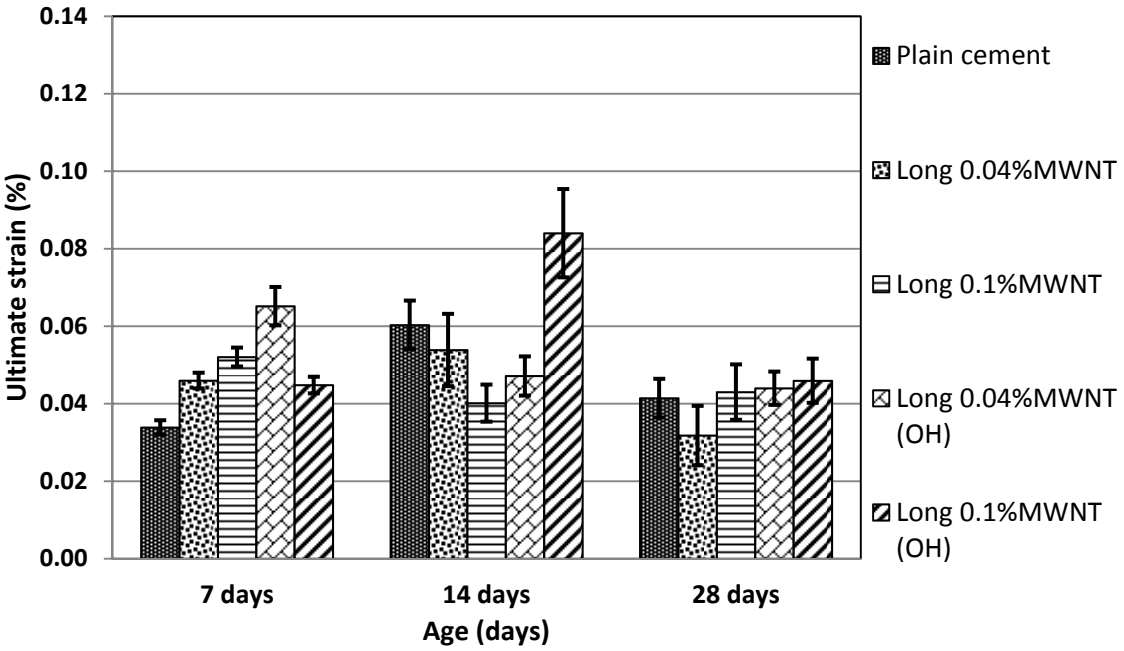

Fig. 37. Average ultimate strain results for the plain cement and the long MWCNTs composite specimens with the standard error of the mean.

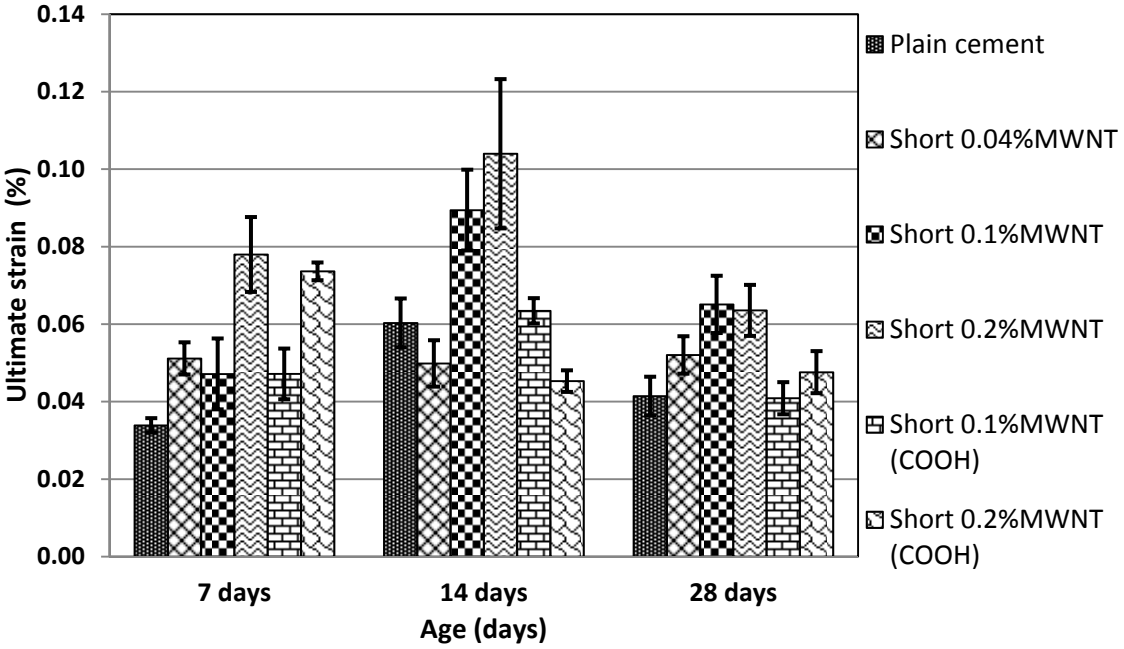

Fig. 38. Average ultimate strain results for the plain cement and the short MWCNTs composite specimens with the standard error of the mean.

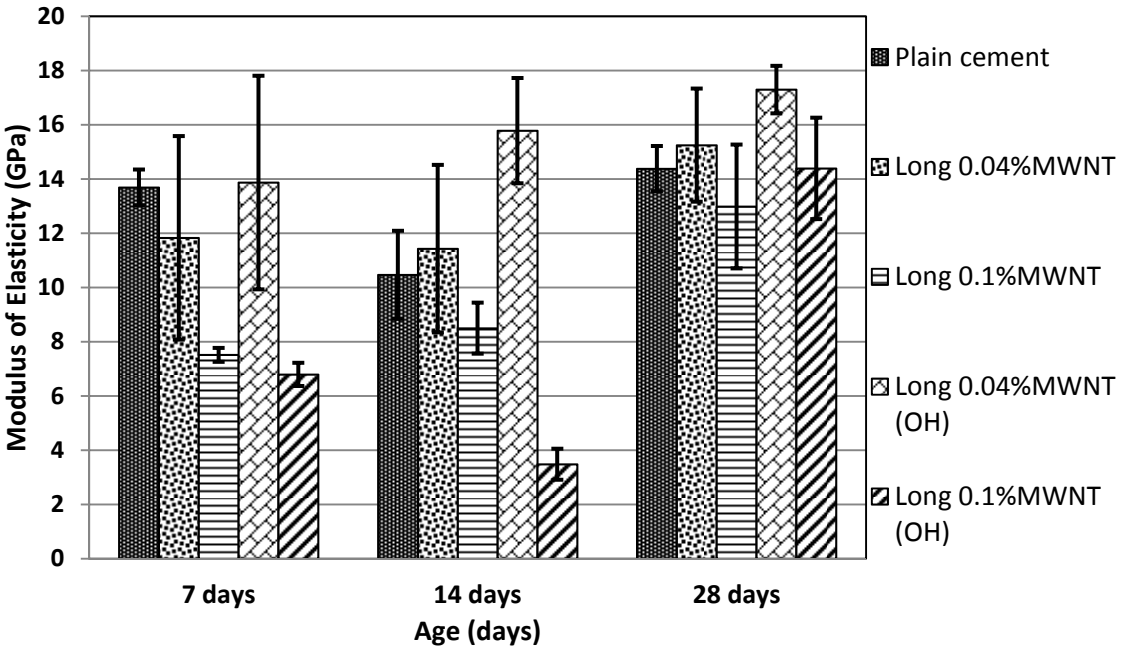

Fig. 39. Average modulus of elasticity results for the plain cement and the long MWCNTs composite specimens with the standard error of the mean.

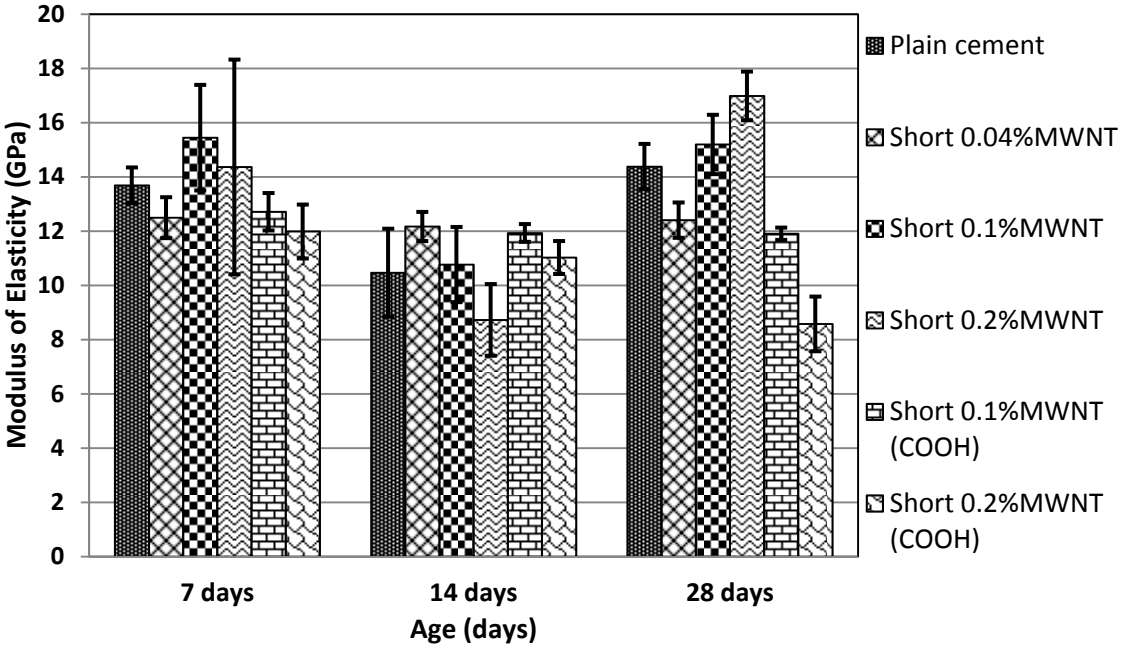

Fig. 40. Average modulus of elasticity results for the plain cement and the short MWCNTs composite specimens with the standard error of the mean.

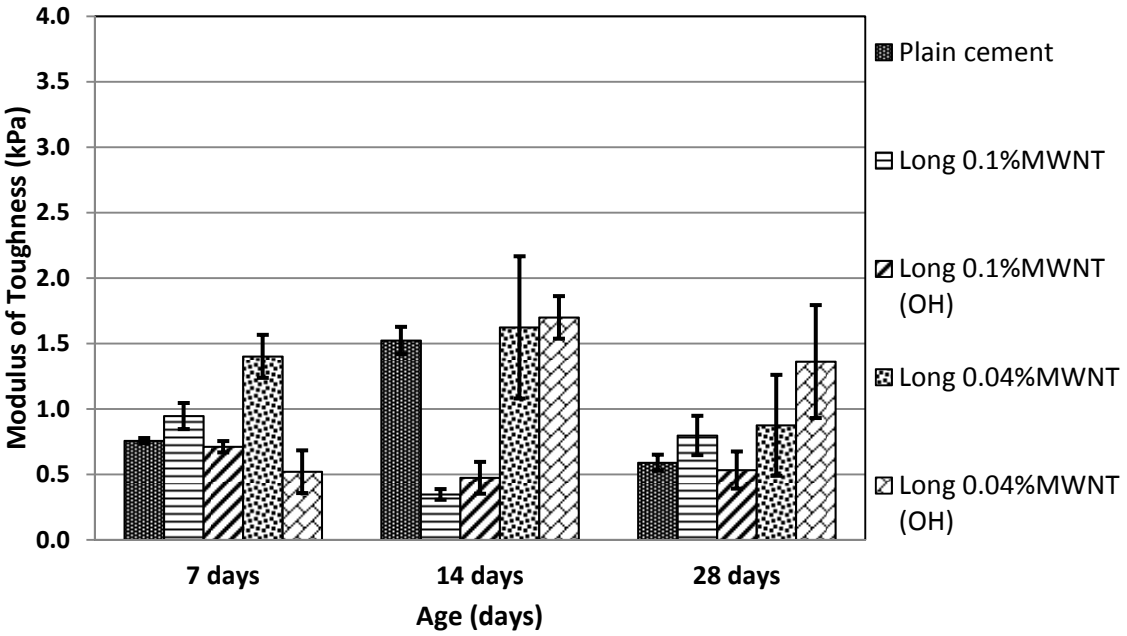

Fig. 41. Average modulus of toughness results for the plain cement and the long MWCNTs composite specimens with the standard error of the mean.

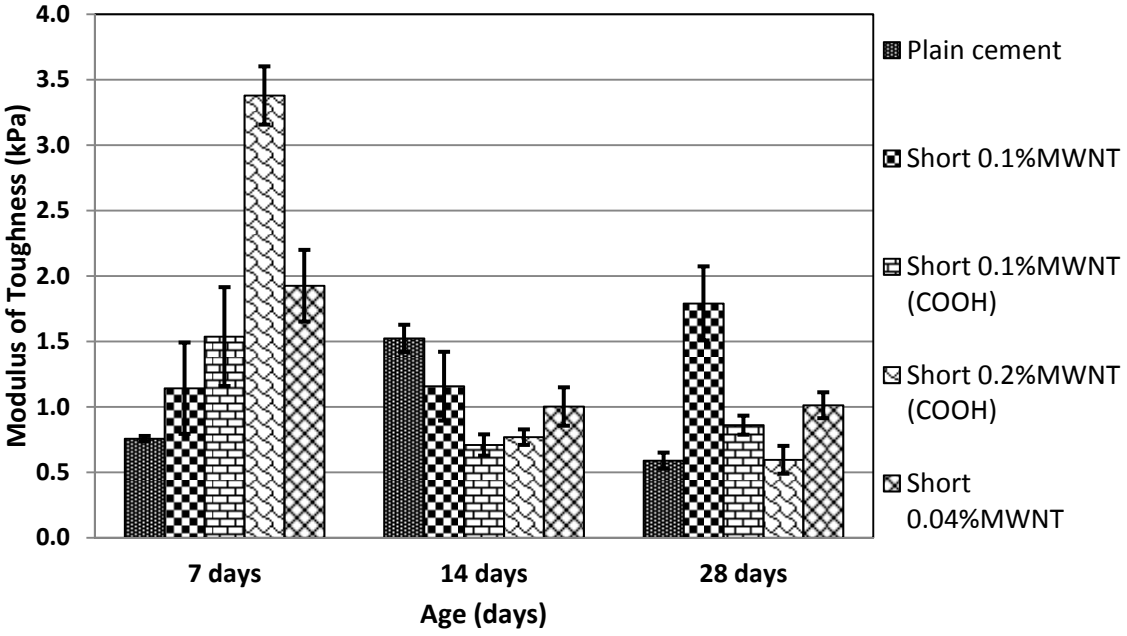

Fig. 42. Average modulus of toughness results for the plain cement and the short MWCNTs composite specimens with the standard error of the mean.

4.4.2 MWCNTs Pull-outs and Results Variability

Based on the observation of the stress-strain diagrams of all specimens, one can notice the multi-peaks behavior that is related to the CNTs pull-out from the cement paste matrix. This action is important to increase the fracture energy stored in the composite (strain energy), which will directly increase the strain capacity (ductility) and the modulus of toughness (fracture resistance). However, the pull-out process is not necessarily improving the strength, since some of the stress-strain curves showed a constant strength or yielding plateau after the first crack without any increase in the strength, while some other specimens showed an increase in the strength after the first crack, as seen in Fig. 22 to Fig. 26. This might be attributed to the dispersivity of the CNTs within the hydrated cement paste.

When investigating the amount of the deviations from the mean value (standard error of the mean), it has been noticed that although all the samples (replicates) of the same batch are identical and casted at the same time from the same mix, there are -in many cases- a noticeable variability in the results from one sample to another of the same composite. This could be due to the size of the specimens and the uniformity of the mixture. The small size of the specimens (beams) would make them more sensitive (size effect) to the existence of any small impurities, like air bubbles or small voids. On the other hand, the uniformity of the distribution of the MWCNTs within the aqueous solution does not guarantee a uniform distribution of the nano-filaments within the cement paste composites, hence the stresses distribution in the cross-sections along the

composite beams length will not be uniform, and will cause variability in the flexural behavior from sample to sample.

4.4.3 Weakening due to Functionalization

On the other hand, many hypotheses were proposed especially to explain the degradation of the functionalized CNTs nanocomposites when compared to the non-functionalized CNTs composites behavior. For example, Musso, et al. [104], reported that the degradation in the flexural strength in many specimens could be related to decrease in the formation of the Calcium Silicate Hydrate (C-S-H), as one of the main products of the cement hydration. Calcium Silicate Hydrate (C-S-H) has many different chemical structures, for example [$Ca_5Si_6O_{16}(OH)_2 \cdot 4H_2O$] and [$Ca_5Si_6(O,OH)_{18} \cdot 5H_2O$]. C-S-H has the main contribution to the strength of the cement hydrate in different stages of hydration, and more details were discussed in [104] and [105]. Degradation in the compressive strength was noticed in composites with functionalized CNTs specimens. It has been shown by Musso, et al. [104] using thermo-gravimeter analysis (TGA), that less amount of C-S-H was produced in the composite with the presence of the functionalized CNTs in the composite.

Another hypothesis to explain the deterioration of the mechanical properties of the functionalized CNTs / cement composites is the excessive formation of ettringite hypothesis [61, 100]. Ettringite [$3CaO\_Al_2O_3\_3CaSO_4\_32H_2O$] is one of the typical products of the cement hydration. It is a needle shaped crystalline structure, which is produced be the hydration of the Tricalcium Aluminate (C_3A) with gypsum (which is

another component of the Portland cement used to control the hydration process and prevent the flash set of the cement paste). Naturally, ettringite expands and causes internal stresses that could lead to micro cracks in the matrix of the hydrated cement paste. Due to the acid treatment of the CNTs, sulfate residue could be left on the surfaces of the CNTs that are not perfectly washed. The existence of the sulfate will cause excessive formation of ettringite in locations near to the CNTs in the matrix. Hence, weakening the material surrounding the CNTs, and as a result, degradation in the composite mechanical properties. More details on ettringite at the microscopic scale will be provided in the next section.

4.4.4 Effect of the Cement Paste Curing Method and the Superplasticizer

The last point in this discussion is about the overall degradation in the mechanical properties (strength, ductility and toughness) of most of the nanocomposites and the plain cement specimen from age 14 days to age 28 days. As seen in Fig. 35 to Fig. 42, most of the specimens, including the plain cement, have shown a decrease in the mechanical properties at age 28 days with respect to age 14 days. This behavior is abnormal, since it is well-known that cement paste gain strength with time. Note that the curing method used for all specimens –including the plain cement- is submerging into lime water. This method for curing has been adopted for many years as a standard method of concrete/cement curing. Many of the researchers who worked on CNTs/cement composites have used this curing method too. This curing method will be the key to explain why this degradation occurred at 28 days, as discussed in the following paragraphs.

A possible explanation for the degradation of most of the nanocomposites at age of 28 days can be derived based on chemical point of view. Based on Mindess and Young, 1981 [106]; the main hydrate components in cement before hydration are Tricalcium Sillicate (C_3S) [$3CaO.SiO_2$], which typically forms about 55% of the cement weight, and it is responsible for the early strength of the cement paste hydrate and will continue for later age, and Dicalcium Silicate (C_2S) [$2CaO.SiO_2$], which typically forms about 25% of cement weigh, will be contributing to the strength at a later stage. Those two components react with water (H_2O) and form the C-S-H, which is a fine amorphous in structure and makes 50% to 65% of the volume of the hydrated cement paste, and mainly responsible for the strength of the cement paste. Another product of the hydration of the C_3S and the C_2S is Calcium Hydroxide (CH) [$Ca(OH)_2$].

Calcium hydroxide, (CH) in cement chemistry notations, is typically a crystalline structure which contributes indirectly in reserving the strength of the cement paste hydrate by reducing the porosity of the matrix, and filling the capillary pores within the cement paste matrix. A scanning electron microscope (SEM) image of the C-S-H and the CH within the cement paste matrix is shown in Fig. 43.

The author believes that leaching of Calcium Hydroxide [$Ca(OH)_2$] from the cement paste submerged into the lime water, would increase the porosity (capillary voids) of the matrix and hence degrade the mechanical properties of the cement paste. Carde, et al. [107] have shown experimentally that the compressive strength of plain cement paste of micro-cylinders (diameters of 10 mm to 30 mm) had degraded significantly due to the leaching process of Calcium Hydroxide. The degradation in the compressive strength for

a 10 mm diameter specimens, which is larger than the specimens in the current study, could reach 50% [107]. It has been proposed that leaching of $Ca(OH)_2$ from the external layers (leaching zone) of the plain cement paste specimens and the loss of Calcium [Ca] ions content due to the progressive decalcification of the C-S-H, have a major contribution in the degradation of the mechanical properties of the cement paste [108].

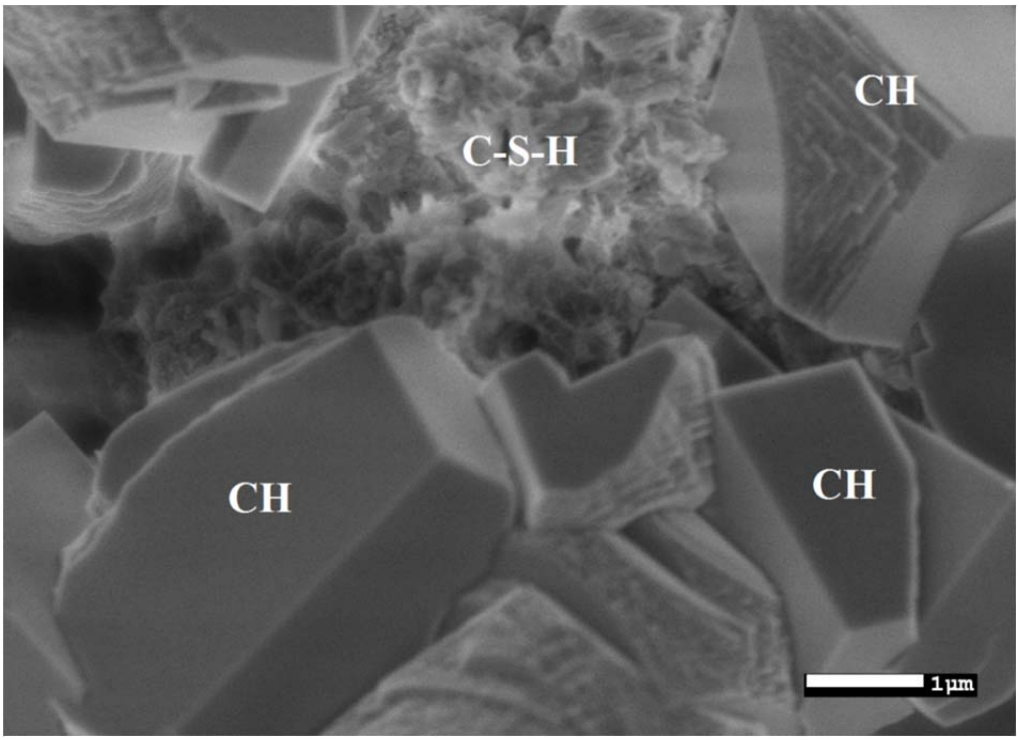

Fig. 43. SEM image showing the C-S-H and the crystalized CH of the cement paste.

Although the leaching kinetics is usually slow, but due to the special case in this study of testing a very small specimens' size (6.5 mm × 6.5 mm cross-section) with large surface area to volume ratio- as in our case-, this will expedite the leaching process due to the increase in the leaching area to total area ratio. The loss of the Calcium Hydroxide

creates macro-voids, since the size of the $Ca(OH)_2$ crystals is close to the size of the capillary porosity, hence effectively increase the overall matrix porosity, which will cause degradation in the mechanical properties, especially for small-sized specimens. In addition, the decrease in the C/S ratio in the C-S-H due to the progressive decalcification process of the C-S-H will increase the micro-voids and the porosity of the material, hence, deterioration in the mechanical properties [109-111].

Calcium hydroxide (CH) are layered structure, the calcium atoms are octahedral and the oxygen atoms tetrahedral in their coordinating, and the unit cell is hexagonal. Ideally, the CH forms hexagonal plates, but the morphology of the crystallization of the CH could vary based on the admixtures in the cement paste mix. Some studies suggested that there is amorphous CH in the calcium silicate pastes, but there is no convincing evidence that this is true, at least experimentally [112]. In cement pastes, TEM images showed small portions of the CH as cryptocrystalline and tightly bounded with the C-S-H [113, 114]. Methods used to determine the CH in hydrated cement paste include; quantitative X-ray diffraction analysis (QXDA), Thermal Gravimetric Analysis (TG), DTG, semi-isothermal DTG, thermal evolve gas analysis, DTA, differential scanning calorimetry (DSC), IR spectroscopy, image analysis of back scattered electron images, and other chemical extraction methods [112]. The dissolution of CH in water is exothermic (ΔH= -13.8 kJ/mol at 25°C) [115], so with the increase of the temperature the solubility decreases. The solubility at 25°C is 1.13 g CaO / l [116].

During the dissolution of the C_3S in cement pastes and the growth of the C-S-H, the concentrations of the Ca^{2+} and OH^- in the solution increases steadily until they reach

the saturation level and then the CH precipitation starts in significant amounts, resulting in drop in the concentrations of Ca^{2+} and OH^{-}. The smaller grains of C_3S, generally, react completely by dissolution and precipitation process during the acceleratory stage [112].

Crumbie et al. [117] tested concrete specimens with w/c ratio of 0.4 and 0.6. The specimens were cured in saturated CH solution after 24 hours of casting. The SEM back scattered images and the methanol-exchange porosity testing confirmed that the porosity and the permeability had increased near the surface. Also they reported that the surface region was depleted in CH content and leaching of the CH occurred although the specimens were immersed in saturated CH solution. When considering the leaching process, the attack or dissolution of CH and other components depends on the type and geometry of concrete, rate of water flow, temperature, and the concentration and types of solutes in the water. A solution of CO_2 (CO_2 per unit volume of the solution) can dissolve $CaCO_3$ or CH from the solid cement paste and free the calcium ions Ca^{2+}. Adenot and co-workers [108, 118] reported that the CH was the first to dissolve from the surface, after that the monosulfate and the ettringite, then the C-S-H is progressively attacked through decalcification.

In order to investigate the leaching effects due to lime water curing on the mechanical properties of cement paste, the author has fabricated a similar batch to the plain cement paste tested before. The new plain cement paste batch has the same size, geometry, procedure and components as the previous one, but this time was cured in a moisture room (closed room with constant humidity of 95% at temperature of $23^{o}C$). The

comparison results showed that higher strength, ductility, and toughness were obtained for the moisture curing approach. Fig. 44 to Fig. 47 show the improvements in the mechanical properties that reached 50% to 60% or more have been recorded for the moisture room curing compared to the lime water curing results. These results matches the experimental results reported by Carde, et al. [107] for similar cross-section area size.

It is noticed also how the plain cement paste batches with superplasticizer, showed a very lower mechanical properties when compared to the plain cement paste batches without any superplasticizer. This is could be due to the excess amount of water available for the cement hydration due to the existence of the water reducing agent (superplasticizer). Simard et al. [119] have tested different batches of cement paste with fixed water/cement ratio (w/c ratio=0.35), and they used two different commercial superplasticizers (Na-PNS and Ca-PNS) [poly-B-naphthalene sulfonates (PNS)] at different concentrations. Their results showed that there are variations in the heat flux of the hydration and retardation in the hydration process with the increase in the concentration of the superplasticizers. The compression tests showed degradations in the strength of all cement paste batches with the increase in the concentration of the superplasticizers. This decrease in strength was also a function of cement type (chemistry). The degradation in the compressive strength varied from 20% to 100% depending on the type and concentrations of the cement and the superplasticizers. They also reported that retardation in hydration was greater for cement types of low C_3A content. However, more investigations on curing methods and superplasticizer effects on the mechanical properties of cement paste will be performed in the future.

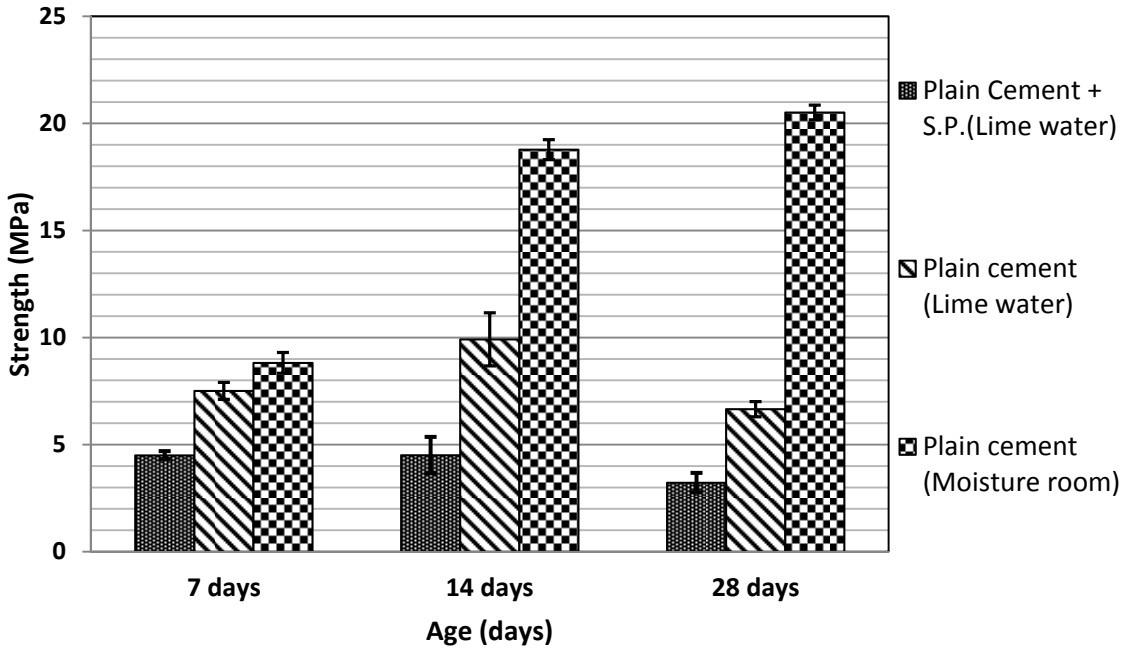

Fig. 44. Average flexural strength results for different plain cement specimens with the standard error of the mean.

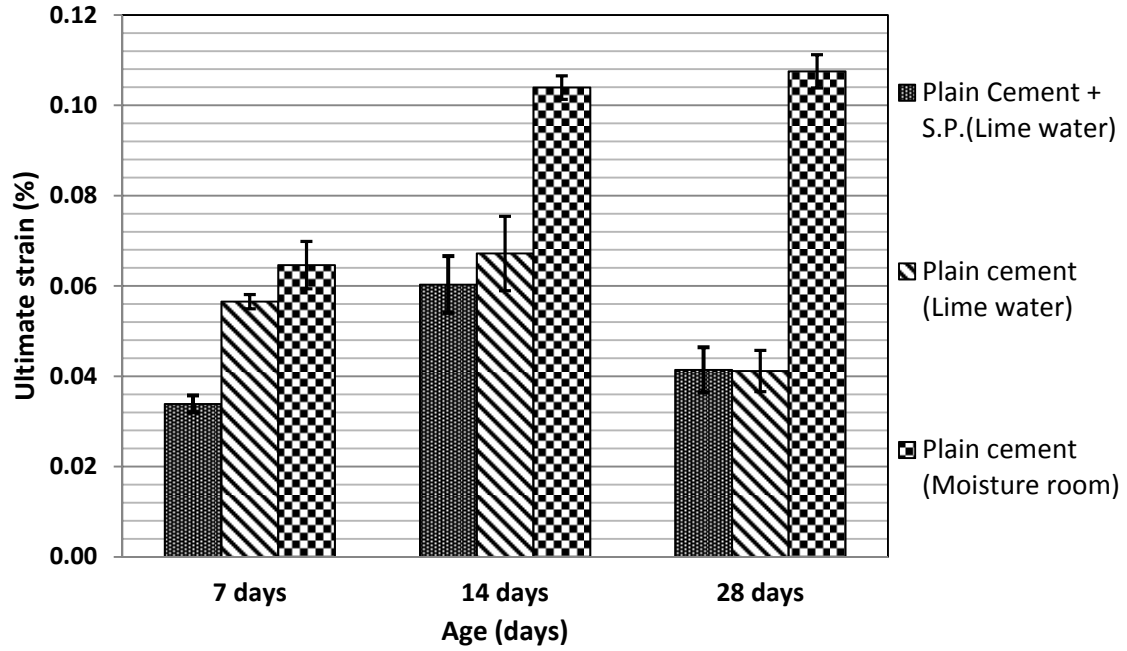

Fig. 45. Average ultimate strain results for different plain cement specimens with the standard error of the mean.

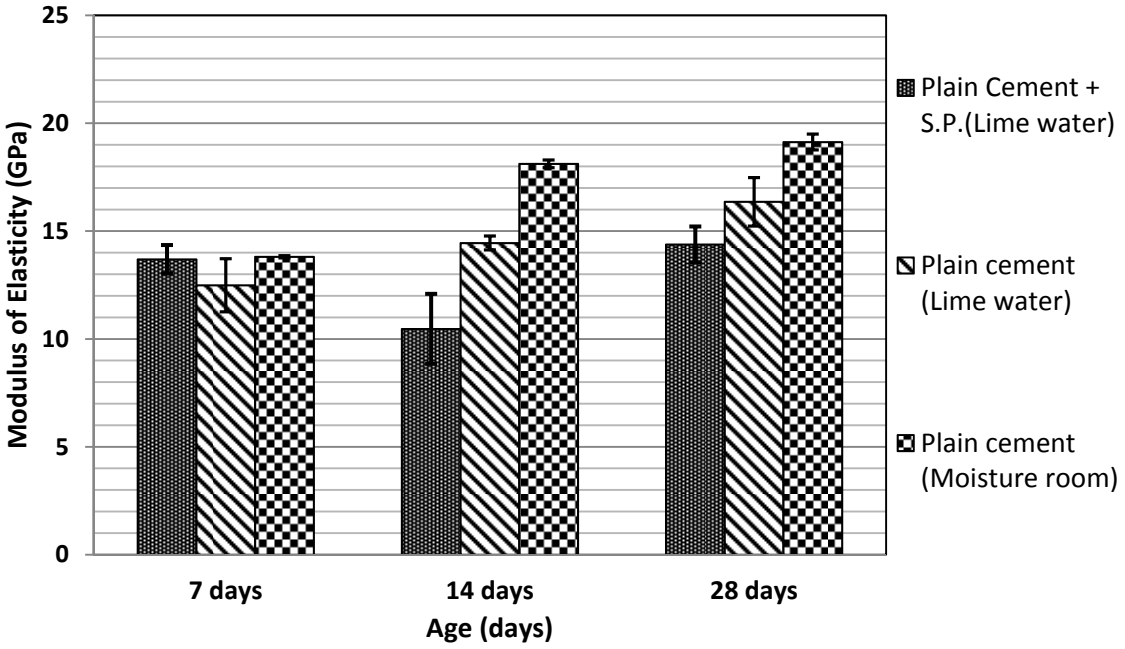

Fig. 46. Average modulus of elasticity results for different plain cement specimens with the standard error of the mean.

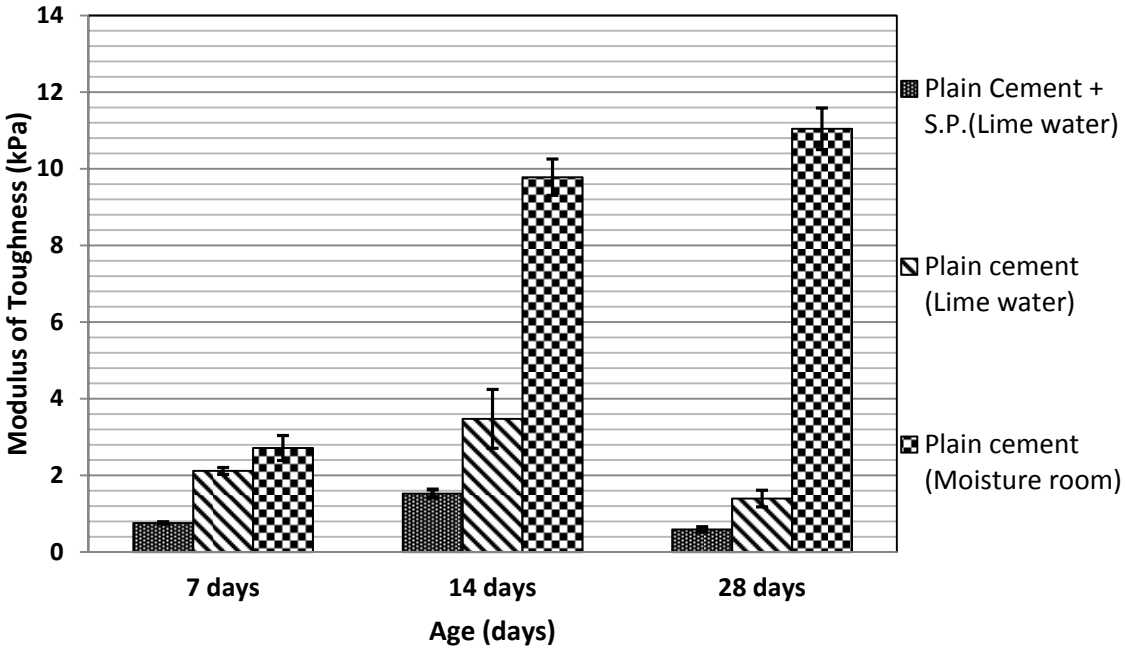

Fig. 47. Average modulus of toughness results for different plain cement specimens with the standard error of the mean.

The reliability of the results obtained for all the ten batches (of this study) is preserved. Since, all the ten batches have been cured for the same time in the same lime water solution, the author believes that they all will have the same effect of the lime water curing. Hence, the comparison between all batches is valid at least qualitatively. However, based on this plain cement study, the author believes that if different curing method was adopted (like moisture curing), the results will show improvements in the mechanical properties of the nanocomposite specimens, due to the reduction in leaching, but the relative behavior and trend of all batches will be the same. The curing method effects need more investigations and will be studied in a future work.

4.5 SEM and TEM Microstructural Imaging

In order to investigate the microstructure of the MWCNTs/cement composites, Scanning Electron Microscope (SEM) images have been taken for the fracture surface of the nanocomposites. A very small portion cut from the fracture surface have been mounted on SEM holder and coated with a very thin layer (3-4 nm) of Platinum/Palladium, to enhance the images quality by improving the charge discharge on the top of the sample under the electron beam of the SEM. A JEOL JSM-7500F machine, an ultra-high resolution field emission scanning electron microscope (FE-SEM), has been used in order to capture the MWCNTs within the cement paste. It should be noticed that finding the CNTs within the cement paste is relatively very challenging, when compared to capturing carbon nano fibers or microfibers. Two main categories have been taken into consideration, which the author believed it has major effects on the

mechanical properties of the CNTs nanocomposites; CNTs crack bridging (pull-out action) and the dispersion of the CNTs within the matrix.

4.5.1 CNTs Pull-out and Crack Bridging

In Fig. 48 and Fig. 49, it is seen that the MWCNTs were effectively bridging micro-cracks within the cement paste matrix. Clear evidence can be obtained from the figures that many CNTs are stretching across the micro-crack. CNTs breakage can also be seen for many of the CNTs bridging the micro-crack. This will imply a good bonding between the CNTs surfaces and the surrounding cement paste. However, it was difficult to capture a clear pull-out image and the corresponding fiber hole in the matrix.

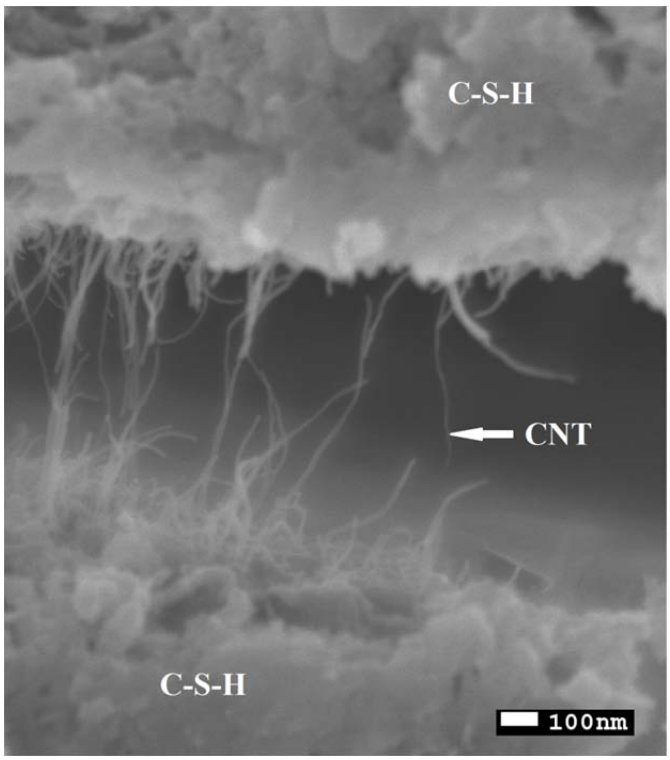

Fig. 48. SEM image showing the micro-crack bridging and breakage of the MWCNTs within cement paste.

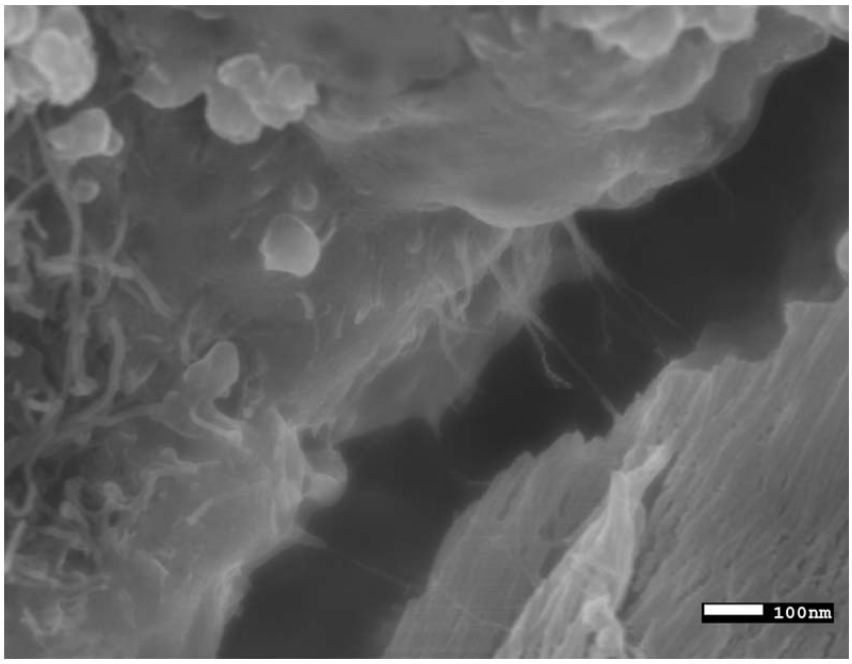

Fig. 49. SEM image showing a micro-crack bridging by few number of MWCNTs within cement paste.

The breakage seen in the images would indicate very high stresses applied to the CNTs. Since the theoretical tensile strength of CNTs is very high, then this means more number of CNTs is needed in order to carry these stresses. This could imply that a very good dispersion is the real key to improve the mechanical properties of cement nanocomposites rather than the bonding between the CNTs and the matrix, at least in cement paste, as breakage not pull-out is seen in the images. However, the effective tensile strength of CNTs is affected by the amounts of defects in the atomic structure of the CNTs walls. The increase of the defects will decrease the strength and make the CNTs to curve and bundle. However, Musso, et al. and Tyson, et al. [62, 104] concluded that even these defects may affects the CNTs as individual, but the overall strength of the composite can be increased with a good dispersion.

4.5.2 Dispersion and Agglomeration

From the previous subsection discussion, it has been proposed that dispersion of CNTs within the cement paste matrix could be more important and critical than bonding, since breakage of the CNTs occurred before the pull-out action. This could imply that -at least for this study case- sufficient bonding was obtained between the CNTs and the surrounding cement paste.

As mentioned before, a good dispersion of the CNTs within the aqueous solution does not guarantee a good dispersion of the CNTs within the cement paste. As seen in Fig. 50, large number of MWCNTs agglomerates and bundle within a very small area on the fracture surface of the cement nanocomposite. Fig. 51 shows a cryo-TEM image of MWCNTs within a thin strip of cement paste.

Based on these SEM and TEM observations of the fractured surface, two main reasons could explain the poor dispersion obtained. The first reason is that the sonication (dispersion) of the CNTs in the mixing water and/or the mixing of the CNTs solution with cement powder, are not very effective, and more enhancements are needed in that area to improve the current mixing and dispersing techniques, or to create new dispersing techniques.

The second reason that could explain the poor dispersion is the cement grain size. It is well known that the cement grain diameter is greater than the size of the CNTs by hundreds of times. When mixing well dispersed CNTs solution with the cement powder, the CNTs will be in the water surrounding the cement grains. When cement paste

hydrates and hardens, the CNTs will be at the original location outside the original perimeter of the cement grains. Hence, locations with agglomerations of CNTs, and locations without any presence of CNTs (the original cement grains areas) will be formed. During the searching process for the CNTs on the fracture surface using the SEM, it was clearly noticed that –at the nano scale- large areas were just empty of the CNTs, while some limited locations contain the CNTs. The second reason proposed could be the main and the most important element to obtain a very well dispersion [49].

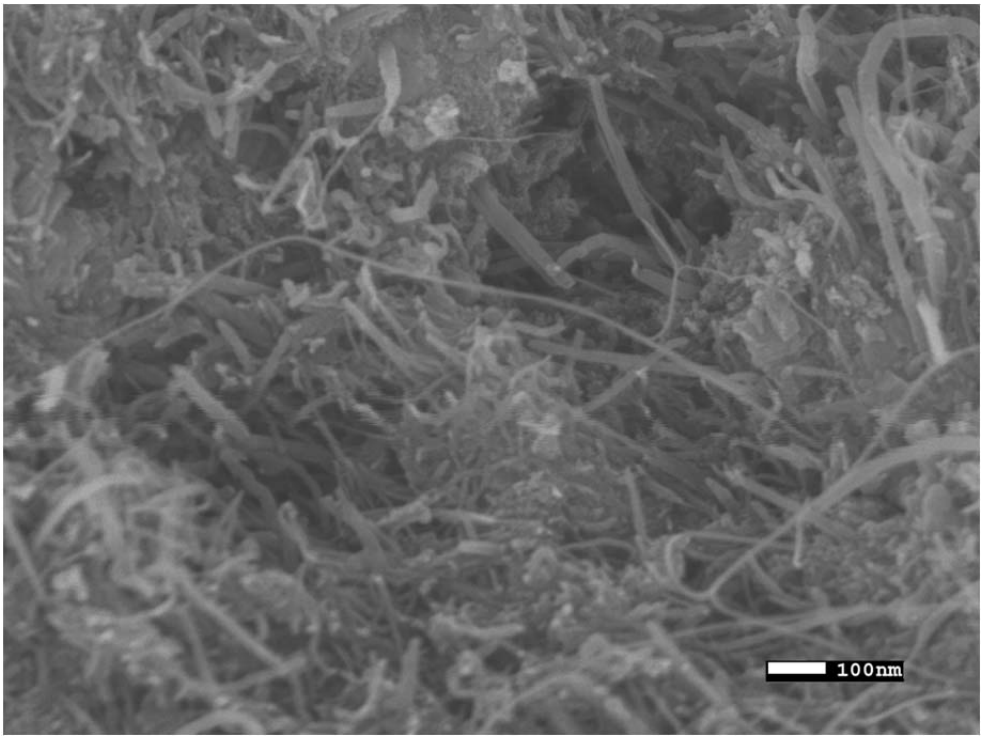

Fig. 50. SEM image of MWCNTs agglomerations within a small area of cement paste.

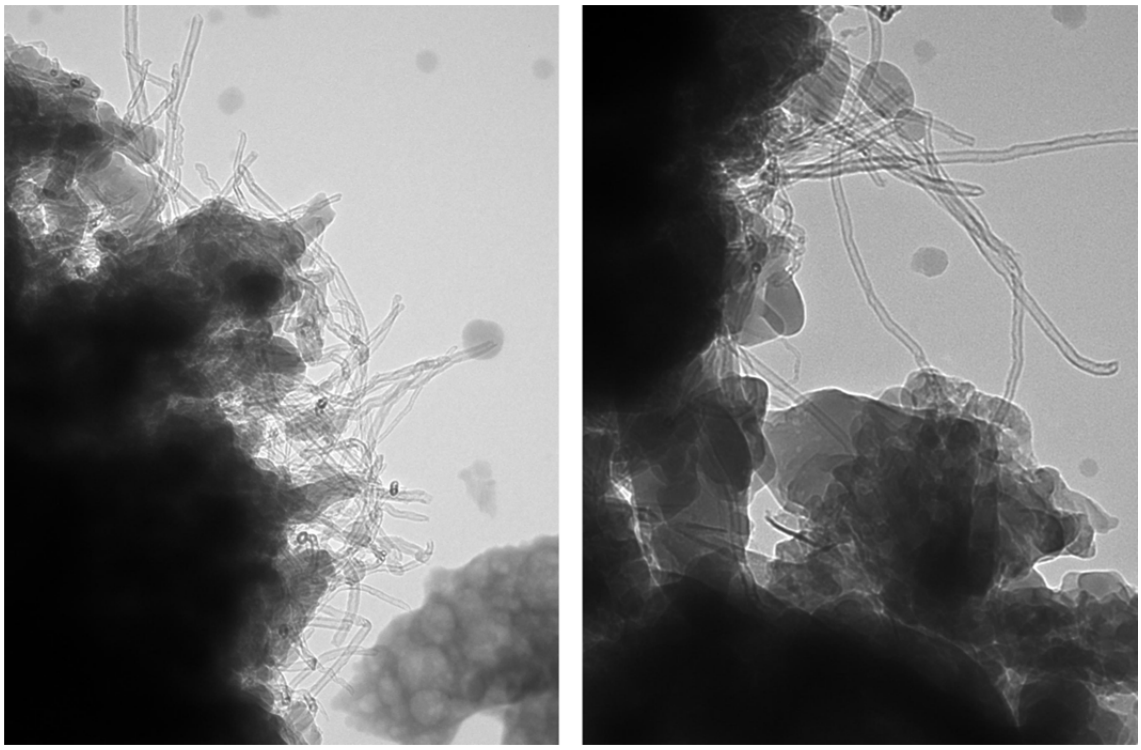

Fig. 51. A cryo-TEM image of MWCNTs within cement paste (picture courtesy of Bryan M. Tyson).

As mentioned in the previous section, the excessive formation of the expansive ettringite needles would cause micro-cracks and damage inside the cement paste matrix, resulting in degradation of the mechanical properties of the material. Fig. 52 shows a SEM image showing a huge formation of ettringite needles within the C-S-H of the cement paste. It is also noticed that air voids (spaces) exist within and around the ettringite formation within the hydrated cement paste.

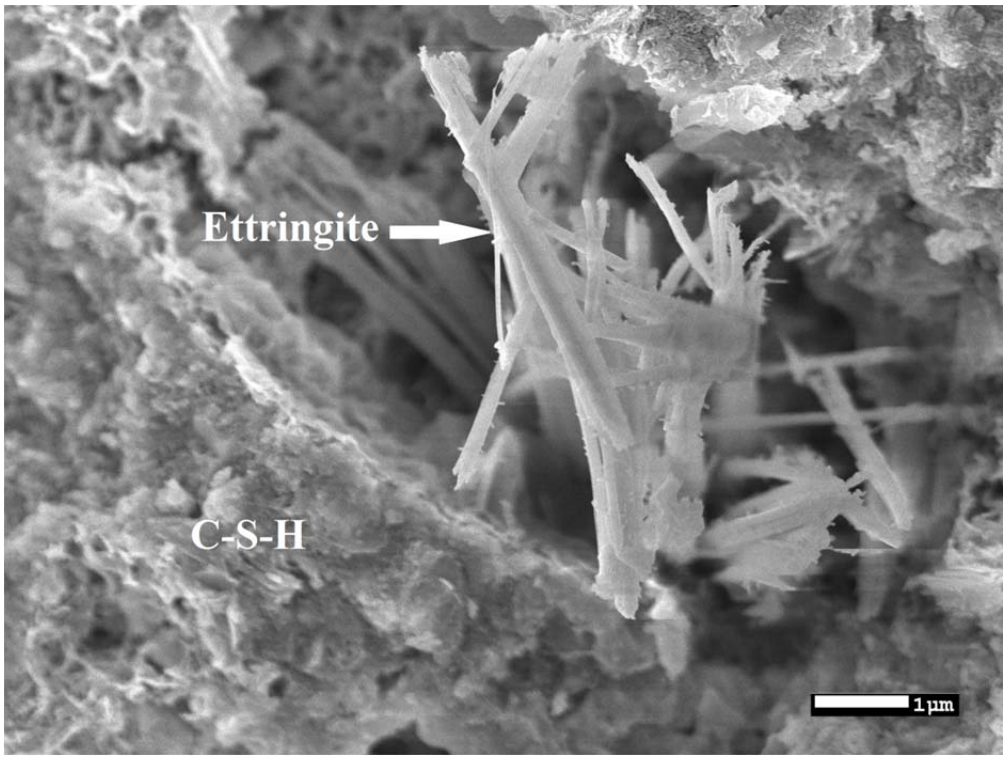

Fig. 52. SEM image showing a huge formation of ettringite needles within the C-S-H of the cement paste. Notice the air void (space) within and surrounding the ettringite formation.

5. CONCLUSIONS AND FUTURE WORK

5.1 Conclusion

In this study, the effects of the aspect ratio of the functionalized and the non-functionalized multi-walled carbon nanotubes on the mechanical properties of cement paste have been investigated. Four different types of MWCNTs have been used as nano-reinforcements for the cement paste composite; two aspect ratio MWCNTs and two functional groups (COOH and OH) of the MWCNTs. Ten different batches of cement composites with different MWCNTs types and concentrations were fabricated and tested. The mechanical properties of the MWCNTs/cement paste composites were tested by a custom made three-point flexural test apparatus. The microstructural characteristics of the MWCNTs/cement composites were investigated by the use of SEM and TEM machines images.

The first step in this work was to disperse the CNTs within water with surfactant. Then this solution was sonicated using ultrasonic wave mixer. It has been mentioned that proper chemical surfactant has to be compatible with cement. Excessive amount of surfactant will enhance the dispersivity of the CNTs, and reduce the amount of ultrasonication power and time, but will have negative effects on the cement paste hydration process. Less surfactant means more energy (sonication) needed for well dispersion, but that will cause breakage and dissolving of the CNTs. Optimum level of both surfactant and ultrasonication needed to be achieved.

Short MWCNTs have been acid treated (functionalized) by combination of sulfuric and nitric acids. The obtained functionalized MWCNTs have the functional

group (COOH). The XPS testing has showed increase in the oxygen content ten times more after the functionalization. The CNTs functionalization process is very important in order to improve the dispersion and to enhance the bonding between the CNTs and the surrounding cement paste matrix. Providing the specific type of the functional group that will bond with the matrix, and optimizing the level of functionalization is crucial, such that providing sufficient side functional groups without excessive damaging to the CNTs.

To investigate the mechanical properties of the MWCNTs/cement composites, ten different batches where made, by sonicating the MWCNTs with the water and the surfactant, then mixing this solution with cement powder using a water/cement ratio of 0.4. The specimens were casted into a small acrylic mold and have been tested under three-point flexural testing, at ages of 7, 14, and 28 days from the casting day. Four different mechanical properties have been measured; flexural strength, ultimate strain (ductility), elastic modulus, and modulus of toughness.

Most of the nanocomposites show multi-peak behavior in the stress-strain diagrams. After the first crack, the material softens or yields in some cases, and sometimes shows gradual increase in the strength to become higher than the first-crack strength. This behavior clearly indicates the CNTs pull-out action, which increases the composite ductility (strain capacity) and toughness.

The mechanical testing results showed that, for flexural strength at 28 days almost all of the MWCNTs composites have increased the flexural strength of the cement nanocomposites. At 28 days, the long MWCNTs have increased the flexural strength more than the short MWCNTs, although the short MWCNTs improved the flexural

strength more at early ages of 7 days. For the ultimate strain (ductility) of the nanocomposite beams, show that over all ages, 7, 14 and 28 days, the ultimate strain (ductility) of the short MWCNTs nanocomposites is more than the ultimate strain (ductility) of the long MWCNTs nanocomposites. This could be because a better level of dispersion has been achieved in the short MWCNTs than in the long ones.

The short 0.2% MWNT showed a significant increase in the flexural strength, specifically increased by 269% compared to the plain cement sample. The long 0.1%MWNT has also increased in the flexural strength by 65%. The long 0.04% MWNT (OH) showed an improvement of 83% in flexural strength at 28 days compared to the plain cement sample. The highest ductility (strain capacity) at 28 days was for the short 0.1% MWNT and short 0.2% MWNT, with improvement of 86% and 81%, respectively. Also, at 28 days, the short 0.2% MWNT (COOH) and the long 0.1% MWNT (OH) ductility increased by 36% and 31%, respectively.

A general degradation in strength and toughness noticed for all specimens at age of 28 days. The author believes that leaching of Calcium Hydroxide [$Ca(OH)_2$] from the cement paste submerged into the lime water, would increase the porosity (capillary voids) of the matrix and hence degrade the mechanical properties.

SEM images implied that the uniformity of the distribution of the MWCNTs within the aqueous solution does not guarantee a uniform distribution of the nano filaments within the cement paste composites. Agglomerations and plain cement area without the CNTs were noticed by the SEM. However, clear evidence can be obtained from the figures that many of the CNTs are stretching across the micro-cracks. CNTs

breakage can also be seen for many of the CNTs bridging the micro-crack. This will imply a good bonding between the CNTs surfaces and the surrounding cement paste.

5.2 Limitations

There are many limitations associated with the experimental work of this research. The first limitation is about the CNTs dispersion measurement and optimization. The evaluation of the dispersion of the CNTs within the aqueous solution is difficult and not accurate, since it depends on the visual evaluation, including the TEM images, which presents limited area that might not be representative. However, it is more difficult and complicated to measure the dispersion of the CNTs within the cement paste composite. The SEM images would only cover a limited area and depth on the distribution of the CNTs within the cement paste volume. The final length of the CNTs after the ultrasonication was not measured to verify the breakage amount of the CNTs due to the ultrasonication process. This could effectively change the actual aspect ratio of the CNTs assumed before the ultrasonication.

Another important limitation regarding the testing is the size of the specimens (beams). The small cross-section area of the specimens will make it very sensitive to any micro defects, like air voids or bubbles. These micro defects will greatly affect the strength and the mechanical behavior of the composite. Also the data collection for the behavior after the first crack would be limited and insensitive, since the first crack usually will fracture the specimen and end the measurement. If larger cross-section beams were tested, the yielding behavior or the crack propagation observations will be

more accurate. As for the nanocomposites behavior the data capturing of the pull-out behavior after the first crack is so important to understand the micro cracks bridging mechanism.

Finally, the three point bending test has a limitation of a peak maximum bending moment at mid-span, which the location of the first crack might not be at mid-span. Introducing a notch (seam) at mid-span for this size of specimens would make it more difficult to capture any ductility and the failure will be very brittle. The four-point bending has the advantage of constant bending moment over the mid part of the beam, and that could reduce the errors.

5.3 Future Work

More investigations are needed in areas like optimization for the dispersion of the CNTs within the aqueous solution, by optimization of the amount of the surfactant needed, the concentration of the CNTs/surfactant ratio, CNTs/water ratio, and the ultrasonication power and duration needed to maximize the dispersion without damaging the CNTs.

On the other hand, optimization and quantification of the dispersion of the CNTs within the cement paste composite. Measuring dispersion and the distribution of these nano-filaments is needed in order to optimize the mixing techniques and effectively use and utilize the CNTs within the cement paste matrix.

Further investigations are needed on the effects of the curing methods on the hydration process, porosity and the chemistry of the cement paste composites, especially

the curing in lime water, in order to support and verify the leaching of the $Ca(OH)_2$ hypothesis. The specimens' geometry and size along with the saturation level of the lime in the curing water will cause the leaching which significantly affects the mechanical properties of the cement paste composites.

Testing larger beams size, using four-point bending testing, will provide more details about the post first-crack behavior.

Performing finite element modeling for the CNTs/cement composites is needed to verify and understands the mechanism of crack bridging and strengthening of the matrix by the existence of the CNTs.

REFERENCES

[1] Altoubat S, Yazdanbakhsh A, Rieder K-A. Shear behavior of macro-synthetic fiber-reinforced concrete beams without stirrups. ACI Mater J. 2009;106(4):381-9.

[2] Fischer G, Li VC. Effect of fiber reinforcement on the response of structural members. Eng Fract Mech. 2007;74(1-2):258-72.

[3] Li VC, Maalej M. Toughening in cement based composites. Part II: Fiber reinforced cementitious composites. Cem Concr Compos. 1996;18(4):239-49.

[4] Mangat PS, Motamedi-Azari M, Shakor Ramat BB. Steel fibre-cement matrix interfacial bond characteristics under flexure. Int J Cem Compos Lightweight Concrete. 1984;6(1):29-37.

[5] Ostertag CP, Yi CK, Vondran G. Tensile strength enhancement in interground fiber cement composites. Cem Concr Compos. 2001;23(4-5):419-25.

[6] Savastano JH, Warden PG, Coutts RSP. Microstructure and mechanical properties of waste fibre-cement composites. Cem Concr Compos. 2005;27(5):583-92.

[7] Wang C, Li K-Z, Li H-J, Jiao G-S, Lu J, Hou D-S. Effect of carbon fiber dispersion on the mechanical properties of carbon fiber-reinforced cement-based composites. Mater Sci Eng A. 2008;487(1-2):52-7.

[8] Demczyk BG. Direct mechanical measurement of the tensile strength and elastic modulus of multiwalled carbon nanotubes. Mater Sci Eng A Struct Mater Prop Microstruct Process. 2002;334(1):173-8.

[9] Collins PG, Avouris P. Nanotubes for electronics. Scientific American. 2000(December 2000):67-9.

[10] Coleman JN, Khan U, Blau WJ, Gun'ko YK. Small but strong: A review of the mechanical properties of carbon nanotube-polymer composites. Carbon. 2006;44(9):1624-52.

[11] Marrs B, Andrews R, Pienkowski D. Multiwall carbon nanotubes enhance the fatigue performance of physiologically maintained methyl methacrylate-styrene copolymer. Carbon. 2007;45(10):2098-104.

[12] Wang JG, Fang ZP, Gu AJ, Xu LH, Liu F. Effect of amino-functionalization of multi-walled carbon nanotubes on the dispersion with epoxy resin matrix. J Appl Polym Sci. 2006;100(1):97-104.

[13] Bacsa RR, Laurent C, Peigney A, Bacsa WS, Vaugien T, Rousset A. High specific surface area carbon nanotubes from catalytic chemical vapor deposition process. Chem Phys Lett. 2000;323(5-6):566-71.

[14] Radushkevich LV, Lukyanovich VM. The structure of carbon produced by thermal decomposition of carbon monoxide on an iron contact (Russian). ЖФХ. 1952;26(1):88-95. http://www.nanometer.ru/2007/04/06/nanotubes.html#.

[15] Iijima S. Helical microtubules of graphitic carbon. Nature. 1991;354(6348):56-8.

[16] Graphite. 2011; http://mrsec.wisc.edu/Edetc/nanoquest/carbon/index.html

[17] Hedberg JA. Schematic image of graphene sheet structure. 2011; http://www.jameshedberg.com/scienceGraphics.php?sort=graphene&id=graphene-wavey-lensBlur

[18] Schematic image of fullerenes (buckyballs) structure made of 60 carbon atoms. 2011; http://mrsec.wisc.edu/Edetc/nanoquest/carbon/index.html

[19] Single-walled carbon nanotube. 2011; http://www.istockphoto.com/stock-photo-10936011-single-walled-carbon-nanotube.php

[20] Multi-walled carbon nanotube. 2011; http://www.topnews.in/law/1-ounce-new-frozen-smoke-can-carpet-3-football-fields-246298

[21] Schematic image of three examples of carbon nanotubes structural orientaions. 2011; http://coecs.ou.edu/Brian.P.Grady/images/nanotube.jpg

[22] Mamalis AG, Vogtländer LOG, Markopoulos A. Nanotechnology and nanostructured materials: Trends in carbon nanotubes. Precis Eng. 2004;28(1):16-30.

[23] Yakobson BI, Smalley RE. Fullerene nanotubes: C-1000000 and beyond. Am Scientist. 1997;85(4):324-37.

[24] Thess A, Lee R, Nikolaev P, Dai HJ, Petit P, Robert J, et al. Crystalline ropes of metallic carbon nanotubes. Science. 1996;273(5274):483-7.

[25] Yu MF, Lourie O, Dyer MJ, Moloni K, Kelly TF, Ruoff RS. Strength and breaking mechanism of multiwalled carbon nanotubes under tensile load. Science. 2000;287(5453):637-40.

[26] Wong EW, Sheehan PE, Lieber CM. Nanobeam mechanics: Elasticity, strength, and toughness of nanorods and nanotubes. Science. 1997;277(5334):1971-5.

[27] Hata K. From highly efficient impurity-free CNT synthesis to DWNT forests, CNT solids, and super-capacitors In: Proceedings of SPIE - The International Society for Optical Engineering. Bellingham, WA, ETATS-UNIS; 2007. p. 64791L.1-L.12.

[28] Qian D, Dickey EC, Andrews R, Rantell T. Load transfer and deformation mechanisms in carbon nanotube-polystyrene composites. Appl Phys Lett. 2000;76(20):2868-70.

[29] Park SH, Bandaru PR. Improved mechanical properties of carbon nanotube/polymer composites through the use of carboxyl-epoxide functional group linkages. Polymer. 2010;51(22):5071-7.

[30] Xu CL, Wei BQ, Ma RZ, Liang J, Ma XK, Wu DH. Fabrication of aluminum-carbon nanotube composites and their electrical properties. Carbon. 1999;37(5):855-8.

[31] Dong SR, Tu JP, Zhang XB. An investigation of the sliding wear behavior of Cu-matrix composite reinforced by carbon nanotubes. Mater Sci Eng, A. 2001;313(1-2):83-7.

[32] Flahaut E, Peigney A, Laurent C, Marliere C, Chastel F, Rousset A. Carbon nanotube-metal-oxide nanocomposites: Microstructure, electrical conductivity and mechanical properties. Acta Mater. 2000;48(14):3803-12.

[33] Deng CF, Wang DZ, Zhang XX, Li AB. Processing and properties of carbon nanotubes reinforced aluminum composites. Mater Sci Eng A. 2007;444(1-2):138-45.

[34] Esawi AMK, Morsi K, Sayed A, Taher M, Lanka S. The influence of carbon nanotube (CNT) morphology and diameter on the processing and properties of CNT-reinforced aluminium composites. Compos Part A: Appl Sci Manuf. 2010;42(3):234-43.

[35] Peigney A, Laurent C, Flahaut E, Rousset A. Carbon nanotubes in novel ceramic matrix nanocomposites. Ceram Int. 2000;26(6):677-83.

[36] Ma RZ, Wu J, Wei BQ, Liang J, Wu DH. Processing and properties of carbon nanotubes–nano-SiC ceramic. J Mater Sci. 1998;33(21):5243-6.

[37] Peigney A, Flahaut E, Laurent C, Chastel F, Rousset A. Aligned carbon nanotubes in ceramic-matrix nanocomposites prepared by high-temperature extrusion. Chem Phys Lett. 2002;352(1-2):20-5.

[38] Balázsi, Kónya Z, Wéber F, Biró LP, Arató P. Preparation and characterization of carbon nanotube reinforced silicon nitride composites. Mater Sci Eng C. 2003;23(6-8):1133-7.

[39] Boo WJ, Sun LY, Liu J, Moghbelli E, Clearfield A, Sue HJ, et al. Effect of nanoplatelet dispersion on mechanical behavior of polymer nanocomposites. J Polym Sci Pt B-Polym Phys. 2007;45(12):1459-69.

[40] Hussain M, Oku Y, Nakahira A, Niihara K. Effects of wet ball-milling on particle dispersion and mechanical properties of particulate epoxy composites. Mater Lett. 1996;26(3):177-84.

[41] Hamming LM, Qiao R, Messersmith PB, Catherine Brinson L. Effects of dispersion and interfacial modification on the macroscale properties of TiO_2 polymer-matrix nanocomposites. Compos Sci Technol. 2009;69(11-12):1880-6.

[42] Pu ZC, Mark JE, Jethmalani JM, Ford WT. Effects of dispersion and aggregation of silica in the reinforcement of poly(methyl acrylate) elastomers. Chem Mat. 1997;9(11):2442-7.

[43] Stoeffler K, Lafleur PG, Denault J. The effect of clay dispersion on the properties of LLDPE/LLDPE-g-MAH/Montmorillonite nanocomposites. Polym Eng Sci. 2008;48(12):2459-73.

[44] Prasad VVB, Bhat BVR, Mahajan YR, Ramakrishnan P. Structure–property correlation in discontinuously reinforced aluminium matrix composites as a function of relative particle size ratio. Mater Sci Eng A. 2002;337(1/2):179-86.

[45] Slipenyuk A, Kuprin V, Milman Y, Spowart JE, Miracle DB. The effect of matrix to reinforcement particle size ratio (PSR) on the microstructure and mechanical properties of a P/M processed AlCuMn/SiCp MMC. Mater Sci Eng, A. 2004;381(1-2):165-70.

[46] Akkaya Y, Shah SP, Ankenman B. Effect of fiber dispersion on multiple cracking of cement composites. J Eng Mech-ASCE. 2001;127(4):311-6.

[47] Akkaya Y, Picka J, Shah SP. Spatial distribution of aligned short fibers in cement composites. J Mater Civ Eng. 2000;12(3):272-9.

[48] Rapoport JR, Shah SR. Cast-in-place cellulose fiber-reinforced cement paste, mortar, and concrete. ACI Mater J. 2005;102(5):299-306.

[49] Yazdanbakhsh A, Grasley Z, Tyson B, Abu Al-Rub R. Carbon nanofibers and nanotubes in cementitious materials: Some issues on dispersion and interfacial bond. ACI Special Publication. 2009;267:21-34.

[50] Yazdanbakhsh A, Grasley Z, Tyson B, Abu Al-Rub RK. Dispersion quantification of inclusions in composites. Compos Part A: Appl Sci Manuf. 2011;42(1):75-83.

[51] Makar JM, Beaudoin JJ. Carbon nanotubes and their application in the construction industry. In: 1st International Symposium on Nanotechnology in Construction. Paisley, Scotland; 2003. p. 331-41.

[52] Cwirzen A, Habermehl-Cwirzen K, Nasibulina LI, Shandakov SD, Nasibulin AG, Kauppinen EI, et al. CHH cement composite. Berlin: Springer-Verlag Berlin; 2009.

[53] Makar JM, Margeson JC, Luh J. Carbon nanotube/cement composite - early results and potential applications. In: 3rd International Conference on Construction Materials: Performance, Innovation and Structural Implications. Vancouver, B.C.; 2005. p. 1-10.

[54] Li GY, Wang PM, Zhao XH. Mechanical behavior and microstructure of cement composites incorporating surface-treated multi-walled carbon nanotubes. Carbon. 2005;43(6):1239-45.

[55] Li GY, Wang PM, Zhao X. Pressure-sensitive properties and microstructure of carbon nanotube reinforced cement composites. Cem Concr Compos. 2007;29(5):377-82.

[56] Cwirzen A, Habermehl-Cwirzen K, Penttala V. Surface decoration of carbon nanotubes and mechanical properties of cement/carbon nanotube composites. Adv Cem Res. 2008;20(2):65-73.

[57] Nasibulin AG, Shandakov SD, Nasibulina LI, Cwirzen A, Mudimela PR, Habermehl-Cwirzen K, et al. A novel cement-based hybrid material. New J Phys. 2009;11:1-11.

[58] Shah SP, Konsta-Gdoutos MS, Metaxa ZS. Highly-dispersed carbon nanotubes-reinforced cement-based materials. Publication USPA US 2009/0229494 A1, 2009.

[59] Konsta-Gdoutos MS, Metaxa ZS, Shah SP. Multi-scale mechanical and fracture characteristics and early-age strain capacity of high performance carbon nanotube/cement nanocomposites. Cem Concr Compos. 2009;32(2):110-5.

[60] Konsta-Gdoutos MS, Metaxa ZS, Shah SP. Highly dispersed carbon nanotube reinforced cement based materials. Cem Concr Res. 2010;40(7):1052-9.

[61] Abu Al-Rub RK, Tyson BM, Yazdanbakhsh A, Grasley Z. Mechanical properties of nanocomposite cement incorporating surface-treated and untreated carbon nanotubes and carbon nanofibers. J Nanomech Micromechan-ASCE. 2011;(in press).

[62] Tyson BM, Al-Rub RKA, Yazdanbakhsh A, Grasley Z. Carbon nanotubes and carbon nanofibers for enhancing the mechanical properties of nanocomposite cementitious materials. J Mater Civ Eng-ASCE. 2011;23(7):1028-35.

[63] Luo JL, Duan ZD, Zhao TJ, Li QY. Effect of multi-wall carbon nanotube on fracture mechanical property of cement-based composite. Adv Mater Res. 2011;Advances in Composites(146-147):581-4.

[64] Luo JL, Duan ZD, Zhao TJ, Li QY. Cement-based composite with carbon nanotubes reinforcement tailored for structural damping. Adv Mater Res. 2011;Advances in Composites(150-151):526-9.

[65] Hunashyal AM, Lohitha SJ, Quadri SS, Banapurmath NR. Experimental investigation of the effect of carbon nanotubes and carbon fibres on the behaviour of plain cement composite beams. IES J Part A: Civil Struct Eng. 2011;4(1):29 - 36.

[66] Vibra-cell liquid processing. 2011; http://www.sonics.biz/lp-vibra.htm

[67] Moore VC, Strano MS, Haroz EH, Hauge RH, Smalley RE, Schmidt J, et al. Individually suspended single-walled carbon nanotubes in various surfactants. Nano Lett. 2003;3(10):1379-82.

[68] Chen W, Auad ML, Williams RJJ, Nutt SR. Improving the dispersion and flexural strength of multiwalled carbon nanotubes-stiff epoxy composites through β-hydroxyester surface functionalization coupled with the anionic homopolymerization of the epoxy matrix. Eur Polym J. 2006;42(10):2765-72.

[69] Kim JA, Seong DG, Kang TJ, Youn JR. Effects of surface modification on rheological and mechanical properties of cnt/epoxy composites. Carbon. 2006;44(10):1898-905.

[70] Li SQ, Wang F, Wang Y, Wang JW, Ma J, Xiao J. Effect of acid and teta modification on mechanical properties of MWCNTs/epoxy composites. J Mater Sci. 2008;43(8):2653-8.

[71] Xie X-L, Mai Y-W, Zhou X-P. Dispersion and alignment of carbon nanotubes in polymer matrix: A review. Mater Sci Eng R. 2005;49(4):89-112.

[72] Zhang HW, Wang JB, Guo X. Predicting the elastic properties of single-walled carbon nanotubes. J Mech Phys Solids. 2005;53(9):1929-50.

[73] Bandyopadhyaya R, Nativ-Roth E, Regev O, Yerushalmi-Rozen R. Stabilization of individual carbon nanotubes in aqueous solutions. Nano Lett. 2001;2(1):25-8.

[74] Islam MF, Rojas E, Bergey DM, Johnson AT, Yodh AG. High weight fraction surfactant solubilization of single-wall carbon nanotubes in water. Nano Lett. 2003;3(2):269-73.

[75] Kuznetsova A, Popova I, Yates JT, Bronikowski MJ, Huffman CB, Liu J, et al. Oxygen-containing functional groups on single-wall carbon nanotubes: Nexafs and vibrational spectroscopic studies. J Am Chem Soc. 2001;123(43):10699-704.

[76] Lee Y-J, Kim H-H, Hatori H. Effects of substitutional b on oxidation of carbon nanotubes in air and oxygen plasma. Carbon. 2004;42(5-6):1053-6.

[77] Ajayan PM, Ebbesen TW, Ichihashi T, Iijima S, Tanigaki K, Hiura H. Opening carbon nanotubes with oxygen and implications for filling. Nature. 1993;362(6420):522-5.

[78] Wiltshire JG, Khlobystov AN, Li LJ, Lyapin SG, Briggs GAD, Nicholas RJ. Comparative studies on acid and thermal based selective purification of hipco produced single-walled carbon nanotubes. Chem Phys Lett. 2004;386(4-6):239-43.

[79] Simmons JM, Nichols BM, Baker SE, Marcus MS, Castellini OM, Lee CS, et al. Effect of ozone oxidation on single-walled carbon nanotubes. J Phys Chem B. 2006;110(14):7113-8.

[80] Mawhinney DB, Naumenko V, Kuznetsova A, Yates JT, Liu J, Smalley RE. Infrared spectral evidence for the etching of carbon nanotubes: Ozone oxidation at 298 K. J Am Chem Soc. 2000;122(10):2383-4.

[81] Ago H, Kugler T, Cacialli F, Salaneck WR, Shaffer MSP, Windle AH, et al. Work functions and surface functional groups of multiwall carbon nanotubes. J Phys Chem B. 1999;103(38):8116-21.

[82] Okpalugo TIT, Papakonstantinou P, Murphy H, McLaughlin J, Brown NMD. Oxidative functionalization of carbon nanotubes in atmospheric pressure filamentary dielectric barrier discharge (APDBD). Carbon. 2005;43(14):2951-9.

[83] Hou Z, Cai B, Liu H, Xu D. Ar, O_2, CHF_3, and SF_6 plasma treatments of screen-printed carbon nanotube films for electrode applications. Carbon. 2008;46(3):405-13.

[84] Kiminobu I, et al. Enhancement of microplasma-based water-solubilization of single-walled carbon nanotubes using gas bubbling in water. Nanotechnology. 2007;18, 335602(33):1-7.

[85] Hamon MA, Hui H, Bhowmik P, Itkis HME, Haddon RC. Ester-functionalized soluble single-walled carbon nanotubes. Appl Phys A-Mater. 2002;74(3):333-8.

[86] Wong SS, Joselevich E, Woolley AT, Cheung CL, Lieber CM. Covalently functionalized nanotubes as nanometre-sized probes in chemistry and biology. (cover story). Nature. 1998;394(6688):52-5.

[87] Fu K, Huang W, Lin Y, Riddle LA, Carroll DL, Sun Y-P. Defunctionalization of functionalized carbon nanotubess. Nano Lett. 2001;1(8):439-41.

[88] Bahr JL, Tour JM. Covalent chemistry of single-wall carbon nanotubes. J Mater Chem. 2002;12(7):1952-8.

[89] Datsyuk V, Kalyva M, Papagelis K, Parthenios J, Tasis D, Siokou A, et al. Chemical oxidation of multiwalled carbon nanotubes. Carbon. 2008;46(6):833-40.

[90] Lakshminarayanan PV, Toghiani H, Pittman Jr CU. Nitric acid oxidation of vapor grown carbon nanofibers. Carbon. 2004;42(12-13):2433-42.

[91] Zhang G, Sun S, Yang D, Dodelet J-P, Sacher E. The surface analytical characterization of carbon fibers functionalized by H_2SO_4/HNO_3 treatment. Carbon. 2008;46(2):196-205.

[92] Wang Y, Iqbal Z, Mitra S. Rapidly functionalized, water-dispersed carbon nanotubes at high concentration. J Am Chem Soc. 2006;128(1):95-9.

[93] Dyke CA, Tour JM. Covalent functionalization of single-walled carbon nanotubes for materials applications. J Phys Chem A. 2004;108(51):11151-9.

[94] Hudson JL, Casavant MJ, Tour JM. Water-soluble, exfoliated, nonroping single-wall carbon nanotubes. J Am Chem Soc. 2004;126(36):11158-9.

[95] Mickelson ET, Huffman CB, Rinzler AG, Smalley RE, Hauge RH, Margrave JL. Fluorination of single-wall carbon nanotubes. Chem Phys Lett. 1998;296(1-2):188-94.

[96] Fu X, Lu W, Chung DDL. Ozone treatment of carbon fiber for reinforcing cement. Carbon. 1998;36(9):1337-45.

[97] Chen CL, Ogino A, Wang XK, Nagatsu M. Plasma treatment of multiwall carbon nanotubes for dispersion improvement in water. Appl Phys Lett. 2010;96(13):131504-6.

[98] Yazdanbakhsh A, Grasley Z, Tyson B, Abu Al-Rub RK. Distribution of carbon nanofibers and nanotubes in cementitious composites. Transp Res Record. 2010(2142):89-95.

[99] Chung DDL. Dispersion of short fibers in cement. J Mater Civ Eng. 2005;17(4):379-83.

[100] Tyson BM. Carbon nanotube and nanofiber reinforcement for improving the flexural strength and fracture toughness of portland cement paste. Masters thesis. College Station, Texas, Texas A&M University; 2010.

[101] Cheap tubes, inc. 2011; http://www.cheaptubesinc.com/

[102] Nanocyl, inc. 2011; http://www.nanocyl.com

[103] Ni labview. 2011; http://www.ni.com/labview

[104] Musso S, Tulliani J-M, Ferro G, Tagliaferro A. Influence of carbon nanotubes structure on the mechanical behavior of cement composites. Compos Sci Technol. 2009;69(11-12):1985-90.

[105] Dweck J, da Silva PFF, Buchler PM, Cartledge FK. Study by thermogravimetry of the evolution of ettringite phase during type II portland cement hydration. J Therm Anal. 2002;69(1):179-86.

[106] Mindess S, Young JF. Concrete. Englewood Cliffs, N.J.: Prentice-Hall; 1981.

[107] Carde C, François R, Torrenti J-M. Leaching of both calcium hydroxide and C-S-H from cement paste: Modeling the mechanical behavior. Cem Concr Res. 1996;26(8):1257-68.

[108] Adenot F, Buil M. Modelling of the corrosion of the cement paste by deionized water. Cem Concr Res. 1992;22(2-3):489-96.

[109] Carde C, François R. Effect of the leaching of calcium hydroxide from cement paste on mechanical and physical properties. Cem Concr Res. 1997;27(4):539-50.

[110] K. L. Scrivener JFY. Mechanisms of chemical degradation of cement-based systems. First ed: Taylor & Francis, Inc.; 1997.

[111] G.J. Verbeck RHH. Structure and physical properties of cement paste. In: Proceedings of the Fifth International Symposium on the Chemistry of Cement. Tokyo: The Cement Association of Japan; 1968. p. 1-32.

[112] Taylor HFW. Cement chemistry. 2nd Edition ed. London: Thomas Telford services Ltd, London; 1997.

[113] Groves GW. Microcrystalline calcium hydroxide in portland cement pastes of low water/cement ratio. Cem Concr Res. 1981;11(5-6):713-8.

[114] Viehland D, Li JF, Yuan LJ, Xu Z. Mesostructure of calcium silicate hydrate (C–S–H) gels in portland cement paste: Short-range ordering, nanocrystallinity, and local compositional order. J Am Ceram Soc. 1996;79(7):1731-41.

[115] Greenberg SA, Copeland LE. The thermodynamic functions for the solution of calcium hydroxide in water. J Phys Chem. 1960;64(8):1057-9.

[116] Bassett H. Notes on the system lime–water, and on the determination of calcium. J Chem Soc. 1934;276:1270-5.

[117] Crumbie AK, Scrivener KL, Pratt PL. The relationship between the porosity and permeability of the surface layer of concrete and the ingress of aggressive ions. In: Roberts LR, Skalny JP, editors. Material Research Society Symposium Proceedings. Pittsburgh1989. p. 279-84.

[118] Adenot F, Richet C. Modelling of the chemical degradation of a cement paste. In: Scrivener KL, Young JF, editors. Mechanisms of Chemical Degradation of Cement-based Systems. London: E & FN Spon; 1997. p. 341-9.

[119] Simard MA, Nkinamubanzi PC, Jolicoeur C, Perraton D, Aïtcin PC. Calorimetry, rheology and compressive strength of superplasticized cement pastes. Cem Concr Res. 1993;23(4):939-50.

APPENDIX A

Stress-strain diagrams for the plain cement (reference) samples:

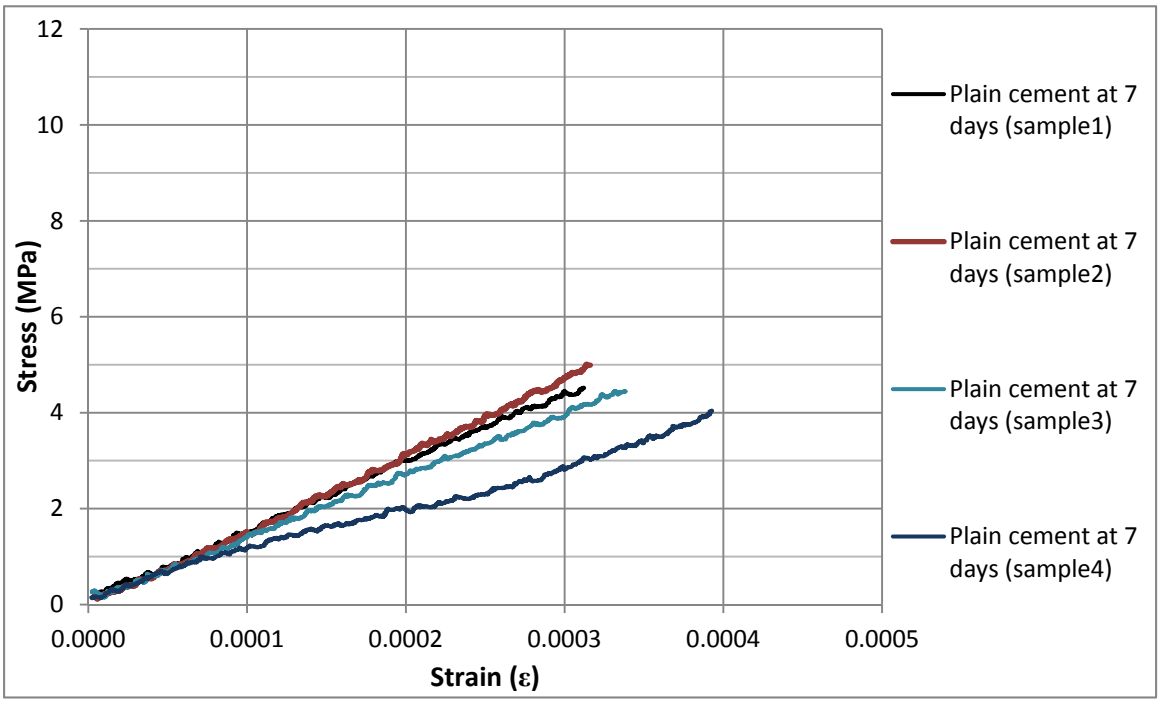

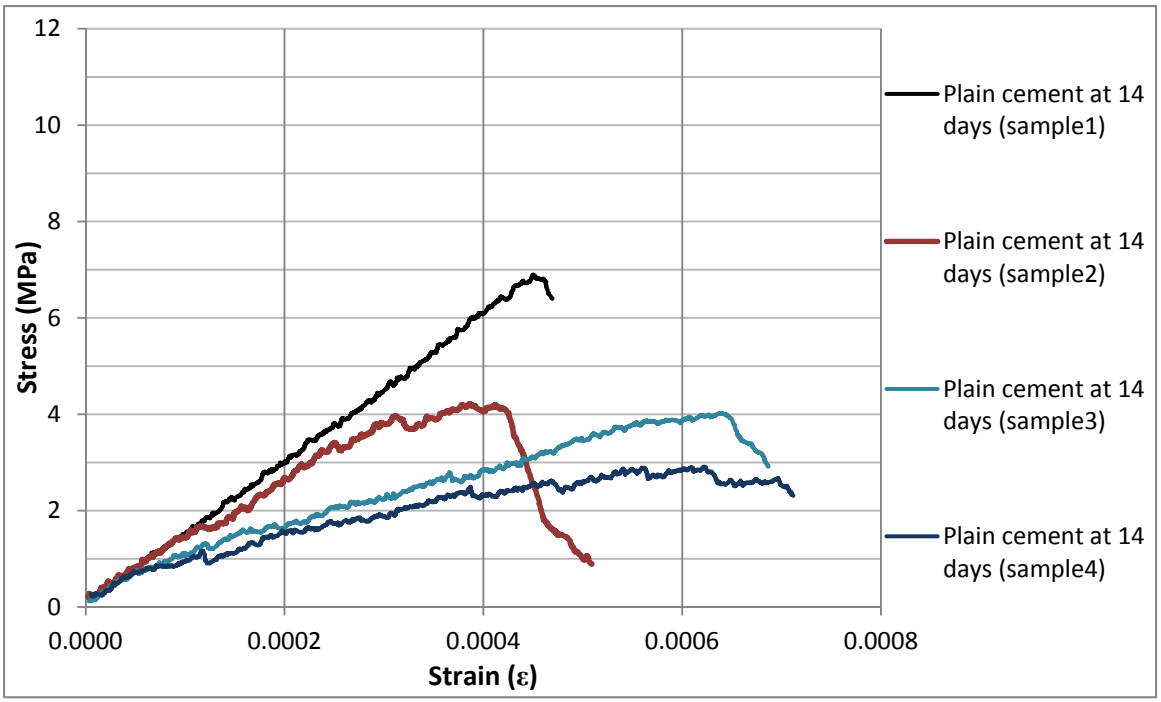

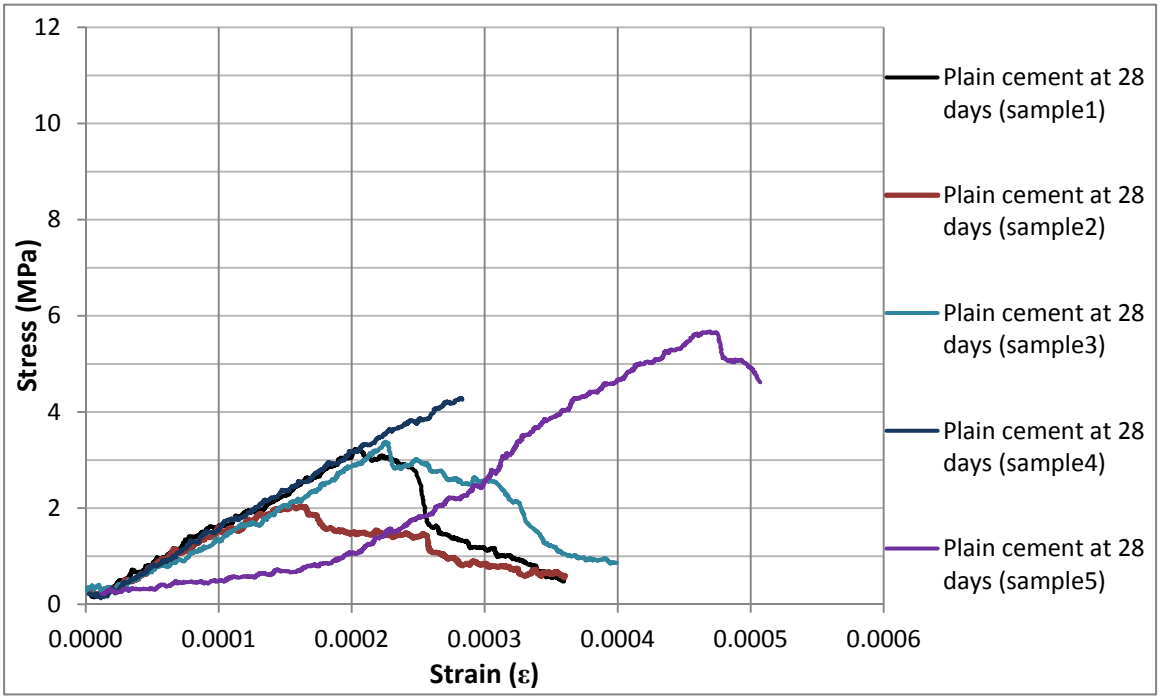
12
10
8
6
4
2
0
Stress (MPa)
0.0000
0.0001
0.0002
0.0003
0.0004
0.0005
0.0006
Strain (ε)
Plain cement at 28 days (sample1)
Plain cement at 28 days (sample2)
Plain cement at 28 days (sample3)
Plain cement at 28 days (sample4)
Plain cement at 28 days (sample5)

Stress-strain diagrams for the 0.1% Long MWCNTs (OH)/cement composite samples:

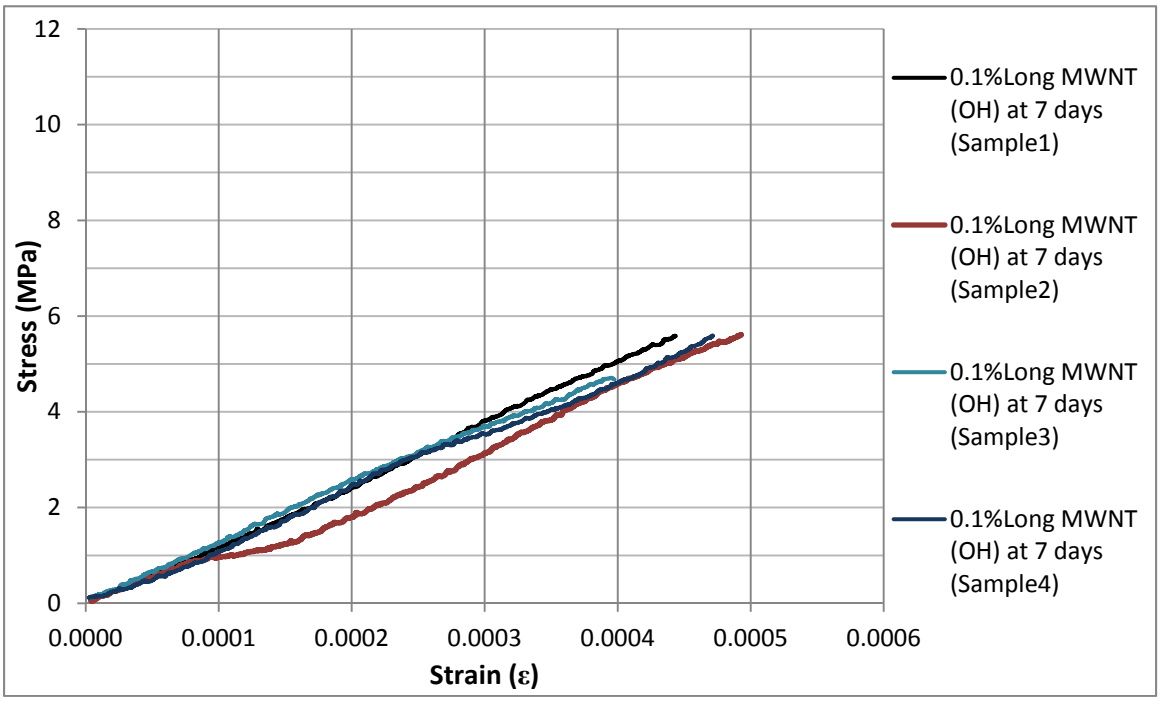

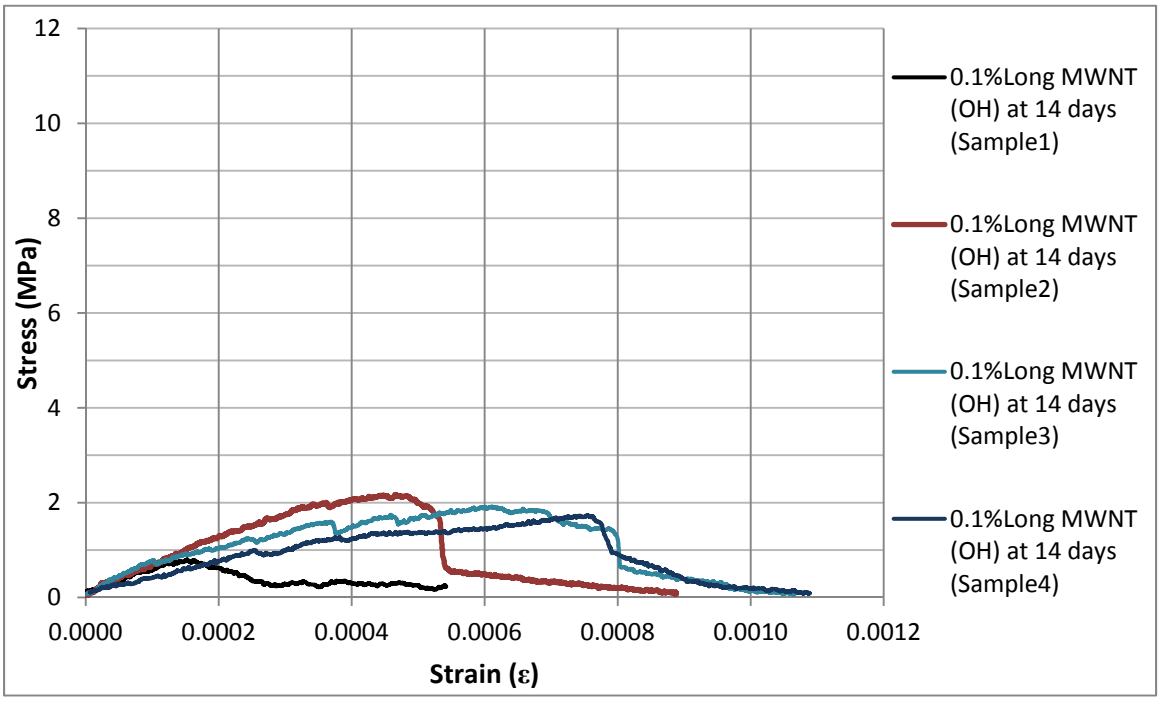

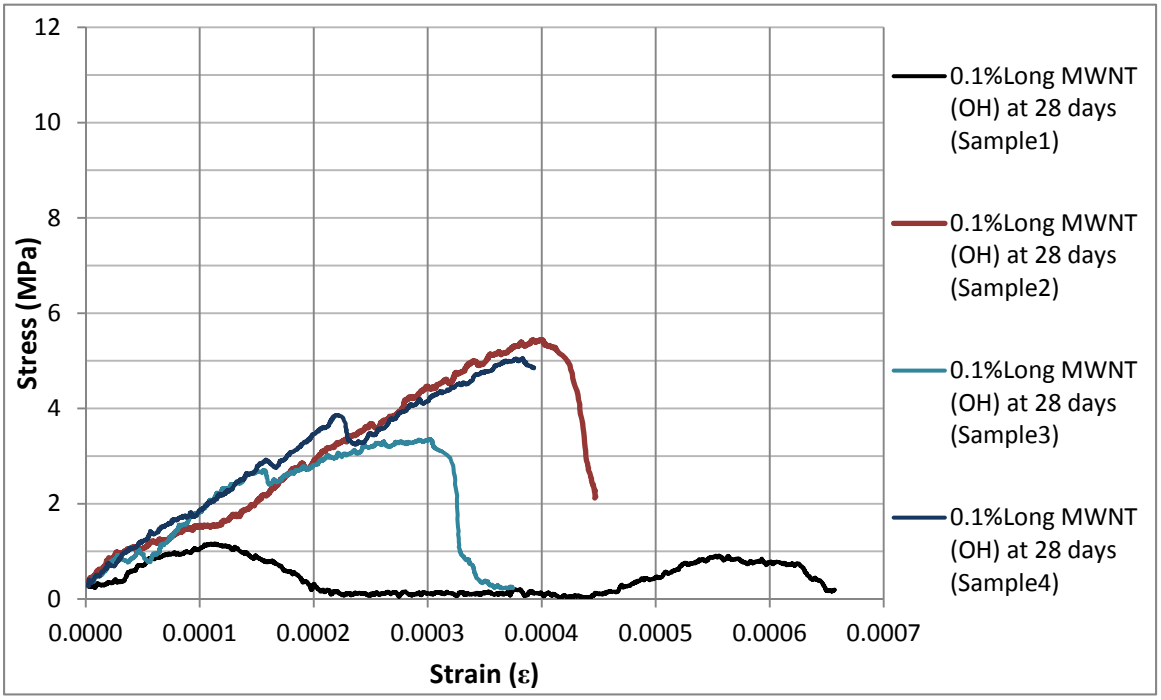
12
10
8
6
4
2
0
Stress (MPa)
0.0000
0.0001
0.0002
0.0003
0.0004
0.0005
0.0006
0.0007
Strain (ε)
0.1%Long MWNT (OH) at 28 days (Sample1)
0.1%Long MWNT (OH) at 28 days (Sample2)
0.1%Long MWNT (OH) at 28 days (Sample3)
0.1%Long MWNT (OH) at 28 days (Sample4)

Stress-strain diagrams for the 0.1% Long MWCNTs /cement composite samples:

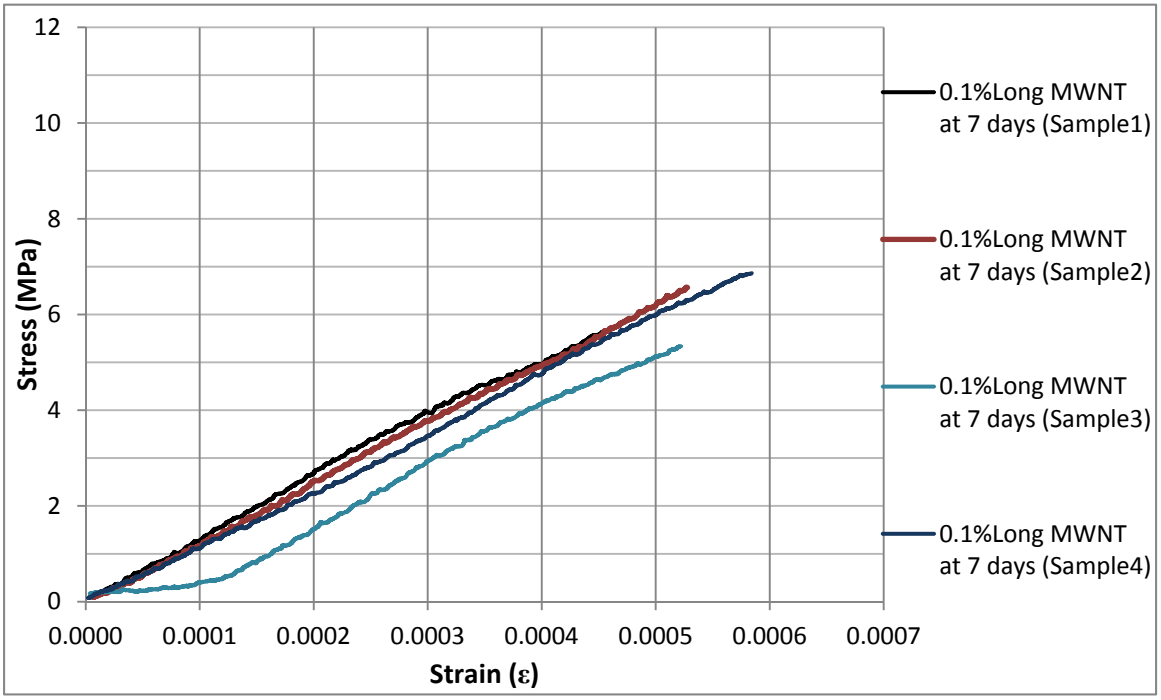

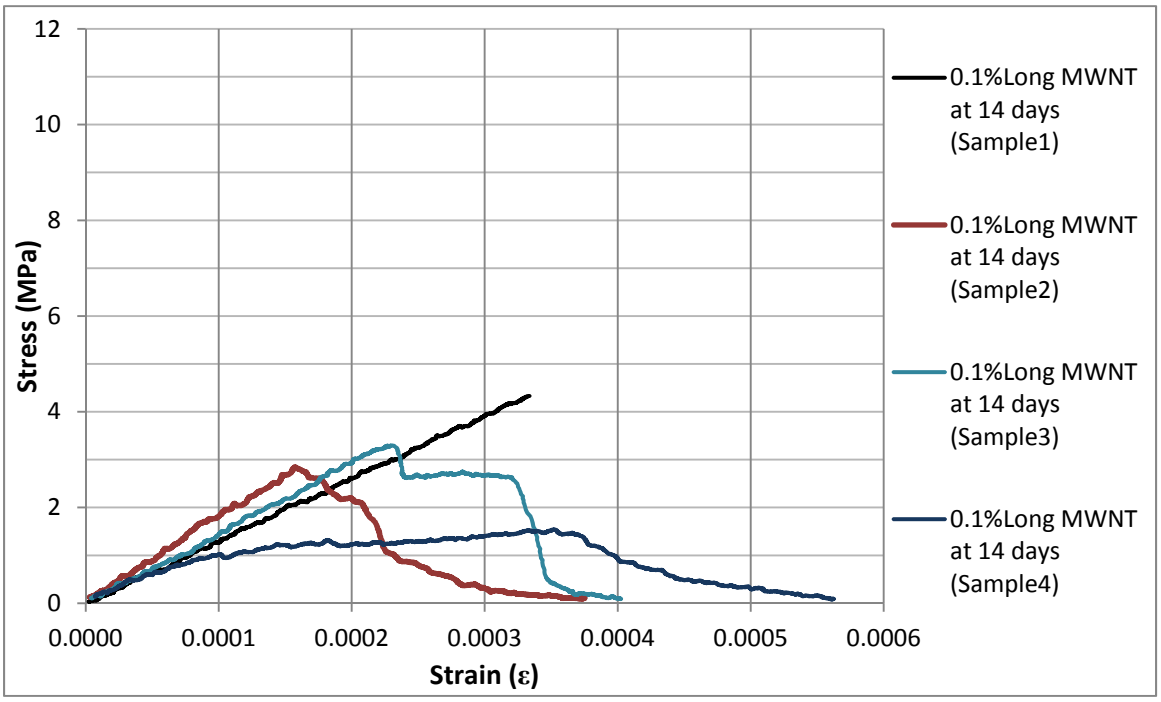

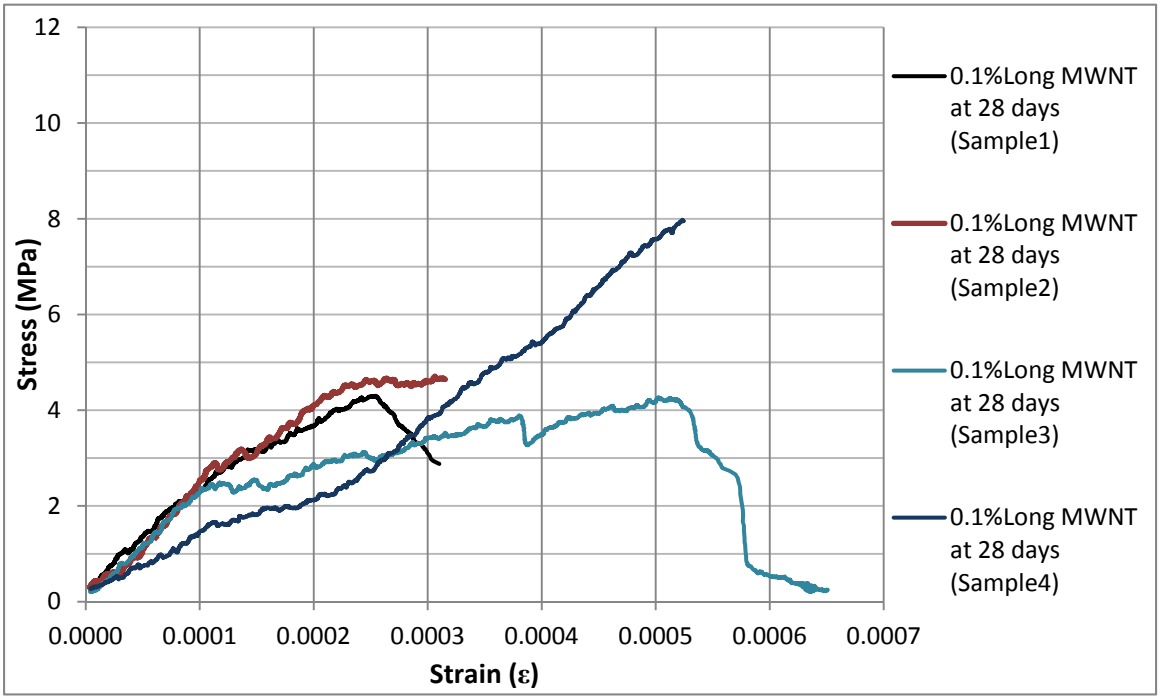
12
10
8
6
4
2
0
Stress (MPa)
0.0000
0.0001
0.0002
0.0003
0.0004
0.0005
0.0006
0.0007
Strain (ε)
0.1%Long MWNT at 28 days (Sample1)
0.1%Long MWNT at 28 days (Sample2)
0.1%Long MWNT at 28 days (Sample3)
0.1%Long MWNT at 28 days (Sample4)

Stress-strain diagrams for the 0.1% Short MWCNTs(COOH)/cement composite samples:

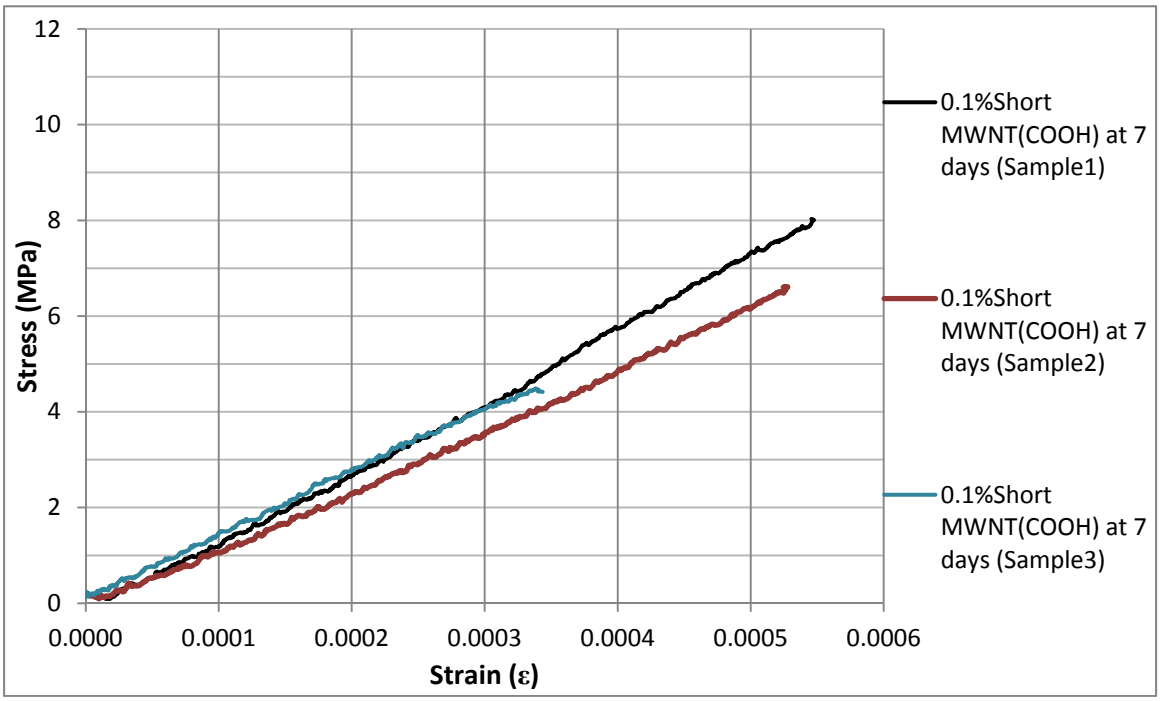

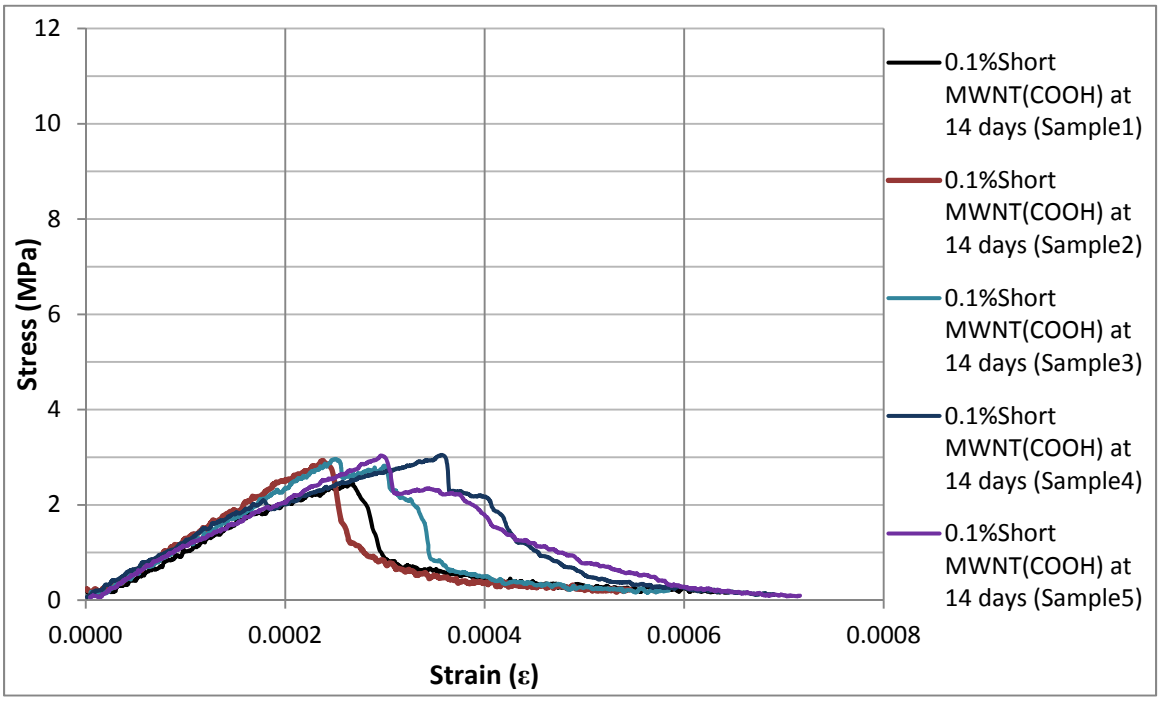

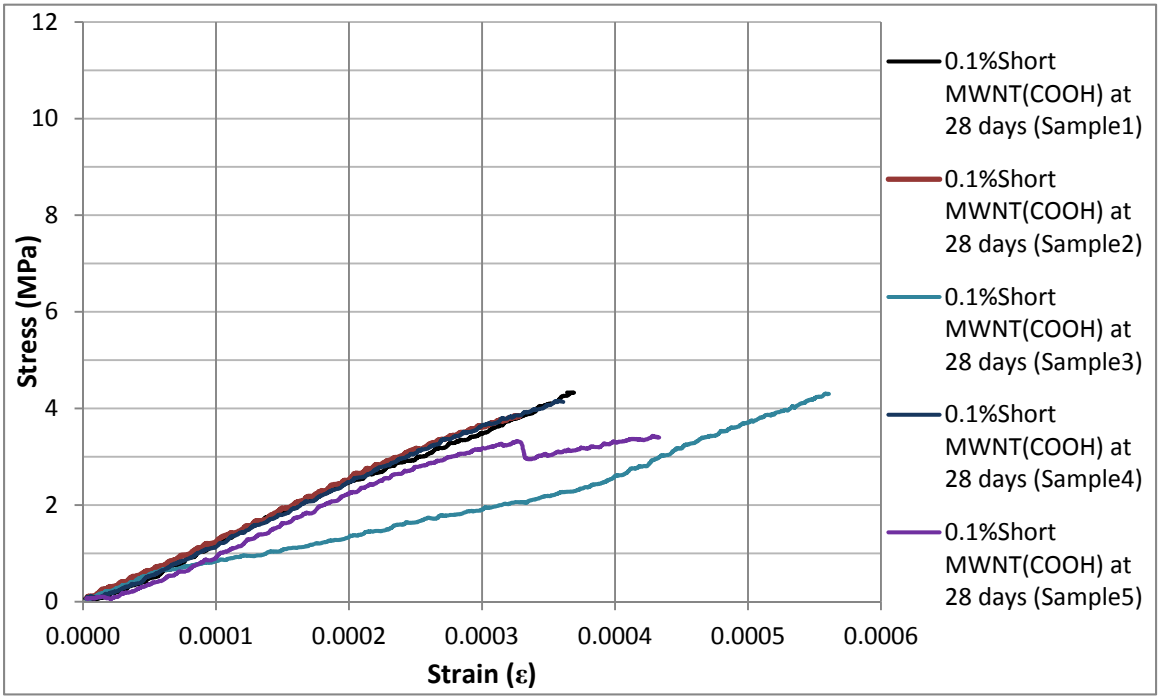
12
10
8
6
4
2
0
Stress (MPa)
0.0000
0.0001
0.0002
0.0003
0.0004
0.0005
0.0006
Strain (ε)
0.1%Short MWNT(COOH) at 28 days (Sample1)
0.1%Short MWNT(COOH) at 28 days (Sample2)
0.1%Short MWNT(COOH) at 28 days (Sample3)
0.1%Short MWNT(COOH) at 28 days (Sample4)
0.1%Short MWNT(COOH) at 28 days (Sample5)

Stress-strain diagrams for the 0.2% Short MWCNTs(COOH)/cement composite samples:

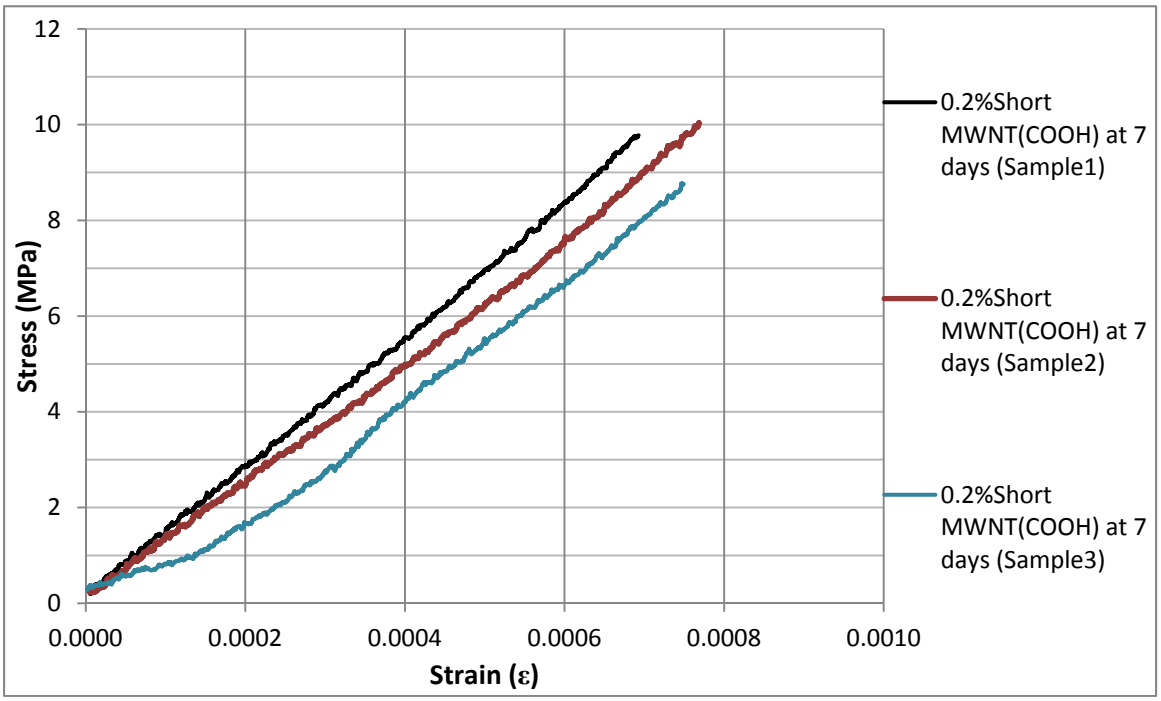

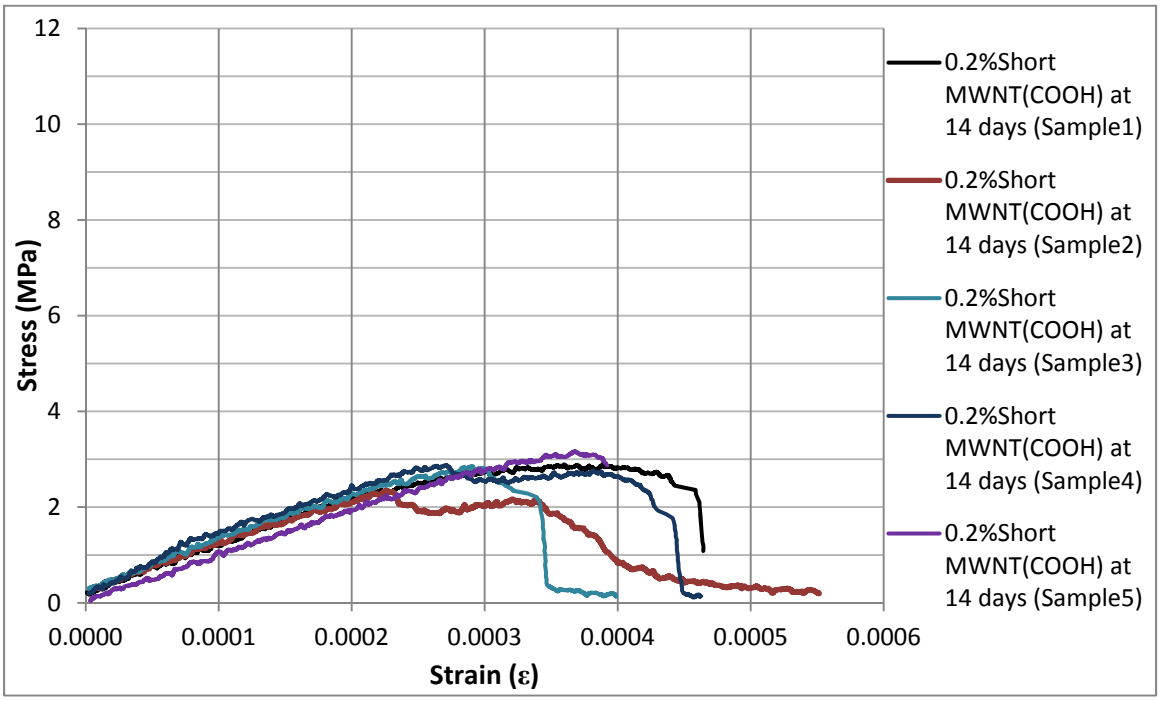

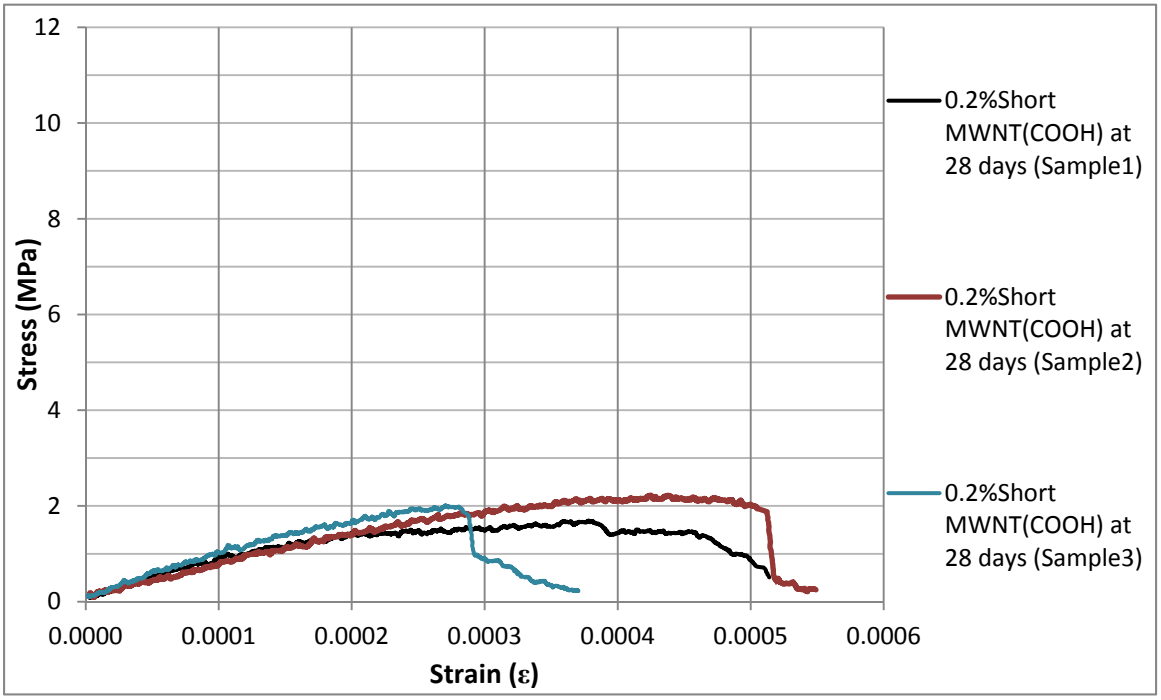
12
10
8
6
4
2
0
Stress (MPa)
0.0000
0.0001
0.0002
0.0003
0.0004
0.0005
0.0006
Strain (ε)
0.2%Short MWNT(COOH) at 28 days (Sample1)
0.2%Short MWNT(COOH) at 28 days (Sample2)
0.2%Short MWNT(COOH) at 28 days (Sample3)

Stress-strain diagrams for the 0.1% Short MWCNTs /cement composite samples:

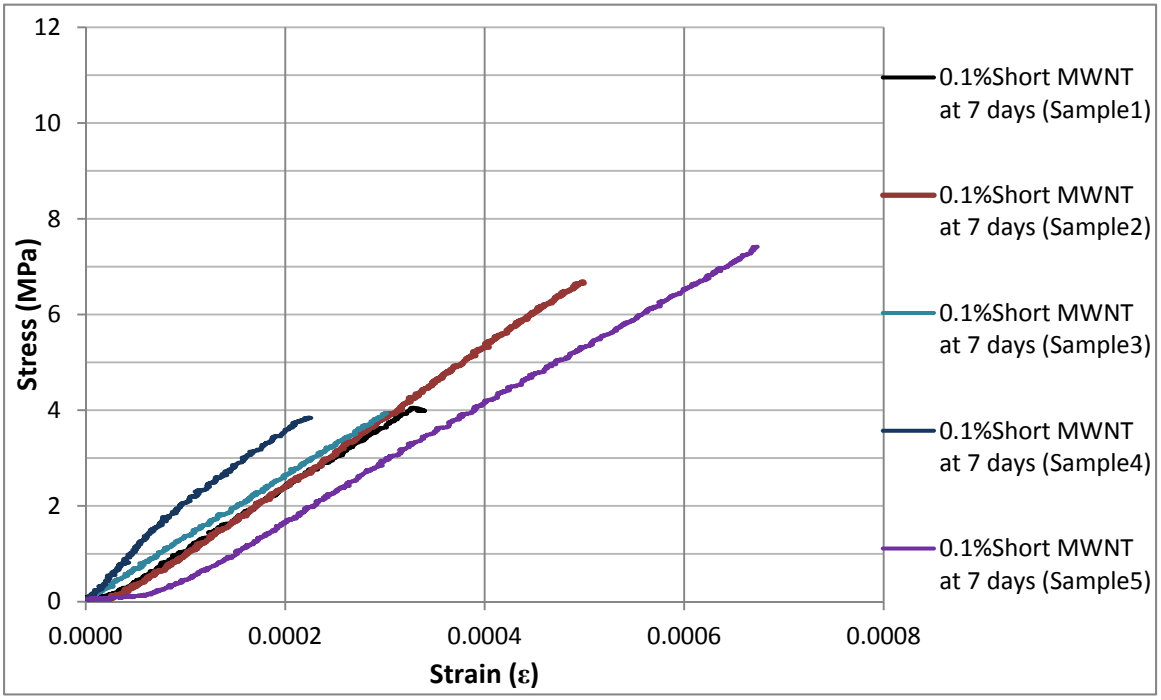

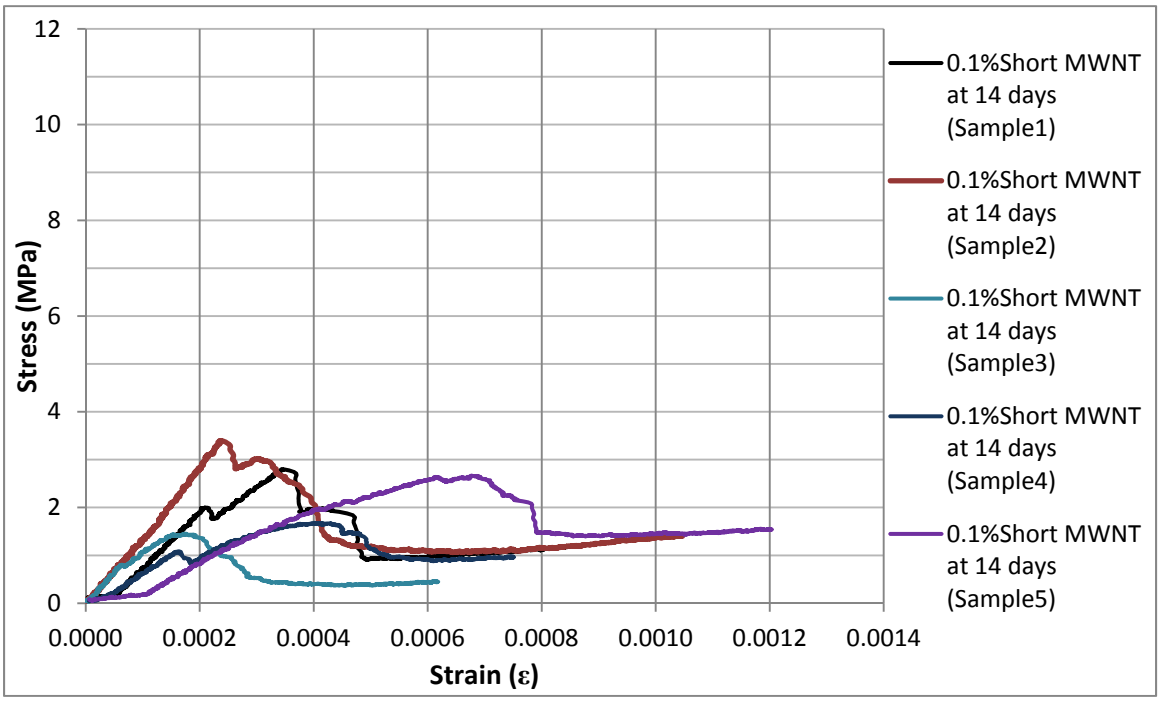

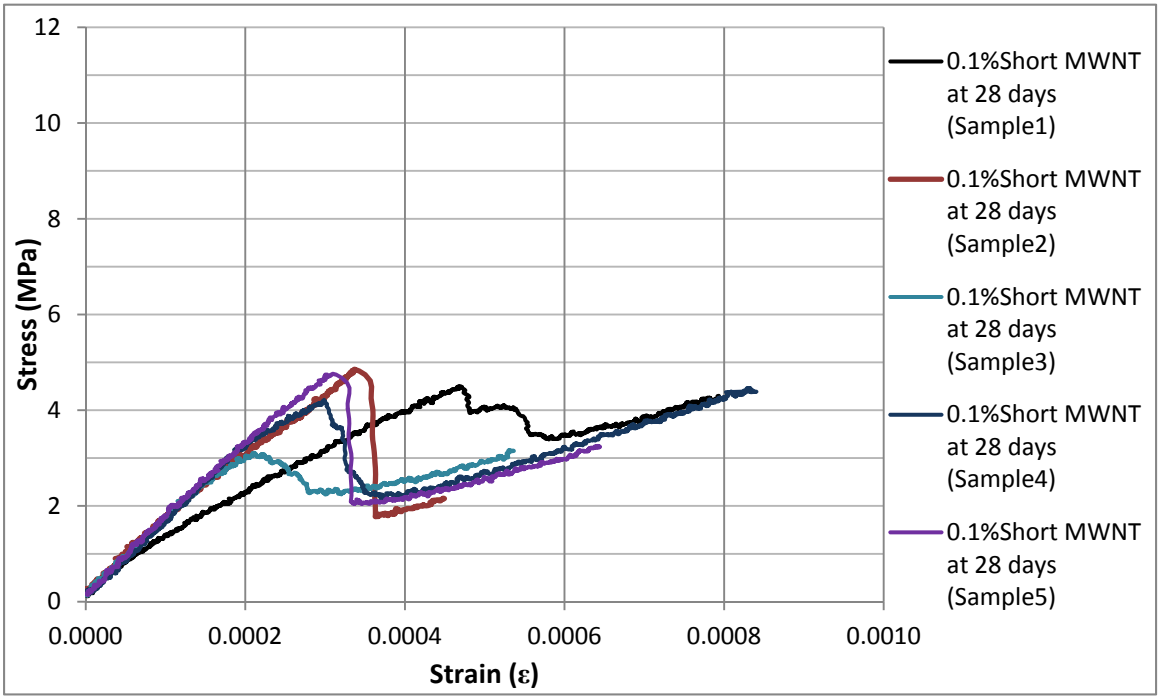
12
10
8
6
4
2
0
Stress (MPa)
0.0000
0.0002
0.0004
0.0006
0.0008
0.0010
Strain (ε)
0.1%Short MWNT at 28 days (Sample1)
0.1%Short MWNT at 28 days (Sample2)
0.1%Short MWNT at 28 days (Sample3)
0.1%Short MWNT at 28 days (Sample4)
0.1%Short MWNT at 28 days (Sample5)

Stress-strain diagrams for the 0.2% Short MWCNTs /cement composite samples:

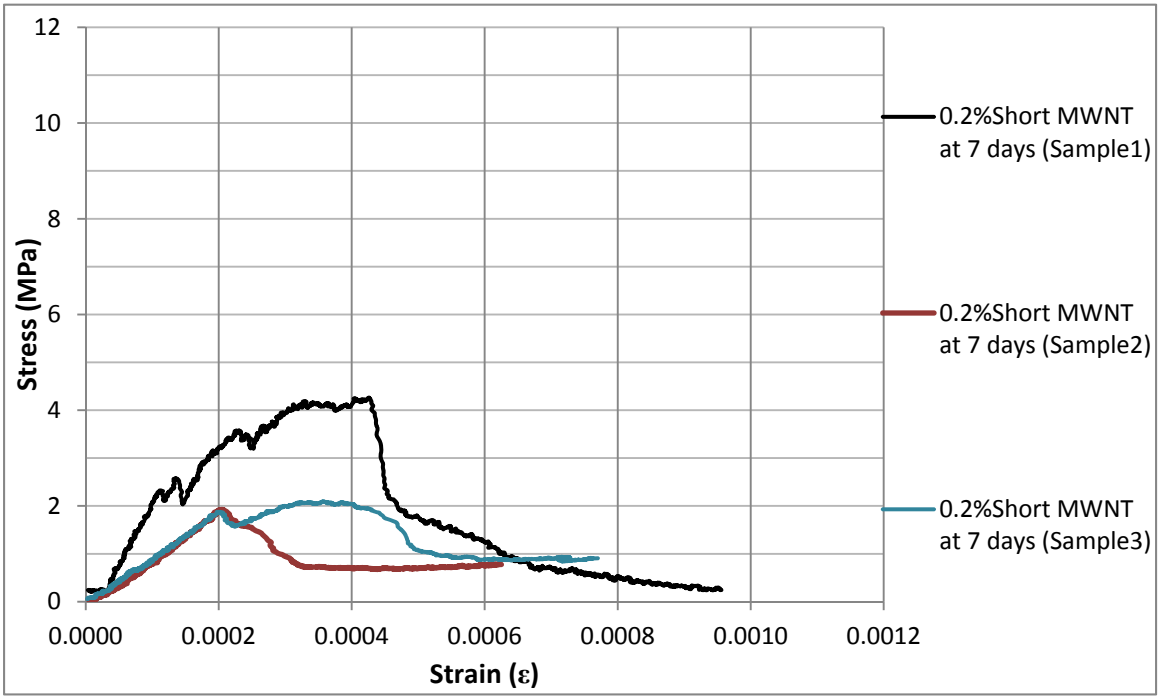

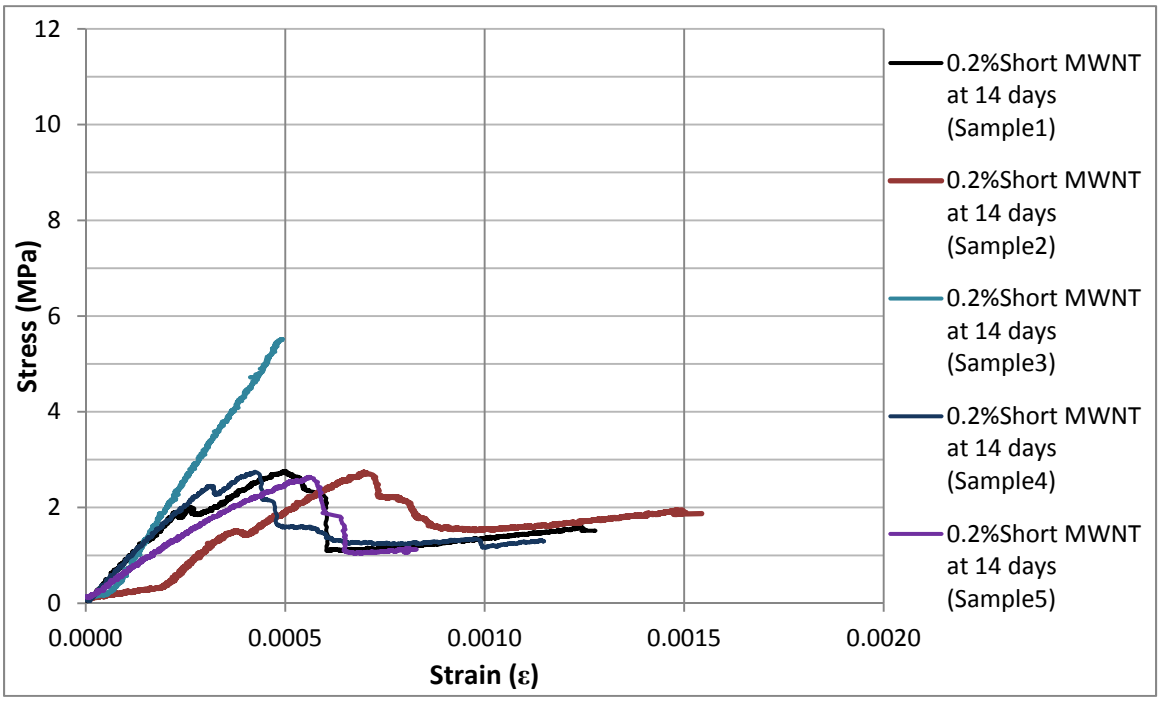

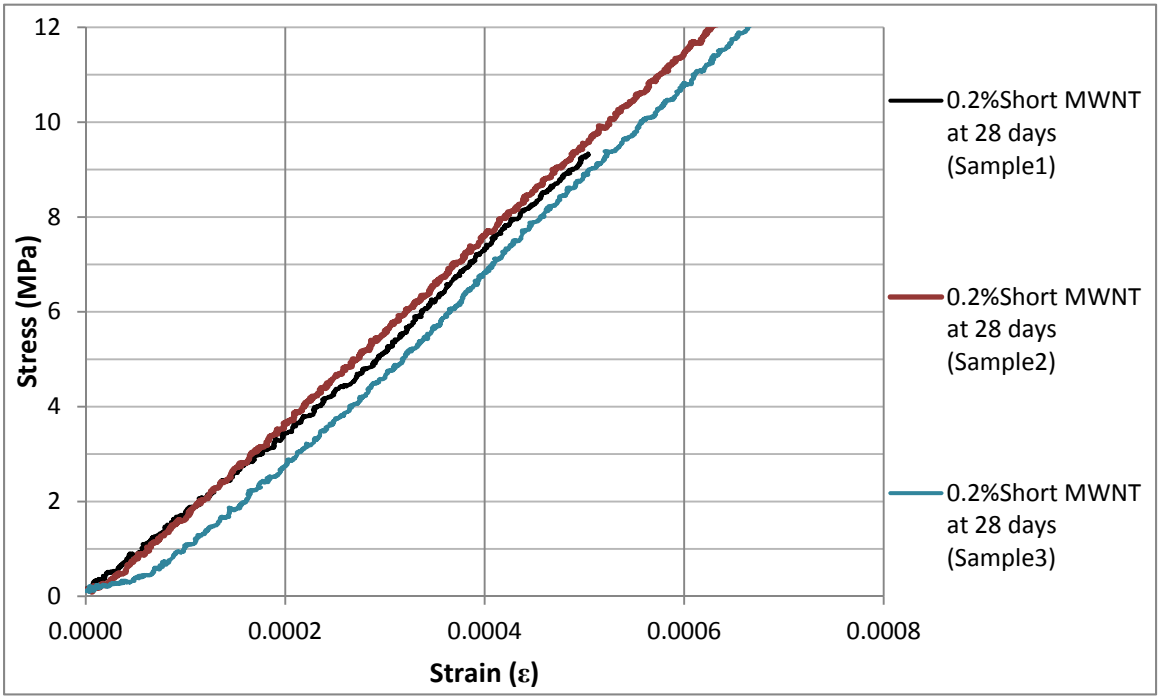
12
10
8
6
4
2
0
Stress (MPa)
0.0000
0.0002
0.0004
0.0006
0.0008
Strain (ε)
0.2%Short MWNT at 28 days (Sample1)
0.2%Short MWNT at 28 days (Sample2)
0.2%Short MWNT at 28 days (Sample3)

Stress-strain diagrams for the 0.04% Short MWCNTs /cement composite samples:

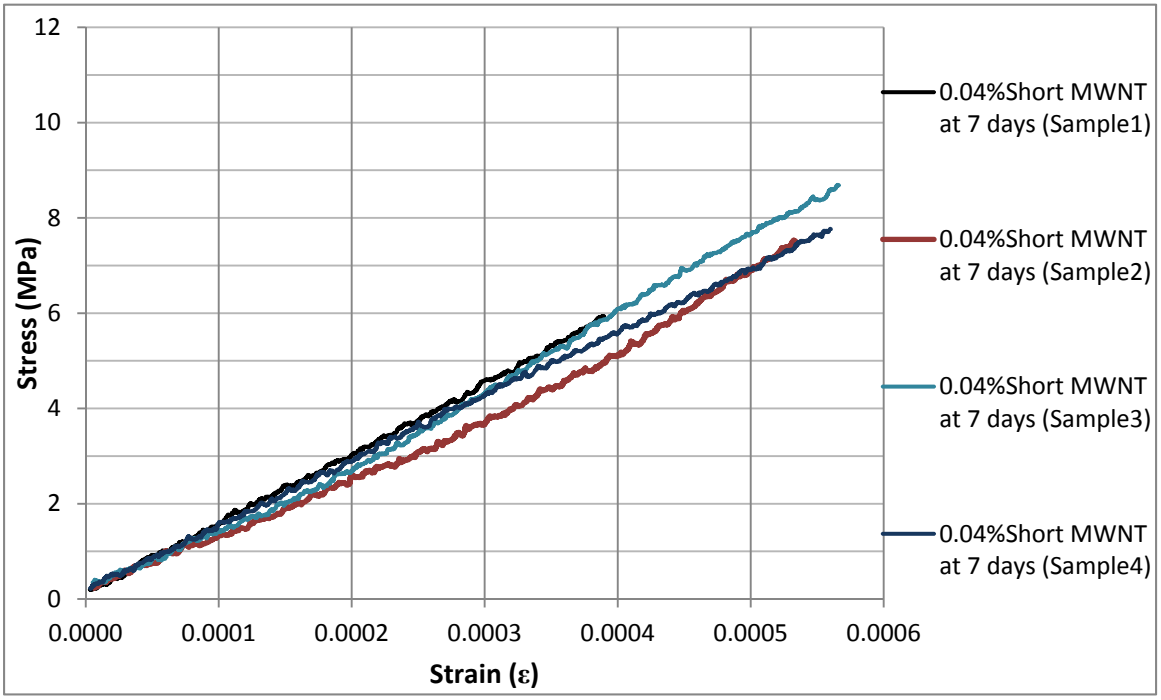

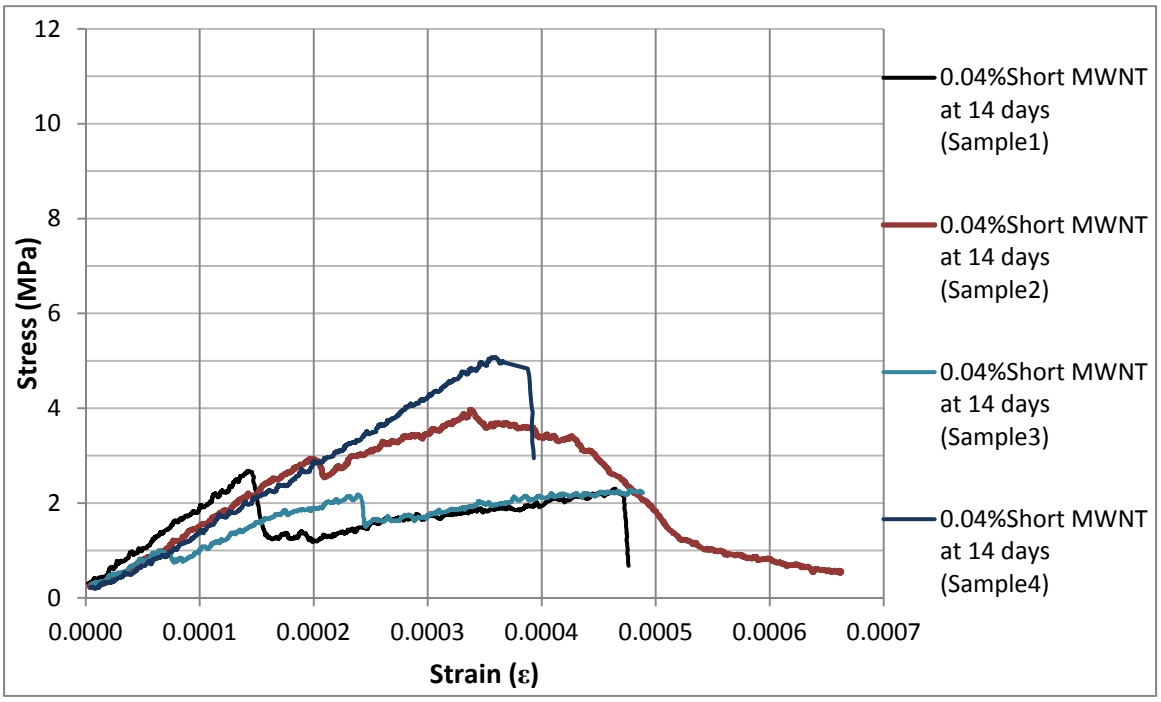

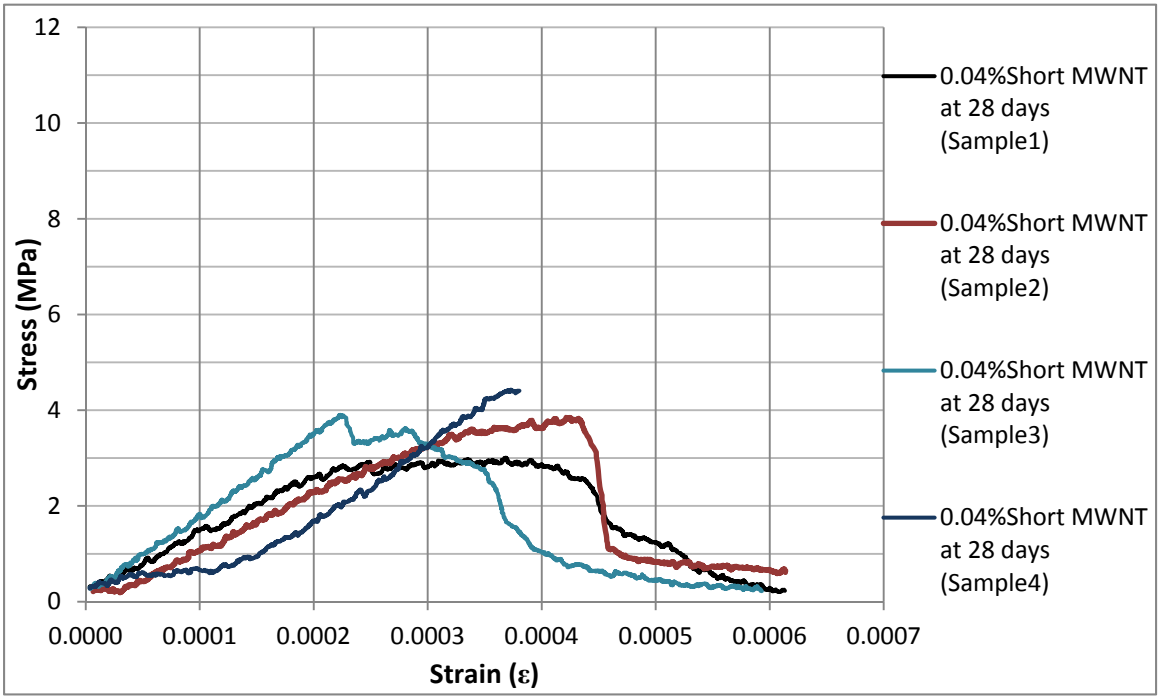
12
10
8
6
4
2
0
Stress (MPa)
0.0000
0.0001
0.0002
0.0003
0.0004
0.0005
0.0006
0.0007
Strain (ε)
0.04%Short MWNT at 28 days (Sample1)
0.04%Short MWNT at 28 days (Sample2)
0.04%Short MWNT at 28 days (Sample3)
0.04%Short MWNT at 28 days (Sample4)

Stress-strain diagrams for the 0.04% Long MWCNTs(OH)/cement composite samples:

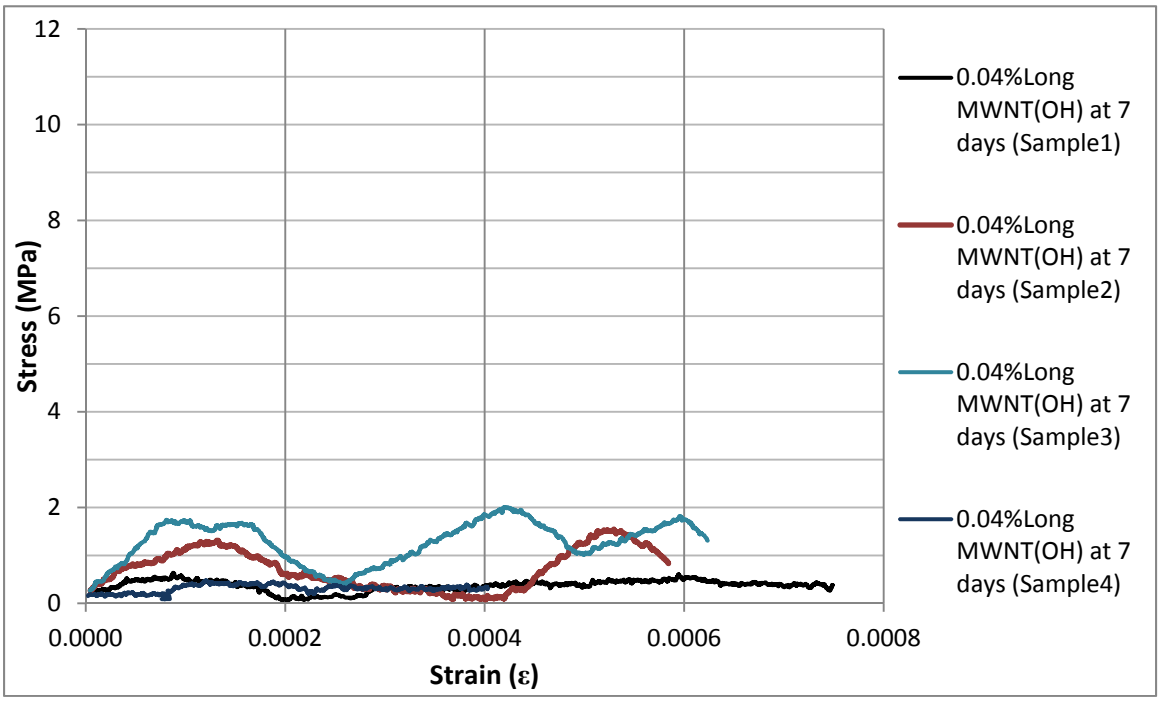

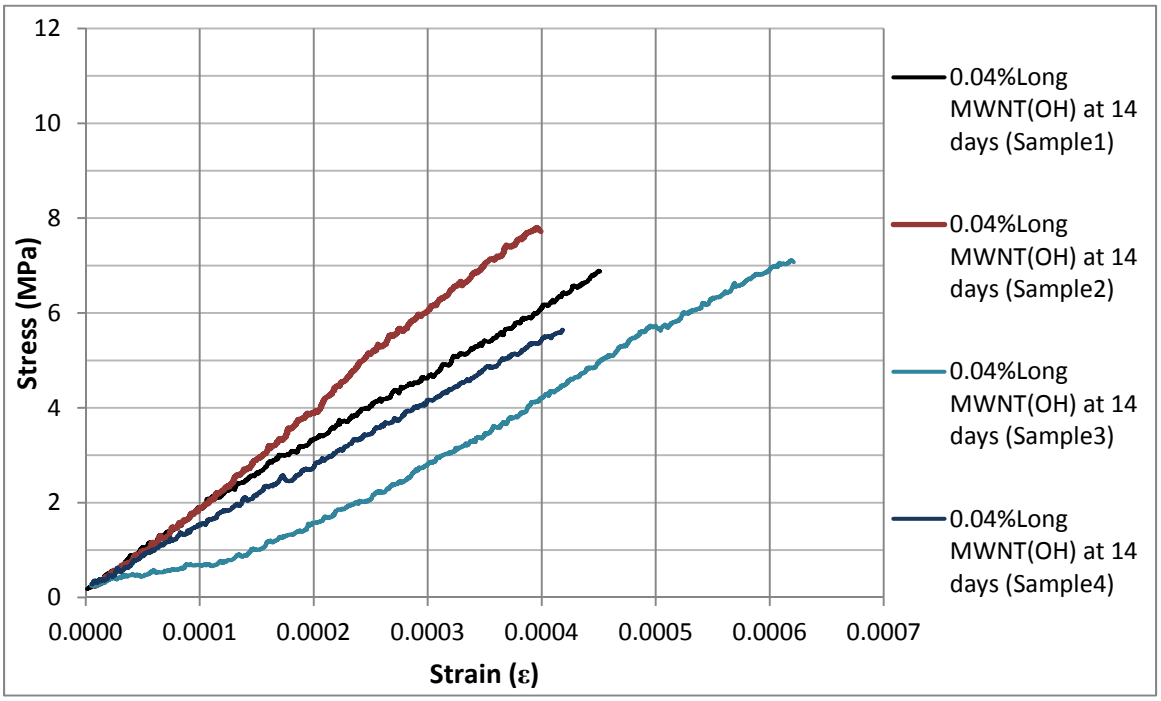

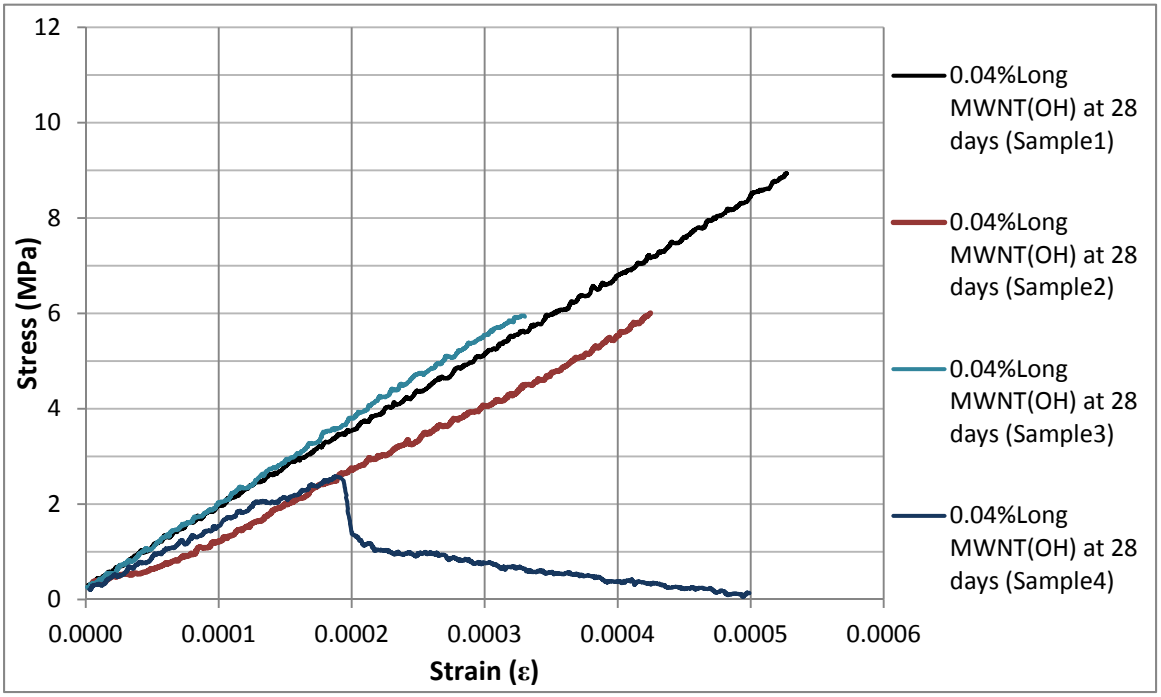
12
10
8
6
4
2
0
Stress (MPa)
0.0000
0.0001
0.0002
0.0003
0.0004
0.0005
0.0006
Strain (ε)
0.04%Long MWNT(OH) at 28 days (Sample1)
0.04%Long MWNT(OH) at 28 days (Sample2)
0.04%Long MWNT(OH) at 28 days (Sample3)
0.04%Long MWNT(OH) at 28 days (Sample4)

Stress-strain diagrams for the 0.04% Long MWCNTs /cement composites samples:

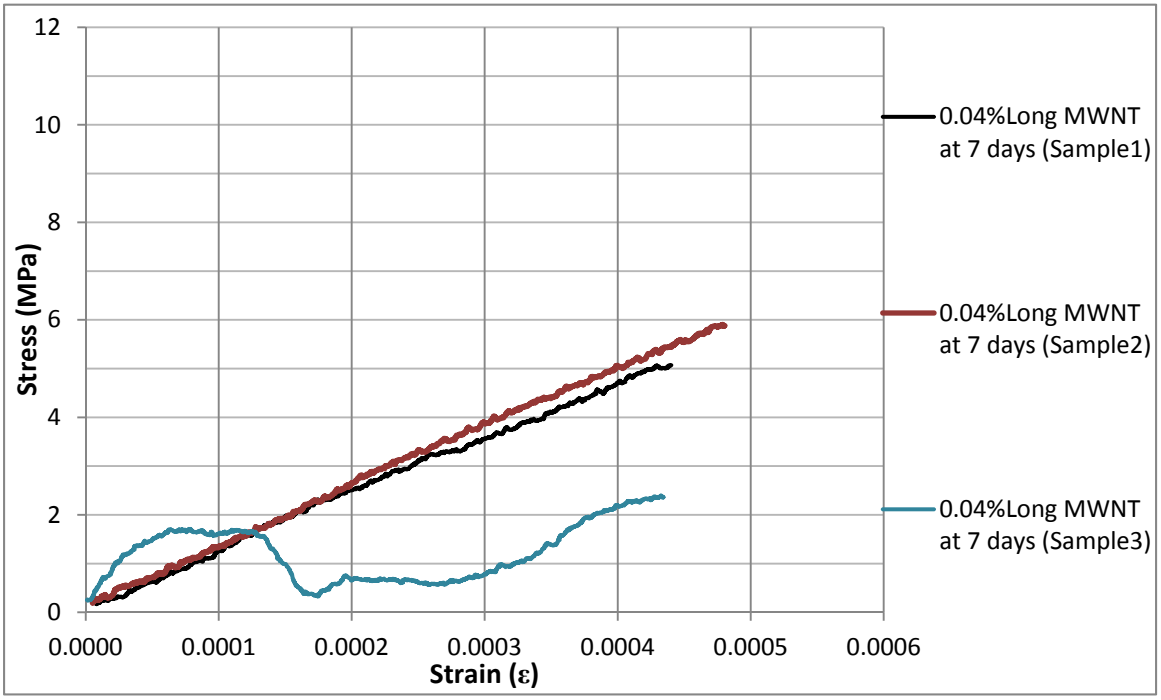

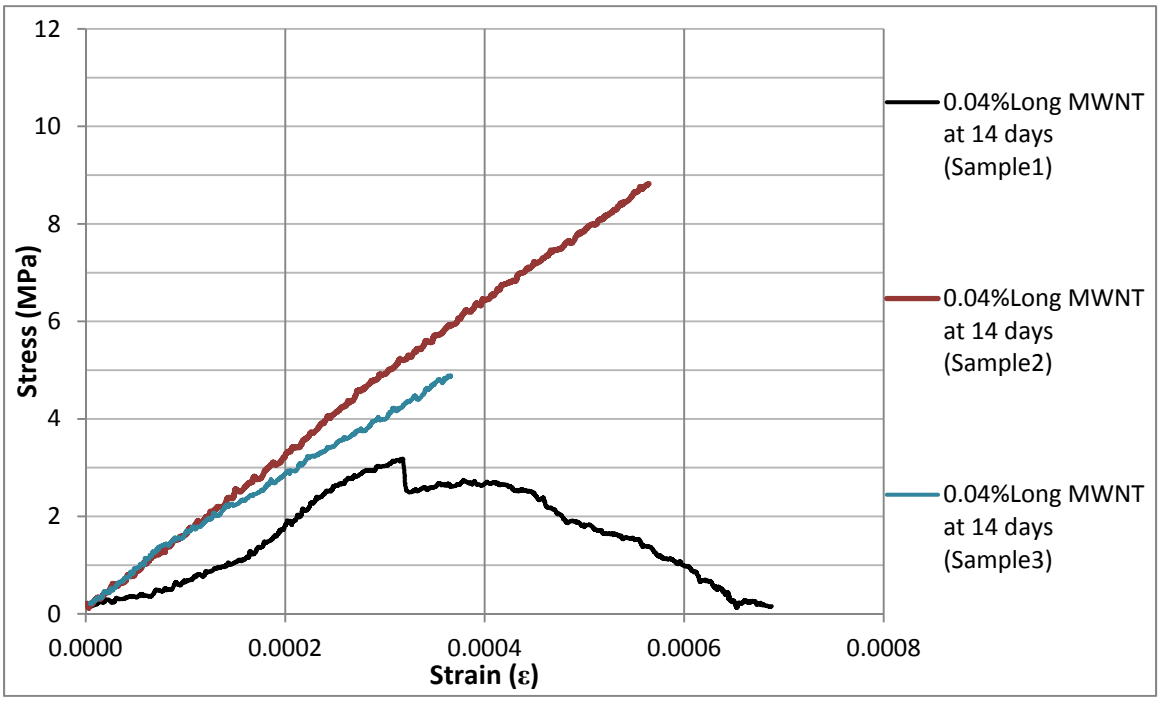

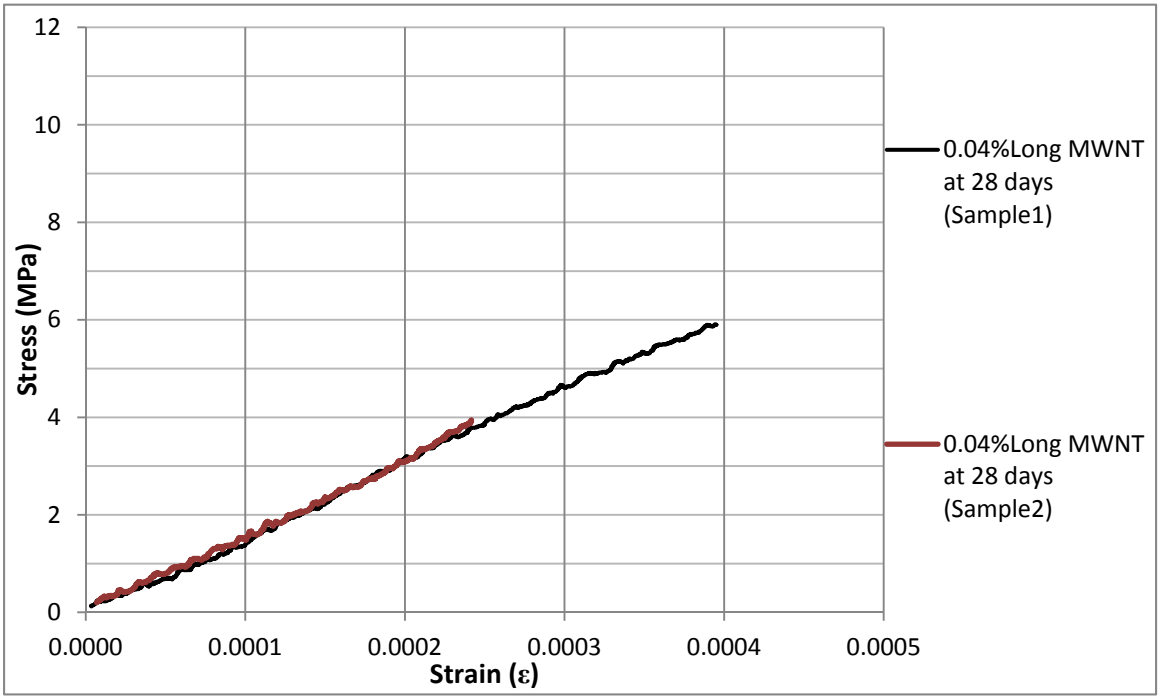
12
10
8
6
4
2
0
Stress (MPa)
0.0000
0.0001
0.0002
0.0003
0.0004
0.0005
Strain (ε)
0.04%Long MWNT at 28 days (Sample1)
0.04%Long MWNT at 28 days (Sample2)

VITA

Name:	Ahmad Ibrahim Ashour
Address:	Construction, Geotechnical, and Structural Division 3136 TAMU College Station, TX 77843-3136
Email Address:	ahmad.ashour@tamu.edu
Education:	M.S., Civil Engineering, Texas A&M University, College Station, 2011 B.S., Civil Engineering, The Hashemite University, Jordan, 2007